

EFFECT OF
GLYCATED ALBUMIN AND SHEAR STRESS
ON ENDOTHELIAL CELL FUNCTIONS

By

ZAHRA MARIA

Bachelor of Science in Mechanical Engineering
Bangladesh University of Engineering and Technology

Dhaka, Bangladesh

2009

Submitted to the Faculty of the
Graduate College of the
Oklahoma State University
in partial fulfillment of
the requirements for
the Degree of
MASTER OF SCIENCE
July, 2011

EFFECT OF
GLYCATED ALBUMIN AND SHEAR STRESS
ON ENDOTHELIAL CELL FUNCTIONS

Thesis Approved:

Dr. David A Rubenstein

Thesis Adviser

Dr. Wei Yin

Dr. Heather Fahlenkamp

Dr. Mark E. Payton

Dean of the Graduate College

To My Parents and Brother

ACKNOWLEDGMENTS

I would first like to thank my advisor and my mentor Dr. David A. Rubenstein for his constant guidance, support and patience. His availability and willingness to guide me through the entire course of my research has been vital in completion of my thesis. I would specially like to thank him for taking the time to correct my abstract and thesis report.

I would also like to thank Dr. Wei Yin for her advice and support. I want to thank Dr. Heather Fahlenkamp for serving in my thesis committee.

My parents and my brother are the source of my inspiration. I am forever indebted to my parents for supporting me through the toughest times of my life.

I thank all my BELOS lab colleagues, especially Saravan Kumar and Farzana Rouf. I would also like to thank my close friends (Natis, David, Shantonu and Sadia) for their support during the time of my research. Lastly I want to take this opportunity to thank everyone who have helped and inspired me during my Masters.

TABLE OF CONTENTS

Chapter	Page
I. INTRODUCTION.....	1
II. BACKGROUND.....	4
2.1 Diabetes Mellitus and Cardiovascular Disease.....	4
2.2 Diabetic Vasculature and Advanced Glycation End Products.....	6
2.2.1 Formation of Advanced Glycation End Products.....	6
2.2.2 The effect of AGE in Endothelial Dysfunction Section.....	9
2.3 Endothelial Cell Biology.....	11
2.3.1 Endothelial Cell Morphology and Function.....	11
2.3.2 Endothelial Cell Cytoskeleton Structure and Function.....	17
2.3.3 Membrane Associated Proteins Related to Diabetes Mellitus.....	19
2.3.3.a Intercellular Adhesion Molecule-1 (ICAM-1).....	19
2.3.3.b Tissue Factor (TF).....	20
2.3.3.c Thrombomodulin (TM).....	20
2.3.3.d Caveolin-1.....	21
2.3.3.e Connexin-43.....	22
2.4 The Effect of shear stress in Endothelial Cell function.....	23
III. MATERIALS AND METHODS.....	28
3.1 Synthesis of Advanced Glycation End Products.....	28
3.2 Endothelial Cell Culture.....	29
3.2.1 Cell Culture Conditions.....	29
3.2.2 Passage of Endothelial Cells.....	29
3.3 Experimental Conditions.....	30
3.3.1 Static Conditions.....	30
3.3.2 Dynamic Conditions.....	30
3.3.2.a Hemodynamic Cell Shearing Device.....	30
3.3.2.b Shearing Experiment.....	31
3.4 MTT Assay.....	33
3.5 Live/Dead Cell Cytotoxic Assay.....	33
3.5.1 Immunofluorescence Staining and Microscopy.....	33
3.5.2 Image Analysis.....	34
3.5.2.a Cell Viability.....	34
3.5.2.b Cell Density.....	34
3.5.2.c Cell Morphology.....	34

Chapter	Page
3.6 Endothelial Cell Connexin-43 and Caveolin-I Expression.....	35
3.6.1 Immunofluorescence Staining and Microscopy	35
3.6.2 Image Analysis.....	36
3.6.2.a Quantification of Connexin-43 and Caveolin-I Intensity.....	36
3.6.2.b Quantification of Connexin-43 and Caveolin-1 Localization.....	36
3.7 Endothelial Cell Actin Structure and Alignment.....	38
3.7.1 Immunofluorescence Staining and Microscopy	38
3.7.2 Image Analysis.....	39
3.7.2.a Actin Fiber Structure.....	39
3.7.2.b Actin Fiber Alignment	39
3.7.2.c Inter-Cellular Connectivity	39
3.8 Enzyme-linked Immunosorbent Assay (ELISA).....	43
3.9 Scanning Electron Microscopy (SEM)	44
3.10 Statistical Analysis.....	44
3.10.1 Analysis of Experiments Under Static Conditions	44
3.10.2 Analysis of Experiments Under Dynamic Conditions.....	44
 IV. RESULTS	 46
4.1 Endothelial Cell Metabolic Activity	46
4.1.1 Static Condition	46
4.1.2 Dynamic Condition.....	48
4.2 Endothelial Cell Viability and Density	50
4.3 Endothelial Cell Morphology	52
4.4 Connexin-43 and Caveolin-1 Expression	54
4.4.1 Static Condition	54
4.4.2 Dynamic Condition.....	57
4.4.2.a Connexin-43 Intensity and Relative Localization.....	57
4.4.2.b Caveolin-1 Intensity and Relative Localization.....	60
4.5 Endothelial Cell Cytoskeletal Structure.....	62
4.5.1 Actin Structure.....	62
4.5.2 Actin Alignment.....	66
4.5.3: Cell Connectivity	69
4.6 Expression of Inflammatory and Thrombotic Mediators.....	72
4.7 Scanning Electron Microscopy.....	75
 V. DISCUSSION	 77
5.1 Endothelial Cell Metabolic Activity	77
5.1.1 Static Condition	77
5.1.2 Dynamic Condition.....	78
5.2 Endothelial Cell Viability and Density	78
5.3 Endothelial Cell Morphology	79
5.4 Connexin-43 and Caveolin-1 Expression	79

Chapter	Page
5.4.1 Static Condition	79
5.4.2 Dynamic Condition	81
5.4.2.a Connexin-43 Intensity and Relative Localization	81
5.4.2.b Caveolin-1 Intensity and Relative Localization	82
5.5 Endothelial Cell Cytoskeletal Structure	83
5.5.1 Actin Structure	83
5.5.2 Actin Alignment	84
5.5.3 Cell Connectivity	85
5.6 Expression of Inflammatory and Thrombotic Mediators	86
5.7 Scanning Electron Microscopy	86
 VI. CONCLUSION	 90
 REFERENCES	 94
 APPENDIX A BASIC PROGRAM USED TO OPERATE CONE AND PLATE SHEARING DEVICE	 105
 APPENDIX B SEM IMAGES FOR THE COMPARISON OF GLYCATION EXTENT FOR DIFEERENT SHEAR STRESS AND CULTURE DURATION	 106

LIST OF TABLES

Table	Page
4.1 Endothelial cell (HUVEC) Morphology	53
6.1 The Effect of Higher Glycation Extent and Shear Stress on Endothelial Cell Structure and Function.....	92
6.2 The combined effect of Higher Glycation Extent and Shear Stress on Endothelial Cell Structure and Function.....	93

LIST OF FIGURES

Figure	Page
2.1 The initial and final stages of AGE formation.....	8
2.2 The coagulation cascade demonstrating the activation of coagulation factors and the anticoagulant factors.....	13
2.3 The sequential steps of leukocyte adhesion and migration controlled by the adhesion molecules on leukocyte and ECs	15
3.1 The modified cone and plate hemodynamic cell shearing device	32
3.2 Digital images of endothelial cell connexin-43 and caveolin-1 expression	37
3.3 The actin structure of the sheared endothelial cells	40
3.4 The alignment of endothelial cells in a shear direction	41
3.5 The inter-cellular connectivity of the endothelial cells.....	42
4.1 Endothelial cell (HUVEC) metabolic activity under static condition	47
4.2 Endothelial cell (HUVEC) metabolic activity under dynamic condition	49
4.3 Endothelial cell (HUVEC) viability and density	51
4.4 Endothelial cell (HUVEC) surface expression of connexin-43 or caveolin-1	55
4.5 Digital images of endothelial cell connexin-43 and caveolin-1 expression	56
4.6 Endothelial cell (HUVEC) surface expression for Cx-43 relative localization and relative intensity	59
4.7 Endothelial cell (HUVEC) surface expression for Caveolin-1 relative localization and relative intensity early	61

Figure	Page
4.8 Endothelial cell (HUVEC) cytoskeletal actin fiber structure	64
4.9 Immuno-fluorescence microscopy image (20X magnification) of Human umbilical vein endothelial cells (HUVEC) actin fiber structure.....	65
4.10 Endothelial cell (HUVEC) cytoskeletal actin fiber alignment	67
4.11 Immuno-fluorescence microscopy image (20X magnification) of Human umbilical vein endothelial cells (HUVEC).....	68
4.12 Endothelial cell (HUVEC) cytoskeletal actin connectivity	70
4.13 Immuno-fluorescence microscopy image (20X magnification) of Human umbilical vein endothelial cells (HUVEC) actin fiber connectivity	71
4.14 Endothelial cell (HUVEC) surface expression of ICAM-1 Thrombomodulin and Tissue Factor	74
4.15 Scanning electron microscopy images of Human umbilical vein endothelial cells (HUVEC)	76

CHAPTER I

INTRODUCTION

Diabetes mellitus or more commonly known as diabetes is by far the most common and serious metabolic disorder with a worldwide prevalence estimated to be around 11% and 8.3% in the United States (National Diabetes Fact Sheet, 2011). Recent statistics have shown that, around 25.8 million people throughout the world are affected with insulin dependent (type-1) or non-insulin dependent (type-2) diabetes. These two forms of diabetes are characterized by a relative or absolute lack of insulin (type-1) or cellular resistance to insulin (type-2) followed by a prolonged period of hyperglycemia (abnormally high fasting glucose level for a significant amount of time) (Ruderman, Williamson, & Brownlee, 1992). Sustained hyperglycemic conditions in a diabetic vasculature, in most cases, lead to the formation of pathogenic advanced glycation end products (AGEs) which alter the healthy cellular structure and function (Goldin, Beckman, Schmidt, & Creager, 2006).

The most common metabolic consequences due to insulin resistance and hyperglycemia in the diabetic vasculature are renal failure, nerve disease, blindness, accelerated atherosclerosis and stroke (Maiti & Agrawal, 2007). According to American Heart Association, a diabetic vasculature induces a two to four folds increases on the risk factors for cardiovascular diseases. The key factors of cardiovascular pathogenesis in coronary, cerebral and peripheral arterial trees are atherosclerosis and thrombosis (Yang et al., 2010). The formation of atherosclerotic lesion

is governed by the structure and location (bifurcations) in the vascular tree and also by the magnitude and pattern of blood flow induced shear stress (Fry, 1968). Endothelial cells (ECs) line the innermost layer of the blood vessel and are continuously subjected to the varying magnitudes of wall shear stress. Therefore, healthy endothelium function is essential to maintaining a healthy vascular condition. High pathological levels of shear stress may cause vascular wall EC damage or induce activation of ECs to cause EC dysfunction in atherosclerotic regions, which could eventually lead to cardiovascular disease conditions.

It is well established that, advanced glycation end products (AGEs) modulate many of the pathologies associated with diabetes mellitus by altering the EC functions and this is a function of glycation extent (Yamagishi et al., 2005). There have been many studies conducted in the past few decades to observe the effect of flow mediated shear stress or AGEs on the effect of EC functionality. However, few studies have been conducted to determine the effect of shear stress on endothelial cell function in the presence of AGEs. To relate diabetic vasculature and cardiovascular disease propagation, the combined effect of shear stress and presence of AGE needs to be thoroughly investigated. Therefore, in this study we propose to observe the effects of AGEs in diabetic culture conditions combined with the application of varying levels of shear stress and investigated whether or not these two conditions have a synergistic effect on cardiovascular disease promotion and propagation.

The major goal of this thesis was to investigate, **how varying glycation extent and physiological shear stress alter endothelial cell function to promote cardiovascular disease pathogenesis *in vitro***. This goal was divided into two aims: (i) to determine the effect of different levels of glycated albumin on EC function in static culture conditions (without the application of shear stress); (ii) to observe the effect of shear stress magnitude on ECs incubated with glycated albumin in dynamic experimental conditions. In this thesis, we **hypothesized** that, **higher glycation extents and high stress (pathological) magnitude would synergistically diminish**

EC culture conditions, promote EC inflammatory and thrombogenic responses, and thereby facilitate cardiovascular disease propagation. The hypothesis (and thesis) was divided into the following specific aims.

Aim 1: To investigate, how the level of glycation alters EC function *in vitro*, by observing EC culture conditions (cell viability, density, morphology and metabolic activity), and to characterize the effect of advanced glycated end products on EC cell-to-cell communication and angiogenic potential.

***Hypothesis:* Higher glycation extents deteriorate healthy EC culture conditions.**

Aim 2: To apply varying levels of hemodynamic shear stress on ECs incubated with glycated albumin, in a cone and plate shear device, to investigate the combined effect of shear stress and glycation extent on EC cytoskeletal structure, inflammatory and thrombotic responses.

***Hypothesis:* Higher shear stress magnitude in the presence of higher glycation extent would synergistically heighten EC inflammatory and thrombotic potential and simultaneously deteriorate EC cytoskeletal structure and function.**

CHAPTER II

BACKGROUND

2.1 Diabetes Mellitus and Cardiovascular Disease

Diabetes mellitus accounts for approximately 225,000 deaths per year and affects nearly 15 million people. Along with cardiovascular diseases (CVD), these two conditions account for the most deaths in the United States annually (National Diabetes Fact Sheet, 2011). The diabetic vasculature differs vastly from the normal vasculature and resembles the pathologies of many cardiovascular diseases (Harja et al., 2008). According to the American Heart Association, the likelihood of having heart disease is two to four times higher among diabetic adults compared to non-diabetic adults. The risk factors associated with CVD are also highly correlated with diabetes. Some of the major risk factors for both of these diseases are hypertension, high cholesterol level, obesity, high blood sugar level and smoking. Therefore, there is a significant connection between CVD and diabetes.

A diabetic condition is defined as the presence of an elevated plasma glucose concentration. The fasting plasma glucose level is 110 mg/dL in a healthy vasculature. A diabetic condition is diagnosed either if the fasting glucose level exceeds 126 mg/dL or if the glucose level is higher than 200 mg/dL two hours after the intake of 75 g of oral glucose (Saydah et al., 2001). The increase in glucose level is caused by the deficiency in insulin production or to a

hyporesponsiveness to insulin in the blood stream. Insulin is a hormone that is produced in the islets of Langerhans of the pancreas and is responsible for the regulation and metabolism of glucose and fat present in the blood stream. In a healthy vasculature, in response to the elevated blood glucose level (after a meal), the pancreatic β cells secrete insulin molecules which circulate in the blood. The insulin in the blood stream binds to the insulin receptors on the cells of the vessel wall and initiates the signaling pathway of glucose transportation into the cells. However, in diabetes pathogenesis, insulin is either inadequate or incapable to facilitate the glucose transportation. Based on the condition and amount of insulin present in the blood, diabetes can be classified into two groups: insulin-dependent diabetes mellitus or type-1 diabetes and noninsulin-dependent diabetes mellitus or type-2 diabetes. In type-1 diabetes the islets of Langerhans do not produce sufficient insulin and thus it is largely absent from the plasma. In type-2 diabetes, insulin is present at a near-normal or above normal level in the plasma. However, it remains ineffective in the metabolism process of glucose (Vander et al. 2001).

Insulin resistance at the cellular level is recognized to be the major factor that is responsible for noninsulin-dependent or type-2 diabetes. Although in this type of diabetic vasculature the insulin level is near normal, the cells that insulin target are not responsive to insulin causing hyperglycemia (Vander et al. 2001). Hypertension or high blood pressure level and obesity are two of the major factors behind the initiation of insulin resistance (Rask-Madsen & King, 2007). Obesity induces an excess of adipose-tissue cells which overproduce messengers (such as leptin and adiponectin) that causes down-regulation of insulin responsiveness and causes postprandial hyperglycemia (Rask-Madsen & King, 2007; Kahn, Hull, & Utzschneider, 2006). During type-1 diabetes the pancreatic β cells incur a defect in their ability to secrete insulin in response to a rise in plasma glucose concentration. As result these cells are no longer able to respond to the hyperglycemic condition in a normal fashion. Regardless of which diabetes type is found, hyperglycemic conditions persist for a prolonged period of time (Vander et al. 2001). It is

the presence of excessive glucose in the vasculature, which leads to many cardiovascular pathology.

The sustained hyperglycemia induces other disease conditions and dysfunctions in the vasculature, such as intracellular accumulation of certain glucose metabolites, endothelial and mitochondrial dysfunction, increase in oxidative stress and the possibility for glucose to cross-links with proteins. As albumin is the most abundant plasma protein, it is most susceptible to such cross-link formations (see section 2.2.1) (Wolff, Jiang, & Hunt, 1991). As a result patients with type-2 diabetes become more susceptible to atherosclerosis, kidney failure, small vessel and nerve disease, infection and blindness.

2.2 Diabetic Vasculature and Advanced Glycation End Products

The persistence of chronic hyperglycemic condition is the first step of many disease conditions that develop from diabetes mellitus. The hyperglycemia originates due to insulin resistance in diabetes mellitus. This excessive glucose in the diabetic vasculature triggers the formation of advanced glycation end products; which is pivotal in the development and progression of diabetic vascular damage leading to cardiovascular disease. This will be discussed in detail in the following section.

2.2.1 Formation of Advanced Glycation End Products

Advanced glycation end products (AGEs) are formed in the diabetic environment when proteins are glycated in the presence of high glucose concentrations. AGEs are generated by the modification of proteins or lipids, which undergo non-enzymatic glycation and oxidation, after coming in contact with aldose sugars (such as glucose) (Marchetti et al. 2009). Glycation may be reversible or irreversible, depending on the exposure time. The initial stages of glycation are the formation of the intermediate Schiff bases (glycation time 1-2 weeks). The Schiff base is generally thought to be reversible, but with longer glycation time this is converted to a very

stable Amadori products (glycation time 6-8 weeks) (Cho, Roman, Yeboah, & Konishi, 2007). The irreversible formation of AGEs requires further molecular rearrangements, but the Amadori products are greatly stable. The protein turnover rate, the degree of hyperglycemia and the extent of oxidative stress are the key factors in the formation of AGEs. Through the presence of any of these conditions in the vasculature both intracellular and extracellular proteins may become glycated (Goldin et al., 2006). Albumin is the most abundant serum protein (approximately 60%) in the vasculature and thereby most susceptible to the formation of AGE. Furthermore, many serum proteins are susceptible to glycation due to their slow turnover rate and restriction to locations with high glucose.

The first stage of the glycation reaction is the formation of Schiff base which arguably is a reversible stage. In this step a condensation reaction takes place between the amine ($R-NH_2$) group from the amino acid in the protein chain and aldehyde ($R-CO-R^*$) group of the reducing sugar ($C_n(H_2O)_n$). The nitrogen (N) atom from the amine and the carbon (C) atom from the sugar form a covalent double bond between themselves during condensation reaction; as a molecule of water (H_2O) is removed. This Schiff base then undergoes the more stable Amadori rearrangement where the hydrogen (H) atom from the carboxyl ($R-COOH$) group adjacent to the carbon nitrogen double bond ($C=N$) moves to form a bond with the nitrogen ($N-H$) leaving a ketone ($R-CO-R^*$) (Marchetti et al. 2009). Figure 2.1 shows the transformation from Schiff base to Amadori product to the formation of AGEs (Yamagishi et al., 2005). The best known Amadori products are HBA1c and fructosamine. Fructosamines are formed by the glycation of serum proteins such as albumin. By a non-oxidative dissociation of fructosamine new reactive intermediates are produced which are finally modify into irreversible AGEs (Marchetti et al. 2009). Once AGEs are formed they tend to accumulate in the vessel wall and alter the normal cellular structure and function.

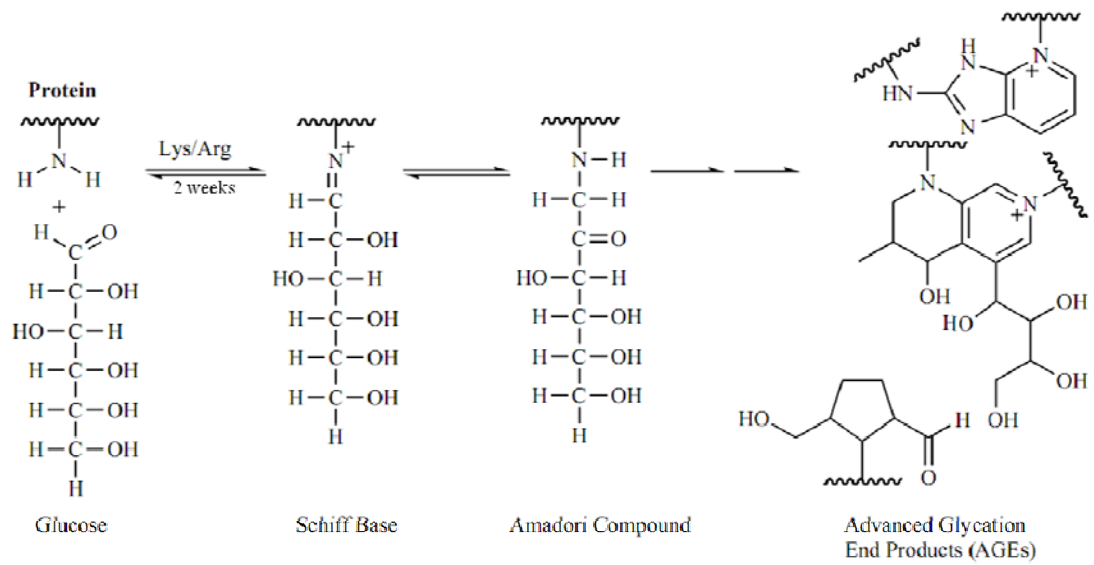


Figure 2.1- The initial and final stages of AGE formation. This figure has been modified from (Yamagishi, Nakamura, & Imaizumi, 2005)

2.2.2 The effect of AGE in Endothelial Dysfunction

AGEs are formed by a series of non-enzymatic glycation reactions in the diabetic vasculature and are responsible for micro and macro vascular complications in diabetes and promote cardiovascular disease (Hori et al., 1996). Formed AGEs alter the cellular functions by associating with several binding sites including the receptor for AGE. RAGE (receptor for advanced glycation end products), are expressed in many tissues, but is most abundant in the heart, lungs, skeletal muscles and blood vessel walls. The endothelial cells and the smooth muscle cells that form blood vessels contain RAGEs (Marchetti et al. 2009). AGEs present in the vasculature interact with receptors of cell signaling pathways, increase oxidative stress, modify the extracellular matrix (ECM), affect the endothelial cell (EC) thrombotic and inflammatory responses and enhance the migration of inflammatory mediators (Yamagishi et al., 2005). AGEs take part in activation of nuclear factor kappa of activated B cells (NF- κ B) (Mohamed et al., 1999), which transform the ECs membrane from anticoagulant to procoagulant.

AGEs alter the function and structure of the ECM by accumulating in the basement membrane on proteins that have a slow turnover rate by forming crosslinks. AGEs can also alter the properties of common matrix proteins such as collagen, vitronectin and laminin by the formation of AGE-AGE covalent bond or by crosslinking. Such links formed between collagen and elastin effectively increases the surface area of the ECM leading to an increase of stiffness in the vasculature (Goldin et al., 2006).

AGEs binding to ECs via cellular receptors induce the activation of NF- κ B, which is a nuclear transcription factor responsible for the DNA transcription and regulation of endothelin-1, vascular adhesion molecule-1 (VCAM-1), intercellular adhesion molecule-1 (ICAM-1), E-selectin, thrombomodulin, tissue factor and proinflammatory cytokines including interleukin-1 α (IL-1 α) and tumor necrosis factor- α (TNF- α), to name a few. Cytokines are small protein structures that regulate the intercellular communication and interaction. NF- κ B greatly increase

high glucose induced monocyte adhesion (Mohamed et al., 1999). AGEs interacting with its cellular receptors increases the cellular surface thrombogenic potential (Marchetti et al. 2009) by reducing antithrombotic thrombomodulin (TM) expression and increasing the tissue factor (TF) expression which may initiate coagulation. TF is a membrane bound glycoprotein in ECs that initiates blood coagulation during vessel injury (Wilcox, Smith, Schwartz, & Gordon, 1989), whereas TM is an EC thrombin receptor that cleaves thrombin, altering its properties from procoagulant to anticoagulant maintaining the hemostatic balance (Dittman & Majerus, 1990). As a result the probability of thrombosis increases with the interaction of AGEs.

The activation of NF- κ B due to AGEs causes an up-regulation of VCAM-1, ICAM-1 and E-selectin in the endothelium which triggers an inflammatory response, monocyte adhesion and migration. Normal endothelium resists adhesion with circulating leukocytes and monocytes in the blood, but due to the increased expression of adhesion molecules the recruitment of monocytes increases. And once these cells adhere to the activated endothelium they penetrate and proliferate within the intima of the blood vessel wall. When the monocytes reach the smooth muscle cells of the intima layer they acquire the characteristics of macrophages and bind to the lipoproteins. After the initialization, these macrophages convert themselves into foam cells which are the hallmark of cardiovascular lesion formation (Maiti & Agrawal, 2007). The foam cells initiate the secretion of proinflammatory cytokines such as IL-1 α and TNF- α . The secretion of these molecules amplifies the inflammatory response and the cycle continues as more monocytes start to migrate and adhere to the endothelium (Maiti and Agrawal 292-306). Although, we are not looking at atherosclerotic lesion formation here, the downstream effects of these markers is a heightened potential of atherosclerosis.

2.3 Endothelial Cell Biology

2.3.1 Endothelial Cell Morphology and Function

Endothelial cells (ECs) form the interior lining of the entire vascular system and provide an anticoagulant barrier between the blood vessel wall and the blood constituents (Sumpio, Riley, & Dardik, 2002). ECs are positioned on a condensed layer of extra cellular matrix known as the 'basement membrane' within the blood vessel wall (Aird, 2007b). In the macrocirculation the larger blood vessels have multiple layers of ECs; whereas smaller vessels in the microcirculation, such as capillaries, contain a monolayer of ECs. One of the primary functions of the ECs is to maintain the blood vessel wall permeability and to regulate the inflow of molecules into the interstitial space (Cines et al., 1998), which is partially governed by the shape and the interactions between the neighboring ECs (Aird, 2007a). The shape of ECs depends partially on its location in the circulatory system. However, they are generally spindle shaped cells with an average length and width of approximately 100 μ m and 20 μ m, respectively (Aird, 2007a). ECs play a major role in the regulation of hemostasis, immune and inflammatory responses, vasomotor tone and angiogenesis (Cines et al., 1998). One of the other major functions of the ECs is the diffusion of oxygen and nutrients from the flowing blood to other cells. In the microcirculation they act as a diffusion barrier against oxygen, nutrients and waste in the capillary structures (Guyton and Hall 2000). EC injury, activation or dysfunction are all hallmarks of many severe pathological conditions, such as atherosclerosis and thrombosis (Sumpio et al., 2002). Therefore a healthy endothelium is important to maintain a healthy vascular condition.

The ECs play a major role in coagulation by regulating the expression of binding sites of anticoagulant and procoagulant factors (Wu & Thiagarajan, 1996a). Thrombomodulin (TM) is one of the major anticoagulant factors expressed by ECs on their surface. In addition, surface bound tissue factor (TF), factor Va and soluble von Willebrand factor are some of the major

procoagulant substances expressed by the ECs (Wu & Thiagarajan, 1996b). Under resting conditions the ECs provide an anticoagulant or non-thrombogenic surface that prevents platelets or other blood constituents from adhering to the endothelial cell surface or to activate the coagulation pathway (Arnout, Hoylaerts, & Lijnen, 2006). Under the stimulation of cytokines or bio-physical force (such as shear stress) or in the occasion of a vessel injury, the cells undergo biochemical changes that lead to the transformation of the cell surface to a prothrombotic state (Wilcox et al., 1989). When a blood vessel is injured, ECs up-regulate TF which binds to coagulation factor VIIa. The TF:VIIa complex initiates the coagulation cascade (Figure 2.2) resulting in the formation of thrombin (Arnout et al., 2006). Thrombin is a serine protease, which converts fibrinogen into insoluble fibrin and promotes platelet activation. The plasma membrane of resting ECs does not favor the assembly of these coagulation factors, which is partly due to the expression of TM on their surface. Thrombin binds to TM to form a 1:1 complex which together with protein S triggers the activation of protein C. Activated protein C triggers the anticoagulant activity by proteolytic inhibition of coagulation co-factors Va and VIIIa (Wu & Thiagarajan, 1996a). In case of endothelial loss or dysfunction the antithrombotic factors may no longer be present or in effect, resulting in a strong prothrombotic environment. Here we are interested in both EC tissue factor and thrombomodulin expression.

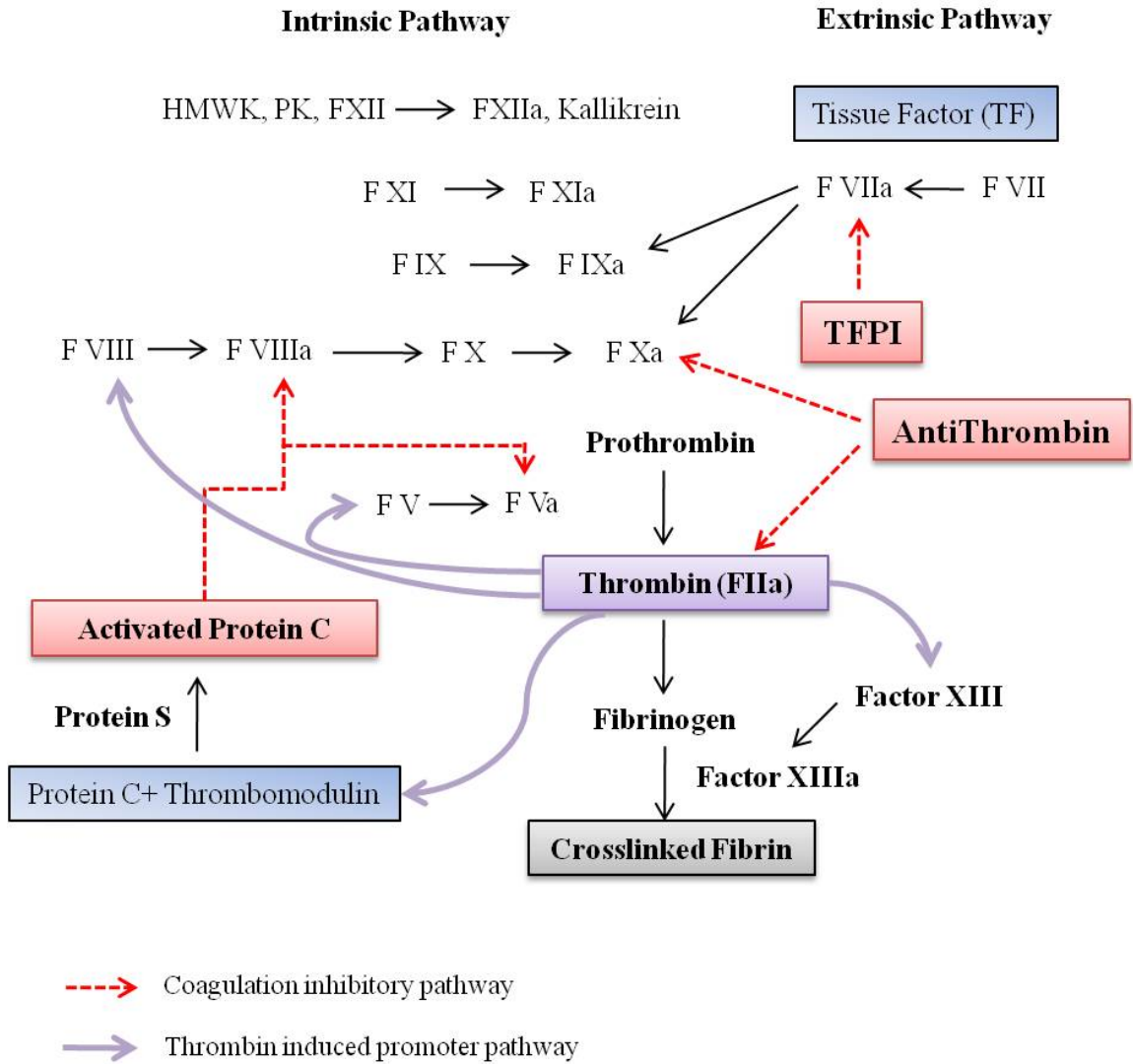


Figure 2.2- The coagulation cascade demonstrating the activation of coagulation factors and the anticoagulant factors.

ECs are positioned in the vascular system as a barrier between the blood and the extravascular tissue and play a major role during inflammatory processes. For instance, ECs play a key role when circulating leukocytes attempt to infiltrate into the extravascular tissue (Cines et al., 1998). The inflammatory response alters the normal resting condition of ECs and causes vessel dilation, increase in blood flow, and a localized recruitment of the leukocytes (Pofer & Cotran, 1990). At the site of EC damage or activation, leukocytes migrate into the extravascular tissue and promote further inflammatory responses to the formation of atherosclerotic plaque (Pofer & Cotran, 1990).

Leukocyte adhesion and migration begins by the accumulation of rolling leukocytes onto the EC surface, after which they get loosely bound to ECs by the initial interaction with selectin molecules (E and P selectin) (Muller, 2002), followed by more permanent interaction with adhesion molecules including ICAM-1 and VCAM-1 (Pofer & Cotran, 1990). Histamines and cytokines produced in the inflammation process cause an up-regulation of E-selectin and P-selectin expression on the EC surface (Kubes & Kanwar, 1994). Certain cytokines such as TNF- α and interleukins induce an elevated expression of these adhesion molecules. Once adhered, leukocytes undergo extravasation where they migrate into the smooth muscle cell layer by passing through the EC junctions (Figure 2.3 demonstrates EC and Leukocyte interaction) (Muller, 2002). The resting non-inflamed ECs suppress the transcription of the adhesion molecules (ICAM-1, VCAM-1). Thus, ECs in the normal resting state regulate the inflammatory response in active and passive ways and safeguard the vascular system from uncontrolled adhesion of leukocyte which could lead to inflammatory and thrombotic disorders (Cines et al., 1998). Here we monitored ICAM-1 expression as a means to quantify inflammation through the process described.

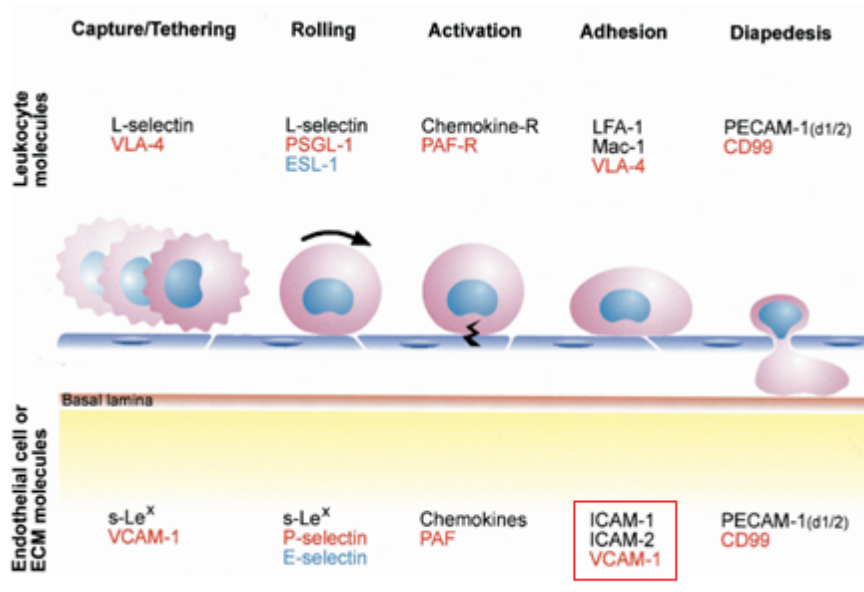


Figure 2.3- The sequential steps of leukocyte adhesion and migration controlled by the adhesion molecules on leukocyte and ECs. Modified from (Muller et al., 2002).

The regulation of blood flow and blood pressure by releasing mediators for vasomotor tone of the vascular smooth muscle cells (VSMCs) is also a major function of the ECs (Busse & Fleming, 2006). They are responsible for the secretion of vasodilators such as NO, prostacyclin (PGI₂) as well as vasoconstrictors, including endothelin (ET), angiotensin and platelet-activating factor (PAF) (Brandes et al., 2000). The productions of these vasomodulators by ECs are modulated by both chemical and mechanical stimuli such as shear stress on the blood vessel wall. By balancing the secretion of vasodilators and vasoconstrictors ECs actively take part in the regulation of blood vessel tone in the resistance vessels. Further, ECs communicate with VSMCs to achieve flow regulation through membrane gap junctions (Yeh, Dupont, Coppen, Rothery, & Severs, 1997). The gap junctions provide a stable mode of communication between two adjacent ECs, and serve to transmit and synchronize vasomotor signals and electrical impulses, transport metabolites, second messengers and ions (Sohl & Willecke, 2004). The junctions are formed by protein clusters of the Connexin family that connect the cytoplasmic compartments of two neighboring cells to facilitate direct exchange of signals and molecules (Dejana, Corada, & Lampugnani, 1995). The connexins that are expressed on the human ECs are mainly connexin-37, connexin-40 and connexin-43 (Sohl & Willecke, 2004) (see section 2.3.3). The couplings of ECs to the VSMCs via gap junctions play a major role in the regulation of EC migration and replication during angiogenesis.

Angiogenesis is the process where new blood vessels are formed from the pre-existing vessels by the proliferation of vascular ECs (Frank, Woodman, Park, & Lisanti, 2003). In an adult human this process is in existence during wound healing and tumor formation. Regulation of angiogenesis is another function of the ECs (Rothberg et al., 1992), which is partially regulated by the presence/activity of caveolin-1. Caveolin-1, a cholesterol binding scaffolding protein, expressed abundantly on the EC membrane is a negative regulator of angiogenic signal transduction (see section 2.3.3). The down-regulation of this protein caused by the angiogenic

growth factors may have an effect in the EC proliferation and subsequent angiogenesis (Frank et al., 2003). A healthy endothelium is therefore pivotal in the events such as angiogenesis, stable network formation and regulation of vasomotor tone.

2.3.2 Endothelial Cell Cytoskeleton Structure and Function

The function of ECs as a semipermeable membrane, at the blood-tissue barrier, is largely dependent upon the cellular organization within the cell itself. The cytoskeleton is the structural component of every eukaryotic cell and is made up of actin microfilaments, microtubules and intermediate filaments. The communication and interaction of these proteins provide a strong dynamic intercellular scaffold that organizes the integral membrane proteins, and modulates the shape of the cell in response to changes in the local environment (Dudek & Garcia, 2001).

Actin microfilaments represent approximately 5-15% of the total protein content of the ECs (Patterson & Lum, 2001) and possess a dynamic structure that can self-assemble as per cellular demand. This property of actin is governed by the polymerization and de-polymerization reaction of the globular G-actin components. The basic structural unit of actin cytoskeleton is made of actin component. The polymerization reaction involves the hydrolysis of ATP molecules. At normal condition a balance exists between the F and G actin components (Prasain & Stevens, 2009).

Based on the organization of F-actin structures, the actin cytoskeleton can be divided into 3 domains: the membrane skeleton, the cortical actin rim and the stress fibers. The cortical rim is made up of long F-actin bundles, whereas the other two consists of short F-actin filaments (De Matteis & Morrow, 2000). The membrane skeleton is positioned adjacent to the cellular membrane and has a thickness of a few nanometers. It is responsible for the membrane architecture and distensibility (Prasain & Stevens, 2009). The cortical rim is situated underneath the membrane skeleton and its structure is organized by the interaction of actin binding (spectrin,

α -actinin, frimbin), nucleating (cofilin, profilin) and severing (gesolin) proteins (Dudek & Garcia, 2001). The cortical rim determines the shape of the cell and provides for the cell to cell adhesion strength (Prasain & Stevens, 2009). The stress fibers take part in generating the tensile forces by the actin-myosin bundles and are responsible for cell motility (Hotulainen & Lappalainen, 2006). The sizes of the inter-cellular gaps are regulated by the contraction and relaxation of the stress fibers. The stress fibers are stretched throughout the cytoplasm and provide an inward tension force that balance the outward force generated by the cortical rim (De Matteis & Morrow, 2000) and conserves the shape of the cell.

Re-organization of the F-actin filaments from its cortical distribution to stress fibers is one of the principle components during EC inflammation and leukocyte transmigration. The inflammatory agonist such as thrombin and histamine reorganizes the cortical actin bundles into fibers that stretch throughout the entire cytoplasm. These fibers exert inward tensile force that leads to the contraction of cell borders and increment of the length of inter-cellular gaps and thereby increase the EC barrier permeability (Dudek & Garcia, 2001).

The actin cytoskeleton binds the ECs to the extra-cellular matrix (ECM) by the interactions between the ECM proteins (collagen, fibronectin, laminin, vitronectin and proteoglycans) and the transmembrane integrin receptors. This interaction provides a bidirectional signaling pathway between the cell and cell-matrix (Jockusch et al., 1995). The actin filaments also link the adhesive proteins complexes such as adherens junctions and tight junctions. Therefore actin filaments also have a role in the EC mechanical stability and can induce signal transduction pathways. Vascular endothelial cadherin (VE-cadherin) is the predominant adhesive protein in the adherens junction and functions to provide EC barrier stability. A down-regulation in VE-cadherin expression could increase the barrier permeability and leukocyte migration (Corada et al., 1999). Therefore, the adhesion between cell to cell and

cell to matrix is necessary to build signal transduction pathway and to maintain a proper EC blood-tissue barrier.

2.3.3 Membrane Associated Proteins Related to Diabetes Mellitus

The diabetic vasculature is known to promote various cardiovascular disease conditions by altering the functional activity of the vascular ECs. The presence of advanced glycation end products (AGEs) in the diabetic vasculature is believed to be one of the major factors behind the EC activation and dysfunction. AGEs have an adverse effect on the EC basal functions, such as EC thrombogenicity and inflammatory responses (as discussed previously). AGEs could also affect EC gap junction activity, permeability and EC angiogenic potential. The salient membrane proteins associated with the regulation of thrombosis and inflammation are namely tissue factor (TF), thrombomodulin (TM) and intercellular adhesion molecule (ICAM-1). Caveolin-1 and Connexin-43 are two of the surface proteins that modulate EC angiogenesis and cell-to-cell network formation via gap junctions. The effect of AGEs on these membrane associated proteins is crucial in the disease progression during diabetic conditions. These five proteins will be discussed in detail in the following sections.

2.3.3.a Intercellular Adhesion Molecule-1 (ICAM-1)

Intercellular adhesion molecule-1 (ICAM-1) is a transmembrane glycoprotein of immunoglobulin superfamily. ICAM-1 is made up of five distinct IgG like domains and a short cytoplasmic tail associated with multiple cytoskeletal linker proteins (Endres, Laufs, Merz, & Kaps, 1997). The main function of ICAM-1 is stable leukocyte adhesion and transendothelial migration during the inflammatory response. ICAM-1 serves as a binding site for leukocyte function associated antigen (LFA-1) (Yang et al., 2005; Rothlein, Dustin, Marlin, & Springer, 2011). ECs at a resting state express lower level of ICAM-1 compared to the activated state. Proinflammatory cytokines (such as TNF- α , IL-1, Interferon- γ) (Poerber et al., 1986) and shear

stress mediated EC activation, cause an up-regulation of ICAM-1 at the EC surface, and induce the leukocyte adhesion and transmigration (Nagel, Resnick, Atkinson, Dewey, Jr., & Gimbrone, Jr., 1994).

2.3.3.b Tissue Factor (TF)

Tissue factor (TF) is a membrane bound glycoprotein that is present in the subendothelial space and within the EC cytoplasm. Each tissue factor molecule consists of three domains; an extracellular domain, a single membrane spanning region and small cytoplasmic domain (Muller, Ultsch, Kelley, & de Vos, 1994). The main function of TF is to initiate and maintain the blood hemostasis during vessel injury by inducing the coagulation cascades' extrinsic pathway. ECs release soluble TF and express surface TF when activated or injured. TF initiates the extrinsic pathway of the coagulation cascade but also facilitates the intrinsic pathway (Figure 2.2). The expression of TF is modulated by the amount of tissue factor pathway inhibitor (TFPI) released by the ECs (Grabowski, Zuckerman, & Nemerson, 1993). Studies have reported that the expression of TF and TFPI are governed by the hemodynamic shear stress on the EC surface (Houston et al., 1999).

2.3.3.c Thrombomodulin (TM)

Thrombomodulin, an integral membrane glycoprotein, is predominantly produced by the vascular endothelial cells and plays an inhibitory role in the coagulation cascade. There are approximately 30,000-100,000 TM molecules present on each EC surface. Each molecule is made up of an extracellular, membrane spanning, and cytoplasmic domains (Esmon, 1993). It is co-factor of thrombin and forms a 1:1 stoichiometric complex that triggers the activation of protein C. Thrombin activates protein C and this activation is amplified by 2.3 orders of magnitude in the presence of TM. The activated protein C is an effective anticoagulant, which in the presence of protein S suppress thrombin generation (Esmon, Esmon, & Harris, 1982). The

expression of TM on the EC membrane is governed by the presence of cytokines and alterations in fluid shear stress. Cytokines such as TNF- α causes the down-regulation of TM on the EC membrane by suppressing its transcription and translation (Moore, Esmon, & Esmon, 1989).

2.3.3.d Caveolin-1

Caveolin-1 is a membrane bound protein that coats the cytoplasmic surface of a specialized micro-domain on ECs known as the caveolae (Minshall, Sessa, Stan, Anderson, & Malik, 2003a). Caveolae is a flask shaped membranous invagination of 50-100 nanometer diameter and is enriched in cholesterol and glycosphingolipid (Palade & Bruns, 1968). The lipid aggregates of the caveolae surface are stabilized by two cholesterol binding scaffolding proteins caveolin-1 and caveolin-2 (Liu & Schnitzer, 1999). Caveolin-1 (cav-1) binds and transports cholesterol from the endoplasmic reticulum to the plasma membrane to regulate the lipid content of the ECs membrane (Minshall, Sessa, Stan, Anderson, & Malik, 2003b).

Caveolin-1 is abundantly expressed on ECs and is responsible for the regulation of transcytosis, membrane permeability, vascular tone and angiogenesis (Minshall et al., 2003a). During angiogenesis cav-1 plays a major role in the modulation of eNOS activity for vascular remodeling and wound healing (Rudic et al., 1998). Studies have reported that cav-1 inhibits the EC nitric oxide (NO) syntheses eNOS. eNOS is seen to associates with cav-1 and remains in an inactive state where it inhibits the release of NO (Bucci et al., 2000). Studies conducted to relate eNOS activity to NO release have shown that over expression of cav-1 decrease eNOS dependent NO synthesis, indicating that eNOS bound to cav-1 loses its enzymatic function (Bucci et al., 2000). A study conducted by Brouet et al. documented that caviling scaffolding domain (CSD) can block the NO dependent angiogenesis *in-vitro* (Brouet et al., 2005). Grattan et al. also reported similar results to show that CSD peptides block NO mediated vascular permeability which is known as an early event in angiogenesis (Gratton et al., 2003). Cav-1 expression in also

affected by the presence of AGE in a diabetic vasculature. Studies have reported that AGE promotes the localization of cav-1 and AGE receptors (RAGE) in the caveolae in a diabetic endothelium (Stitt, Burke, Chen, McMullen, & Vlassara, 2000). Bucci et al. reported that hyperglycemic condition in a diabetic mouse lead to an increase in the expression in cav-1 (Bucci et al., 2000). Therefore diabetic vasculature tends to inhibit angiogenesis by upregulating eNOS inhibiting protein cav-1.

2.3.3.e Connexin 43 (Cx-43)

Connexins are component proteins of gap junction channels that link the cytoplasmic compartments (Yeh et al., 1997). The junctions are formed by the head to head alignment of two hemi channeled connexons which are composed of six connexin (Cx) molecules (Van et al., 1997a). Human ECs express Cx-43, Cx-40 and Cx-37, among which Cx-43 is by far the predominant connexin expressed in cultured ECs. Its function is to form a stable network among the neighboring ECs and/or SMCs by synchronizing the propagation of electrical and chemical signals and transporting metabolites. Several reports have shown a down-regulation of Cx-43 during EC dysfunction (Van et al., 1997b). EC dysfunction caused by diabetes mellitus, hypertension and atherogenic factors could affect the Cx-43 expression. Studies have shown that pro-inflammatory cytokine TNF- α down-regulates Cx-43 in HUVECs and thereby decreases gap junction activity (van Rijen, van Kempen, Postma, & Jongasma, 1998). Animal studies have reported that induced diabetic condition on ApoE mouse down-regulates Cx-43 expression and gap junction activity (Hou et al., 2008). The presence of advanced glycation end products is responsible for many of the EC dysfunctions in the diabetic vasculature. A number of studies have been conducted and most of the results concluded that hyperglycemic conditions and presence of AGEs downregulates Cx-43 expression and reduces gap junction intercellular activity.

2.4 The Effect of shear stress in EC function

Endothelial cells (ECs) located within the innermost layer of the blood vessel and are constantly subjected to hemodynamic forces of varying magnitude, frequency and direction. These forces are mainly pressure forces, acting perpendicular to the vessel wall or cyclic strain and shear stress, acting longitudinally to the vessel wall. This shear stress creates a frictional force on the surface on the endothelium (Benson, Nerem, & Pedley, 1980) known as the wall shear stress. Of all the forces, the hemodynamic shear stress is of particular importance as it stimulates various functional pathways, cell metabolism and alters cell morphology. The range of physiological shear stress in the large arteries (>4mm diameter) is 10-40 dynes/cm², which could be higher or lower during pathological conditions (Davies, Mundel, & Barbee, 1995a). The nature and magnitude of the wall shear stress is a function of the blood flow pattern throughout the vasculature. In the linear locations (without branch formations or bifurcations) the flow is majorly laminar and therefore imposes a laminar pulsatile shear stress (cardiac cycle dependent) that yields a net positive shear stress on the endothelium (Traub & Berk, 1998). Studies have shown that a constant positive shear stress usually generates similar EC responses compared to a pulsatile shear stress with varying magnitudes (Hsieh, Li, & Frangos, 1993; Helmlinger, Berk, & Nerem, 1995). In unique locations of the vasculature such as curvatures and bifurcations, the laminar flow pattern is disrupted, which creates flow separation and recirculation zones. A constant laminar shear stress is regarded as atheroprotective, as it induces the ECs to release factors that inhibit coagulation, leukocyte migration and smooth muscle proliferation. It also increase the production of vasodilators such as prostacyclin, while suppressing the release of vasoconstrictors, inflammatory mediators and adhesion molecules (Malek, Alper, & Izumo, 1999). Distributed oscillatory shear stresses (in flow separation and recirculation zones) enhance the atherogenic factors (Malek, Izumo, & Alper, 1999). Therefore, laminar blood flow is essential in order to maintain a healthy endothelium function.

In the case of laminar blood flow, the magnitude of the shear stress is greatest at the vessel wall and is a function of the fluid (blood) velocity (v), viscosity (μ), and the radius of the fluid conducting vessel (r) (equation 2.1). Although blood constitutes of blood cells and proteins, it behaves as a continuous single phase fluid in the large arteries and can be assumed as a Newtonian fluid. The magnitude of the shear stress can be estimated using the Hagen Poiseuille formulation (equation 2.2) which assumes a constant μ , v , r at the cross section of interest.

$$\tau_{\omega} = \mu \frac{dv}{dr} = \mu \dot{\gamma} \quad \text{Equation 2.1}$$

$$\tau_{\omega} = \frac{4\mu Q}{\pi r^3} \quad \text{Equation 2.2}$$

Here, τ_{ω} , $\dot{\gamma}$ and Q represent the wall shear stress, shear rate and fluid flow rate respectively.

The major function of ECs is to regulate coagulation, initiate angiogenesis, promote/inhibit inflammatory response, maintain the vascular tone, and form a communicative network among the adjacent tissues. Shear stress plays a major role in modulating the expression of the functional molecules responsible for healthy endothelium function. ICAM-1, TF and TM are the major surface proteins that mediate the inflammatory response and EC thrombogenic activity. Caveolin-1, a caveolae protein on EC surface, takes part in regulating angiogenesis. The gap junction protein Cx-43 builds the communicative network among the surrounding ECs. The effect of shear stress on the expression of these proteins will be further discussed in this section.

ICAM-1 is a transmembrane glycoprotein that plays a major role in leukocyte adhesion and migration during inflammation (Yang et al., 2005). A number of studies have been conducted to investigate the effect of shear stress on the EC ICAM-1 expression. Nagel et al. conducted a study that showed an up-regulation of ICAM-1 expression in a time dependent manner where ECs were exposed to constant shear stress (10 dynes/cm²) for 48 hours. Another study by Tsuboi

et al. reported that HUVECs exposed to constant shear (15 dynes/cm²) for 4 hours has an ICAM-1 expression that was 1.27 times higher compared to the no shear control (Tsuboi, Ando, Korenaga, Takada, & Kamiya, 1995). In a previous study by Yin et al. it was reported that exposure to high pulsatile shear stress (1 dynes/cm²- 6 dynes/cm²) increased ICAM-1 expression on BMECs (Yin et al., 2011). All these studies indicated that shear stress cause an upregulation of the EC surface expression of ICAM-1. As previously mentioned in section 2.2, the diabetic vasculature containing AGEs is also partially responsible for inducing an increase in ICAM-1 expression. How shear stress would modulate this protein expression in a diabetic condition in the presence of AGEs is yet unclear and leaves further scope of research. The protein expression of tissue factor (TF) and thrombomodulin (TM) in ECs is also altered when exposed to shear stress. Numerous studies have reported an up-regulation of thrombogenic TF and a down-regulation of anti-thrombogenic TM under the influence of constant laminar shear stress. In a study, Houston et al. reported that ECs exposed to laminar shear stress (15 dynes/cm²) incurred an increase in TF expression in a time dependent fashion (Houston et al., 1999). Similar results were obtained by Lin, M. C. et al. where they saw that, ECs exposed to a constant shear stress (12 dynes/cm²) resulted in an increase of coagulation factor Xa generation (under normal hemostasis Xa is generated from the TF:VIIa complex), indicating that shear stress caused an upregulation in TF procoagulant activity (Lin et al., 1997). Shear stress also plays a modulating role in the surface expression of TM which inhibits the activities of TF. In a study by Takada et al., HUVECs were exposed to low (1.5 dynes/cm²) and high (15 dynes/cm²) constant shear stress (Takada et al., 1994). In both cases there was an increase in TM expression when compared to control, in both a time and magnitude dependent manner. However in a study conducted by Malek et al., it was reported that, there was a significant down-regulation of TM expression when ECs were exposed to 15 dynes/cm² and elevated 36 dynes/cm² (Malek, Jackman, Rosenberg, & Izumo, 1994a), which contradicts some of the preliminary work. The results from these experiments indicate that

shear stress actively modulates the TM protein expression, under various shear stresses and play a major role in coagulation and thrombus formation.

The function of cav-1, the major surface protein on the glycosphingolipid rich caveolae, is affected by hemodynamic shear stress. Cav-1 impairs the NO dependent angiogenesis, by forming a bond with EC nitric oxide synthase (eNOS) rendering it inactive. A study conducted by Rizzo et al. reported that shear stress alters the tension bearing, coiled spring structure of caveolae (Sargiacomo et al., 1995). The pressure induced alteration of the cav-1 morphology may cause eNOS to be released from the cav-1 clamp, permitting eNOS activity and facilitating NO synthesis (Rizzo, McIntosh, Oh, & Schnitzer, 1998). These studies indicate that shear stress promotes angiogenesis, which is the opposing effect that AGEs incur on the cav-1 mediated angiogenesis (section 2.3.3.d) and further research is required to investigate the effect of shear stress in AGE mediated cav-1 expression.

The cell-to-cell communication and signal transduction via gap junction proteins such as Cx-43 is essential in maintaining a healthy endothelium. Studies conducted to demonstrate shear stress mediated Cx-43 activity have reported that, shear stress has an up-regulating effect in the localization and expression of Cx-43. Kawk et al. reported an up-regulation of Cx-43 in the presence of oscillatory shear stress (Kwak, Silacci, Stergiopoulos, Hayoz, & Meda, 2005). In a study conducted by DePaola et al. it was demonstrated that a controlled distributed flow *in vitro* regulates time and location dependent Cx-43 expression (DePaola et al., 1999). However not many studies have been conducted to investigate the effect of constant shear stress. Opposing the effect of shear, AGEs induce a down-regulating effect on Cx-43 expression (section 2.3.3.e). The combined effect of AGEs and shear stress is yet unclear.

The actin cytoskeleton of ECs undergoes profound morphological changes under the influence of blood flow induced shear stress. *In vivo* and *in vitro* studies have demonstrated that,

under steady flow conditions, ECs elongate in shape, reorganize the structure of F-actin fibers, align the cell longitudinal axis with the flow direction with a simultaneous increase of cytoskeleton stiffness. An *in vitro* study by Theret et al., on cultured bovine aortic endothelial cells (BAECs), documented a 10 fold increase in cytoskeleton stiffness of sheared cells, in comparison with its static control counterparts (Theret, Levesque, Sato, Nerem, & Wheeler, 1988). Levesque et al., in a study on cultured BAECs reported that, cells exposed to shear stress (30 dynes/cm²) for 24 hours, lose their static “cobblestone” shaped morphology and alter to an elongated spindle like structure aligned to the flow direction (Levesque, Liepsch, Moravec, & Nerem, 1986). It was also demonstrated that the degree of alignment is a function of the level of shear stress and duration of exposure. F-actin microfilaments are the major structural component of the EC cytoskeleton, and are present in bundle like structures at the cell periphery (cortical actin rim, section 2.3.2) and in long filament like stress fibers at the cell centers. In an *in vivo* study by Kim et al., the documented results showed, at locations of elevated shear stress, there was a disruption of the F-actin bundles in the cortical rim and formation of new elongated stress fibers at the center of the cell (Kim, Langille, Wong, & Gotlieb, 1989). A similar study by Langille et al., demonstrated the time and shear dependent formation of the stress fibers and their alignment to the shear direction (Langille, Graham, Kim, & Gotlieb, 1991). Disintegration of the cortical rim actin bundles have also been reported in cell culture models exposed to high glucose levels (Salameh, Zinn, & Dhein, 1997) imitating diabetic vascular condition. This disruption could result in an increase in cell permeability, enhance cellular adhesion properties and facilitate cell proliferation (Langille et al., 1991). Therefore high shear stress in diabetic vasculature could increase the risk factors in CVDs.

CHAPTER III

MATERIALS AND METHODS

3.1 Synthesis of Advanced Glycation End Products

Bovine serum albumin was glycosylated as per the following procedure. 50 mg/mL albumin ($\geq 98\%$ pure, Sigma-Aldrich, St. Louis, MO, USA, all materials purchased from Sigma-Aldrich unless otherwise noted) was incubated with 250 mM D-(+)-glucose, 5mM phenylmethylsulfonyl-fluoride (Pierce, Rockford, IL, USA), 2 mg/mL aprotinin, 0.5 mg/mL leupeptin, 100 $\mu\text{g}/\text{mL}$ penicillin and 100 U/mL streptomycin in phosphate buffered saline (PBS, pH 7.4) at 37°C for 8 weeks. Control albumin samples were incubated as above without the addition of glucose. After 2, 6 and 8 weeks, 12 mL glycosylated and control samples were dialyzed extensively against 200 mL of PBS for 2 hours. Every 2 hours the PBS was exchanged with fresh PBS for a total of 4 exchanges. After dialysis, the albumin concentration and the glycation extent was quantified using mass spectrophotometry. Molecular mass of glycosylated and non glycosylated control samples were measured using spectrophotometer absorbance at 280 nm. The difference of molecular mass between the samples was attributed to the association of glucose molecules to albumin. The number of glucose molecules was quantified from this mass difference. After 2 weeks of incubation albumin was glycosylated with an average 5 of glucose molecules. After 6 and 8 weeks the average numbers of glucose molecules were increased to 26 and 31 respectively. The

glycated samples (AGE) and the control samples (BSA) were aliquoted and frozen at -4°C until use.

3.2 Endothelial Cell Culture:

3.2.1 Cell Culture Conditions

Human umbilical vein endothelial cells (HUVECs) were purchased from ScienCell Research Laboratories (Carlsbad, California, USA) as passage one and used for experiments from passage two through seven. Upon arrival of the HUVECs, the cells were seeded onto a T-75 culture flask. The flask was coated with 2% gelatin for at least 15 minutes prior to seeding. The cells were maintained in endothelial cell growth media (ScienCell) supplemented with 5% fetal bovine serum, 1X growth supplement, 10 U/mL penicillin and 10 µg/mL streptomycin (all purchased from ScienCell). The cells were maintained in the culture flask at 37°C and in the presence of 5% CO₂. Cell media was replaced with fresh media every other day. The cells were fed by tilting the flask sideways and aspirating the old media off. This was followed by 2 PBS washes and then 15 mL of fresh warmed media was added. The cell culture and feeding took place inside a laminar flow hood with sterile environment and laminar air flow. The conditions of the cells were examined prior to each feeding using transmitted light microscope, to verify that the cells had normal endothelial cell morphology.

3.2.2 Passage of Endothelial Cells

Confluent HUVECs were passed to either T-75 flasks, 24well plates or 6 well plates. The cells were fed one day prior to passing. The old media was aspirated off and 1.5mL of trypsin-EDTA (ethylene-diamine-tetra-acetic-acid) was added immediately to detach the cells from the culture flask. Using transmitted light microscope the retraction process was observed. This process was stopped when the majority of endothelial cells (90-95%) detached from the culture flask. 13.5mL of media (warmed to 37°C) was added to neutralize the trypsin which brings the

total volume to 15 mL. 5 mL (x3) was removed and added to new T-75 culture flasks coated with 2% gelatin (for at least 15 minutes). This makes a 1:3 passage by area. The cell media was exchanged the day following the passage, and then put back on to the normal feeding schedule. At this point the cell passage number has increased; i.e. a passage one flask has now become passage 2 flask.

3.3 Experimental Conditions

3.3.1 Static Conditions

At the beginning of an experiment one confluent T-75 flask was trypsinized and passed onto 6 or 24 well plates. The wells were coated with 2% gelatin (for at least 15 minutes) prior to the passage. For some experiments glass coverslips prior to gelatin coating were added. 80 μ L and 20 μ L of glycated albumin (AGE) and non-glycated albumin (BSA) were added to each well in a 6 and 24 well plate and the final volume was brought to 2 mL and 0.5 mL (media plus cells after trypsin was neutralized) respectively. The final concentration of AGE and BSA in culture conditions were 2 mg/mL. The glycated serum albumins are termed 2, 6 and 8 week AGE and non-glycated albumin are termed 2, 6 and 8 week BSA. The cells were incubated with AGE and BSA for 3 or 5 days which were termed as “Early” or “Late” conditions respectively. The 6 or 24 well plates were maintained at 37°C in the presence of 5% CO₂ throughout the culture duration. During the feeding cycle fresh AGE and BSA was added along with the media (all warmed up to 37°C).

3.3.2 Dynamic Conditions

3.3.2.a Hemodynamic Cell Shearing Device

A hemodynamic cell shearing device was used to investigate the response of ECs to various shear stress conditions. The shearing device was developed using the principles of a

viscometer. The shearing device was custom made for 6 well plates in this study. The cone was fabricated with ultra-high molecular weight polyethylene (UHMWP) and was coupled with a precise micro-stepper motor and control system (Figure 3.1) (Yin & Rubenstein, 2009). The micro-stepper motor provides the ability to uniformly and accurately produce the desired shear stress on the confluent EC monolayers in 6 well plates. This device consists of four such motors and can be used to apply shear stress to 4 wells at a time with up to 2 different shear waveforms. The micro-stepper motors were air cooled during shearing in order to avoid overheating.

The magnitude of the shear stress on the EC monolayer depends on the cone angle and the angular rotational speed of the cone, which is coupled to the micro-stepper motor. The cone angle and the radius used in this study are 0.5° and 1.733 cm. The stepper motor is driven by a control system interfaced to a computer and controlled by a BASIC program. The required shear stress values were first converted to angular velocity which was then programmed to the stepper motors to drive the cone.

3.3.2.b Shearing Experiment

Confluent HUVECs were treated with 0.6 mL of fresh media (warmed to 37°C) and placed on an isothermal plate to maintain the cells at a temperature of 37°C throughout the duration of shearing. In healthy blood vessels, EC are exposed to a normal average shear of approximately 10 dynes/cm². To observe responses of the ECs when subjected to a low (4 dynes/cm²), medium (10 dynes/cm²) or high shear (40 dynes/cm²) stress of constant shear stress was applied to the cells for the duration of one hour. For each experiment 2, 6-well plates were sheared. Each well of the 6-well plates had ECs incubated with a different condition (BSA or AGE). One well on each six well plate was always kept as a control. The control well contained ECs that were not exposed to any AGE or BSA. The basic program used in the cone and plate controller for replicating this constant shear is attached in Appendix A.

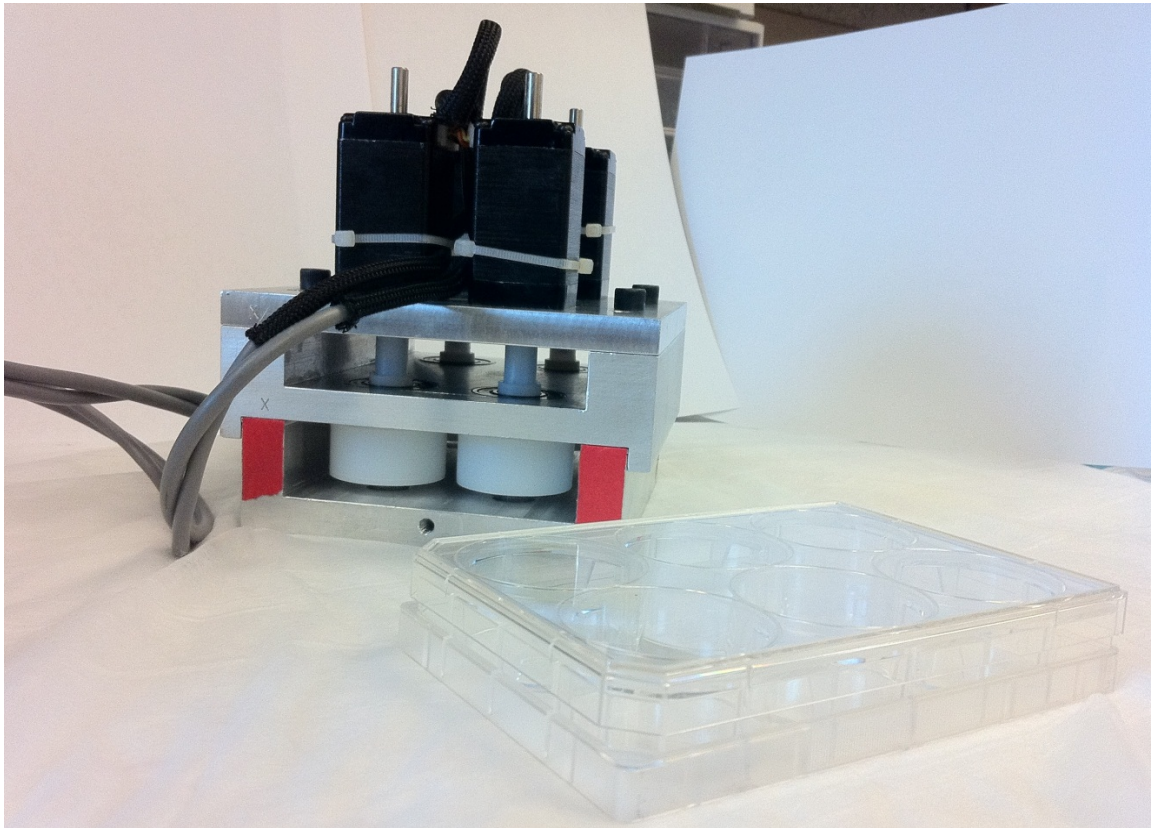


Figure 3.1 – The modified cone and plate hemodynamic cell shearing device. Showing the arrangement of cones attached to motors and a 6-well plate used in this study.

3.4 MTT Assay

A standard MTT assay was used to quantify the metabolic activity of endothelial cells which were exposed to different glycation extents and subjected to low, medium and high shear stress. For experiments, ECs were incubated with 2, 6 and 8 weeks of AGE and BSA for different durations (3 or 5 days) and subjected to various shear stress for the duration of 60 minutes.

A standard MTT assay was carried out by incubating the cells with MTT reagent (Sigma) for up to three hours at 37°C. The key component of MTT reagent is 3-[4, 5-dimethylthiazol-2-yl]-2,5-diphenyl tetrazolium bromide. The formazan crystals formed due to the activity of mitochondrial dehydrogenases of the living cells were solubilized using a solution consisting 10% Triton-X and 0.1 N HCl in anhydrous isopropanol. The cells were mixed gently and the absorbance at 630nm was measured using an optical microplate reader (Beckman Coulter, DTX 880). All MTT data were normalized by control sample data.

3.5 Live/Dead Cell Cytotoxic Assay

3.5.1 Immunofluorescence Staining and Microscopy

The viability of endothelial cells under the various glycation conditions was determined using a live/dead cytotoxic assay (2 μ M calcein and 4 μ M ethidium in PBS). This assay is used to determine the cell viability, density and morphology of the cultured ECs. Calcein can be transported through the cell membrane of live cells; while ethidium stains the DNA of compromised cells (ethidium can only enter cells that have holes in the cell membrane). Thus the calcein positive cells were marked as live cells, while the ethidium positive were marked as dead. To stain the ECs, the culture media was aspirated from the well and the cells were washed with PBS (at 37°C). The glass coverslip (with monolayer of EC) was carefully removed from the well and the bottom was dried with lens paper. 2 drops (~100 μ L) of calcein and ethidium dye was added to the coverslips and incubated for 15 minutes before imaging. During the incubation

period the cells were maintained at 37°C. A Coolsnap Fast Cooled (ES2) digital camera interfacing with NIS Elements Software was used with 10X (Nikon, Plan Fluor DL, N.A. 0.3) or 20X (Nikon, Plan Fluor ELWD, N.A. 0.45) objectives to image the ECs. For each well 3 random locations were chosen using transmitted light at 10X magnification. For each location 3 images were documented (1 transmitted light, 1 fluorescent image with green excitation and 1 fluorescent image with blue excitation). The images were obtained within 15 minutes after incubating with the dyes, after which time live cells will start to uptake ethidium and the dye will start to photobleach.

3.5.2 Image Analysis

3.5.2.a Cell Viability:

Cell viability was determined from the digital images of calcein and ethidium positive cells. From each image the total number of calcein positive (live) and ethidium positive (dead) cells was counted manually. The viability was defined as the ratio of total number of live cells (calcein positive) to the total number of cells per image (calcein or ethidium positive).

3.5.2.b Cell Density:

Cell density was determined from the digital images of the calcein and ethidium positive cells. The cell density was defined as total number of calcein positive (live) cells divided by the image area. The image area was calibrated and documented for each objective and the camera combination. Cell density provides a relative measurement of cell proliferation. Cell density was normalized by the seeding density for each experiment.

3.5.2.c Cell Morphology

The morphology of live cells was determined using a customized MATLAB program developed by Dr. Rubenstein (Rubenstein et al., 2007). The program identifies a cell at a

particular location, detects the cell boundary and calculates the area of the cell based on the cell perimeter. The images were manually thresholded (converted to 2 channel 8bit black and white) to ensure good contrast and to enable a better edge detection. The cells in the images were identified by manually selecting the long axis and the short axis of individual cells. The cell area was approximated for each cell using Boole's rule for numerical integration. This approximation uses the identified perimeter of each cell as the boundary. Cells were further classified as elongated, if the short axis is less than 80% of the long axis or circular if the short axis is greater than or equal to 80% of the long axis, for data analysis.

3.6 Endothelial Cell Connexin-43 and Caveolin-I Expression

3.6.1 Immunofluorescence Staining and Microscopy

The surface expression and the localization of connexin-43 and caveolin-1 under both static and dynamic conditions were quantified by immunofluorescence microscopy. ECs were washed (2X) with PBS (pH-7.4, warmed to 37°C) and fixed with 1.5% glutaraldehyde (300 µL per well) for 15mins at 37° C. After washing (2X with PBS), gluteraldehyde was neutralized and non-specific binding was blocked with 100 mM glycine – 0.1% BSA (1 mL per well for 30mins, 37°C). The cells were again washed (2X) with PBS-0.1% BSA and incubated with 0.6 µg/mL rabbit anti-human connexin-43 (300 µL per well, Abcam, Cambridge, MA, USA) and 2 µg/mL murine anti-human caveolin-1 (300 µL per well Invitrogen, Carlsbad, CA, USA) for 60 minutes in at 37°C. The cells were washed (2X with PBS-0.1% BSA) and then incubated for 60 minutes with FITC conjugated goat anti rabbit secondary antibody (5 µg/mL) and goat anti mouse Cy5 secondary antibody (5 µg/mL) to detect connexin-43 and caveolin-1 expression.

A Coolsnap Fast Cooled (ES2) digital camera interfacing with NIS Elements Software using 10X (Nikon, Plan Fluor DL, N.A. 0.3) or 20X (Nikon, Plan Fluor ELWD, N.A. 0.45) objectives was used to image the stained ECs. For each well 5 random locations were chosen

using transmitted light at 20X magnification. For each location 3 images were documented (1 transmitted light, 1 fluorescent image with green excitation and 1 fluorescent image with blue excitation).

3.6.2 Image Analysis

3.6.2.a Quantification of Connexin-43 and Caveolin-I Intensity

The surface connexin-43 and caveolin-1 intensity was measured using a method customized in Rubenstein Lab. The images were split into red-green-blue channels. The intensity of each channel was measured using a custom written MATLAB program. The green channel intensity was reported as the surface intensity of connexin-43 and the red channel intensity was reported as the caveolin-1 intensity. The intensity of the individual channels were quantified and normalized to control (no glycation). Figure 3.2 (A) and (B) shows sample data for connexin-43 and caveolin-1 intensity. The brighter red in Figure (A) and the green spots in Figure (B) mark connexin-43 and caveolin-1 respectively.

3.6.2.b Quantification of Connexin-43 and Caveolin-1 Localization

The localization of connexin-43 and caveolin-1 was measured using a method customized in Rubenstein Lab. The paired connexin-43 (green image) and caveolin-1 (red image) were merged together by an image editing software (Adobe Photoshop CS5). The discrete clusters were then manually counted to quantify the localized connexin-43 and caveolin-1 expression, and then normalized to the control (no glycation). Figure 3.2 (C) shows sample data for connexin-43 and caveolin-1 localization and are yellow in color when the red and green images were merged.

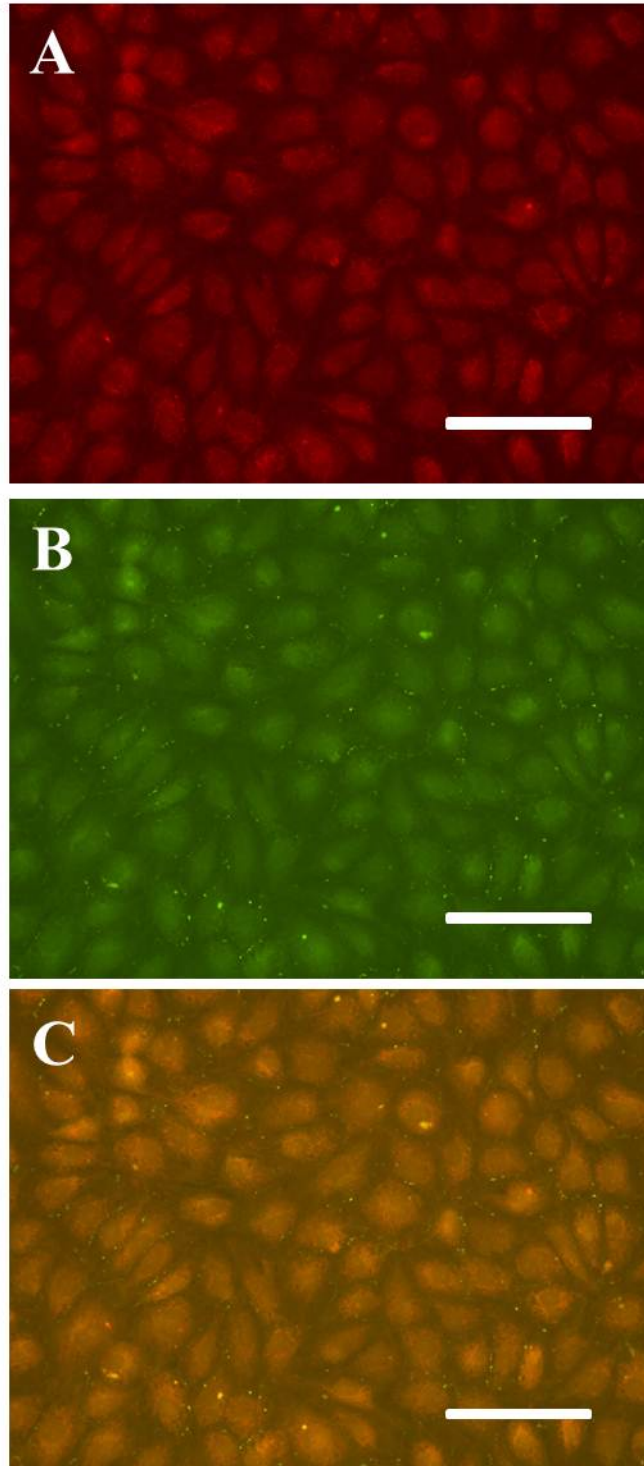


Figure 3.2 – Digital images of endothelial cell connexin-43 (A) and caveolin-1 (B) expression. Merged image (C) show where these proteins were localized. All scale bars represent 100 μ m.

3.7 Endothelial Cell Actin Structure and Alignment

3.7.1 Immunofluorescence Staining and Microscopy

Immunofluorescence microscopy was used to quantify the changes in cytoskeleton actin structure, altered alignment of the actin fibers and the inter-cellular connectivity when ECs were exposed to shear. After applying shear stress to the ECs, the cells were washed (2X) with PBS (pH-7.4, warmed to 37°C). The cells were then fixed with 1.5% glutaraldehyde (300 μ L per well) for 15mins at 37° C. After washing (2X with PBS), glutaraldehyde was neutralized and non-specific binding was blocked with 100mM glycine – 0.1% BSA (1mL per well for 30mins, 37°C). To stain the plasma membrane the cells were incubated with wheat germ agglutinin (WGA) at a concentration of 5 μ g/mL for 10 minutes, in the dark at room temperature followed by a wash (2X with PBS). For the purpose of permeabilizing, the cells were incubated with 0.2% triton-X for 5 minutes, in dark at room temperature which was followed by a wash (2X with PBS). In order to stain the actin fibers the cells were incubated with 5 U/mL phalloidin (Ph) for 20 minutes in dark at room temperature. After this incubation the cells were washed (2X with PBS). To stain the nucleus the cells were incubated with 300 nM DAPI for 5 minutes in dark at room temperature. After this incubation the cells were washed (2X with PBS) and imaged.

A Coolsnap Fast Cooled (ES2) digital camera interfacing with NIS Elements Software using 10X (Nikon, Plan Fluor DL, N.A. 0.3) or 20X (Nikon, Plan Fluor ELWD, N.A. 0.45) objectives were used to image the ECs. In each well 5 random locations were chosen using transmitted light at 20X magnification. For each location 4 images were documented. One image with transmitted light, first fluorescent image with green excitation (red image, the plasma membrane), second fluorescent image with blue excitation (green image, the actin fibers) and the third fluorescent image (blue image with UV excitation, the nucleus).

3.7.2 Image Analysis

3.7.2.a Actin Fiber Structure

Actin fiber structure was quantified to determine the percentage of the actin fibrous structure that is intact after the application of the different shear stresses under the varying glycosylated culture conditions. The percent actin structure was defined as the number of cells that have preserved the fibrous structure of actin after exposure to shear. It is quantified by dividing the total number of fibrous cells by the total number of cells per image. The structure is examined and counted manually. Figure 3.3 shows sample data for actin structure.

3.7.2.b Actin Fiber Alignment

Actin fiber alignment was quantified to determine the combined effect of varying shear stress and glycation on altering the EC alignment towards what we expect to be, the shear direction. The percentage of alignment is determined by dividing the number of ECs that were aligned to the shear directions (in a single direction) by the total number of ECs in the image. The alignment was analyzed and counted manually. Figure 3.4 shows the sample data for actin alignment.

3.7.2.c Inter-Cellular Connectivity

The inter-cellular connectivity of the actin fibers were determined to observe the network formation of actin fibers under varying glycosylated culture conditions and the application of shear stress. Based on percentage of connectivity, a rating scale of 0-5 was set with 0 being no network formation among the adjacent cells and 5 being 80-100% cells forming actin fiber networks among themselves. EC images were manually analyzed and appropriate rating was awarded. Figure 3.5 shows the sample data for inter-cellular connectivity.

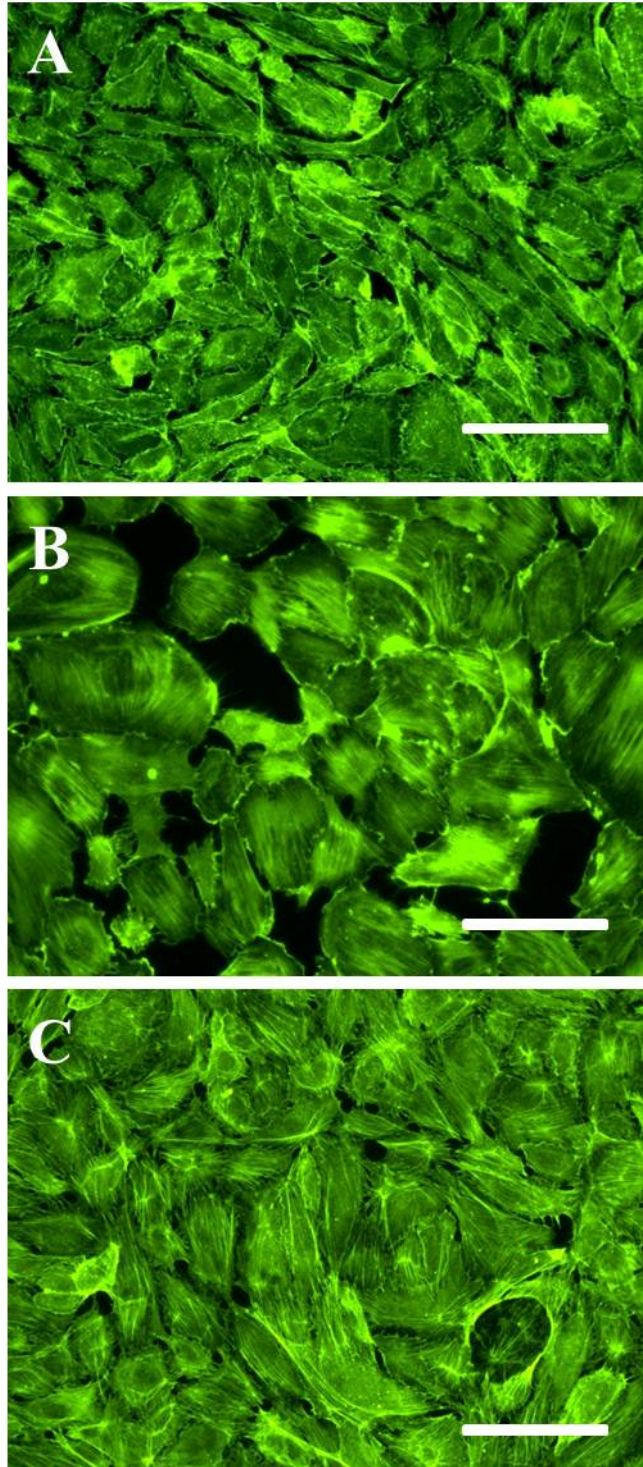


Figure 3.3- The actin structure of the sheared endothelial cells. Figure A,B,C approximates 0%, 50% and 100% fibrous cells respectively. All scale bars represent 100 μ m.

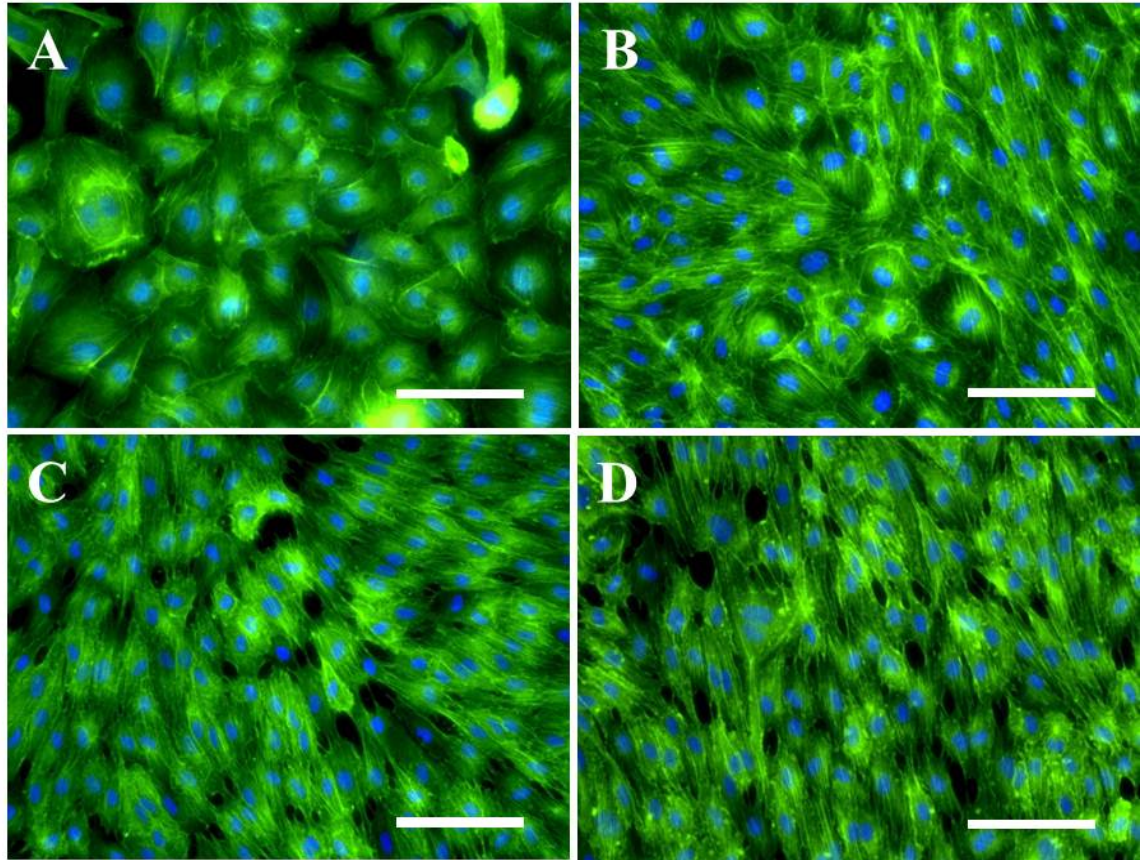


Figure 3.4- The alignment of endothelial cells in a shear direction. Figure A, B, C, D show approximately 25%, 50%, 75% and 100% cells aligned in the shear direction respectively. All scale bars represent 100 μ m.

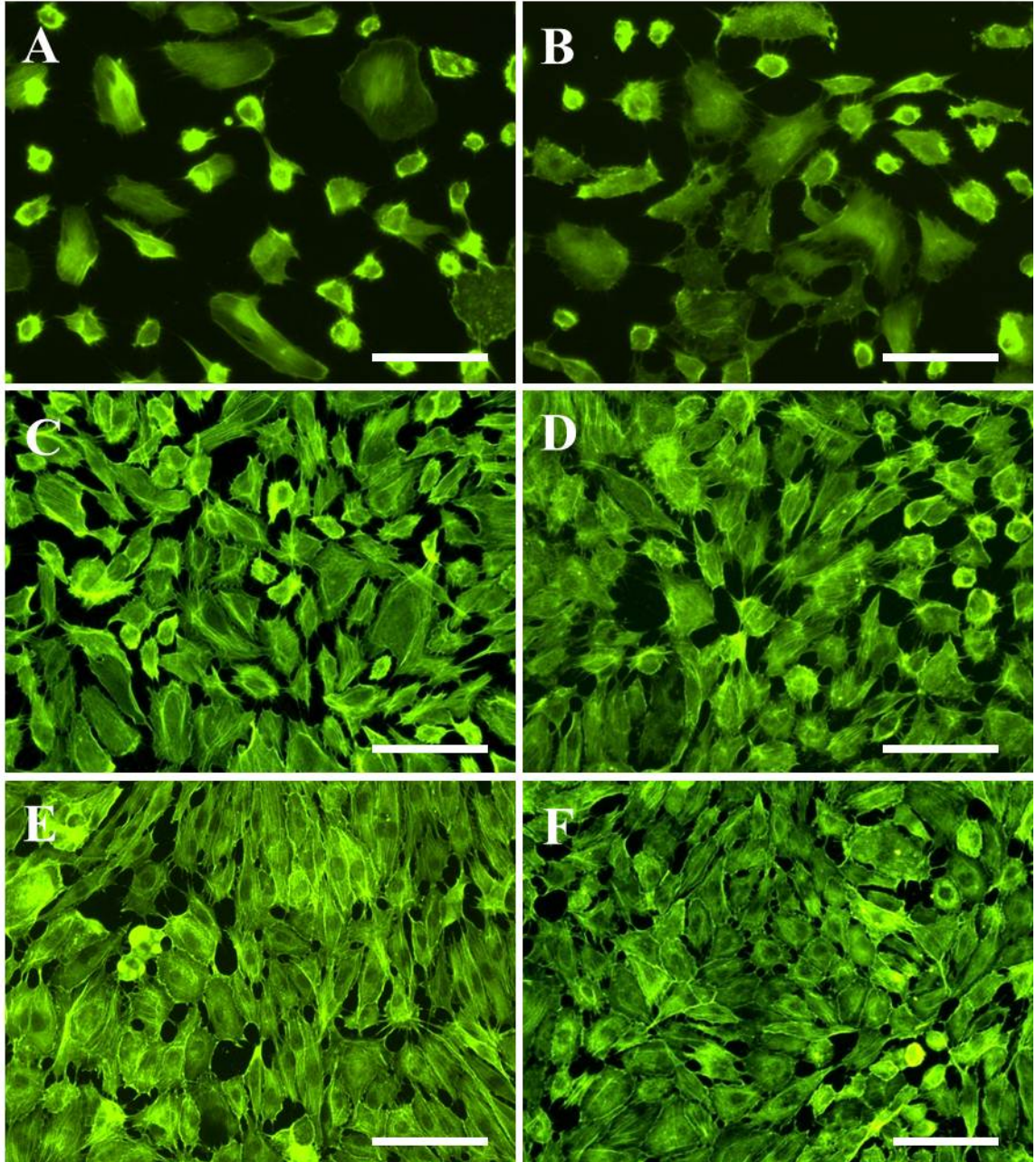


Figure 3.5- The inter-cellular connectivity of the endothelial cells. Figure A,B,C,D,E,F shows 0 (0%), 1 (<20%), 2 (20-40%), 3 (40-60%), 4 (60-80%), 5 (80-100%) rated connectivity respectively. All scale bars represent 100 μ m.

3.8 Enzyme-linked Immunosorbent Assay (ELISA)

The effects of albumin glycation, glycation extent and shear stress magnitude on the surface expression of intracellular adhesion molecule-1 (ICAM-I), thrombomodulin (TM) and tissue factor (TF) was quantified using ELISA. This experiment was carried out both for static and sheared samples.

After the incubation of the cells with glycated albumin for different durations the cells were either sheared (dynamic condition) then investigated with ELISA or investigated directly (static condition) with ELISA. Post shearing or incubation the supernatant was aspirated off of the cells and the cells were washed (2X) with PBS (pH-7.4, warmed to 37°C). ECs were then fixed with 0.5% glutaraldehyde (300 µL per well) for 15mins at 37° C. After washing (2X with PBS), gluteraldehyde was neutralized and non- specific binding was blocked with 100 mM glycine – 0.1% BSA (1mL per well for 30 mins, 37°C). After washing (2X) with TBS, (Tris buffer saline, pH 7.4) ECs were treated with the primary antibody to measure EC surface activation and inflammatory responses (37°C, 60 minutes). The primary antibodies were a murine monoclonal anti-human ICAM-1 antibody (1 µg/mL in PBS, Ancell Corporation, San Diego, CA), which was used to measure EC activation; a murine monoclonal anti-human TF antibody (2 µg/mL in PBS, Abcam), which was used to measure EC hemostasis potential; and a murine monoclonal anti-human TM (10 µg/mL in PBS, Abcam), which was used to measure the EC regulation on coagulation. The primary antibody binding was then detected by treating the cells with an alkaline phosphatase conjugated goat anti-mouse secondary antibody (1:1000 in PBS) for 60 minutes at 37°C followed by a wash (2X with TBS). The cells were then incubated with pNPP (p-Nitrophenyl Phosphate, yellow, Sigma) solution for 20 minutes and the absorbance at 450nm was measured using an optical microplate reader (Beckman Coulter, DTX 880). Data was normalized to the non-albumin control after subtraction of the negative control.

3.9 Scanning Electron Microscopy (SEM)

Scanning electron microscopy was used to perform a qualitative morphological analysis. The SEM images were obtained at the OSU Microscopy Laboratory. The supernatant was aspirated out and the ECs were washed (2X) with PBS (pH-7.4, warmed to 37°C). ECs were then fixed with 0.5% glutaraldehyde (300 µL per well) for 15mins at 37°C. After washing (2X with PBS), glutaraldehyde was neutralized and non-specific binding was blocked with 100mM glycine – 0.1% BSA (1mL per well for 30mins, 37°C). After washing (2X with PBS), the ECs were incubated in osmium tetroxide (Electron Microscopy Sciences, Hatfield, PA, USA) for 60 minutes in the dark at room temperature. This was followed by a wash (2X with PBS) and finally stored at -4°C in 1 mL PBS. Prior to imaging the ECs were first dried in absolute ethanol for 15 minutes (three exchanges). And then in hexamethyldisilazane (Electron Microscopy Sciences) for 10 minutes (two exchanges). Finally the cells were coated with gold (Blazers Union MED 010 Au/Pt Sputter Coater) for 30 seconds and imaged.

3.10 Statistical Analysis

3.10.1 Analysis of Experiments Under Static Conditions

Statistical analysis was performed using the Primer for Biostatistics (V 4.02) with a significance level of $\alpha = 0.05$ for all statistical tests. The data was tested for significance using ANOVA, with the combination of Tukey's test or Student's *t*-test to determine the difference among the different treatment groups. Normalized data for a minimum of 4 independent experiments were used.

3.10.2 Analysis of Experiments Under Dynamic Conditions

Statistical analysis was performed using SAS (V9.0) and significance was tested at $\alpha = 0.05$. In most cases, a 3-way ANOVA was used to analyze the differences within the data. Significant differences were found based on the least squares means values from the ANOVA

results. To conduct the three way ANOVA, the data was grouped into glycation extent (2, 6 and 8 weeks AGE or BSA), culture duration (3 or 5 days) and magnitude of shear stress (4, 10 and 40 dynes/cm²). Normalized data for a minimum of 4 independent experiments were used.

CHAPTER IV

RESULTS

4.1 Endothelial Cell Metabolic Activity

4.1.1 Static Condition

The metabolic activity of endothelial cells exposed to diabetic culture conditions, i.e. in the presence of AGEs, was measured using a standard MTT assay. The metabolic activity of ECs when exposed to different glycation extents (2, 6, and 8 week AGE) in an early and late growth duration was documented (Figure 4.1, n=4-5). The results suggested that, in early culture condition there were no significant differences due to the different glycated conditions. But with longer growth duration, there was a significant improvement in metabolic activity in the control, non-glycated conditions (BSA) and 2 week AGE samples. However there was no significant improvement in metabolic activity when the cells were incubated with 6 and 8 week AGE, and the activity was significantly less than the paired 6 and 8 week BSA conditions. Figure 4.1 indicates that longer glycated conditions (6 & 8 week AGE) significantly impaired the EC metabolic activity.

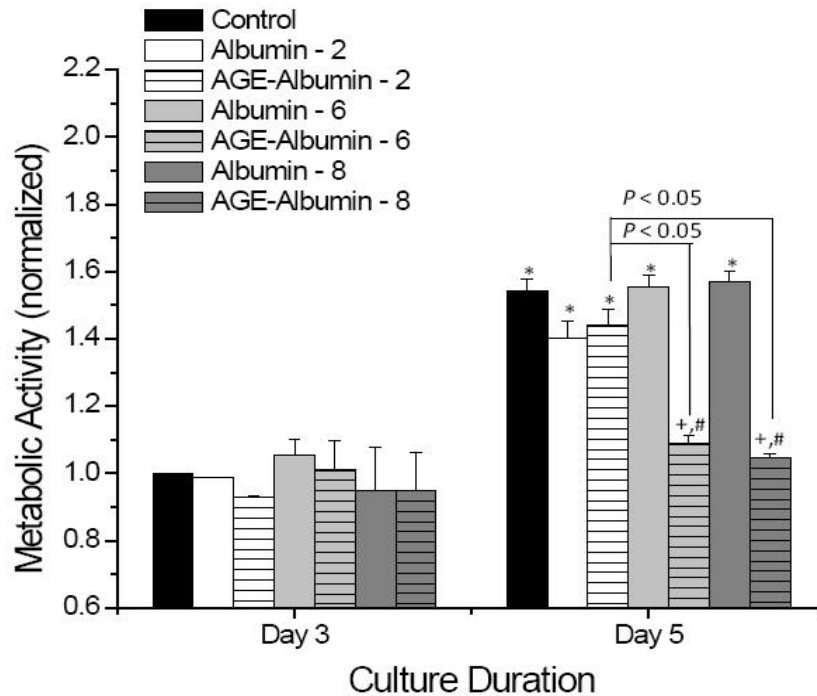


Figure 4.1-Endothelial cell (HUVEC) metabolic activity under static condition, as a function of culture duration and glycation extent. Metabolic activity was calculated from 2–3 samples from 4–5 independent experiments. Each bar represents the mean + standard error of the mean of the pooled data from each experiment. +, significantly different from no added albumin (paired by culture duration, two-way ANOVA, $p < .05$); *, significantly different from day 3 (paired by treatment, two-way ANOVA, $p < .05$); #, significantly different from nonglycated albumin (paired by culture duration, two-way ANOVA, $p < .05$). Some data presented here was collected by the Rubenstein lab. This figure has been taken from (Rubenstein et al. 2011).

4.1.2 Dynamic Condition

The combined effect of glycation extent (2, 6 and 8 week AGE) and varying shear stress levels on the EC metabolic activity was measured using a standard MTT assay. The ECs incubated with different glycation extents for early and late culture durations were exposed to low (4 dynes/cm²) medium (10 dynes/cm²) or high (40 dynes/cm²) constant shear stress for 1 hour. The results (Figure 4.2, n=4-5) indicated that in early culture duration, the level of shear stress did not have significant effect on the EC metabolic activity (Figure 4.2.A). However in late culture duration, there was a reduction in metabolic activity when the cells were exposed to high shear stress (40 dynes/cm²), with significant difference in ECs incubated with 8 weeks AGE and BSA compared to the ECs exposed to medium shear stress (10 dynes/cm²) (Figure 4.2.B). The glycated (AGE) and non glycated (BSA) albumin conditions increased the overall metabolic activity compared to the control in most of the shear conditions, but with no definite trends. The increase in metabolic activity of ECs incubated with AGEs could be due to the combination of AGEs and shear stress. Figure 4.2 illustrates that higher shear stress levels at a longer growth duration could impair EC metabolic activity.

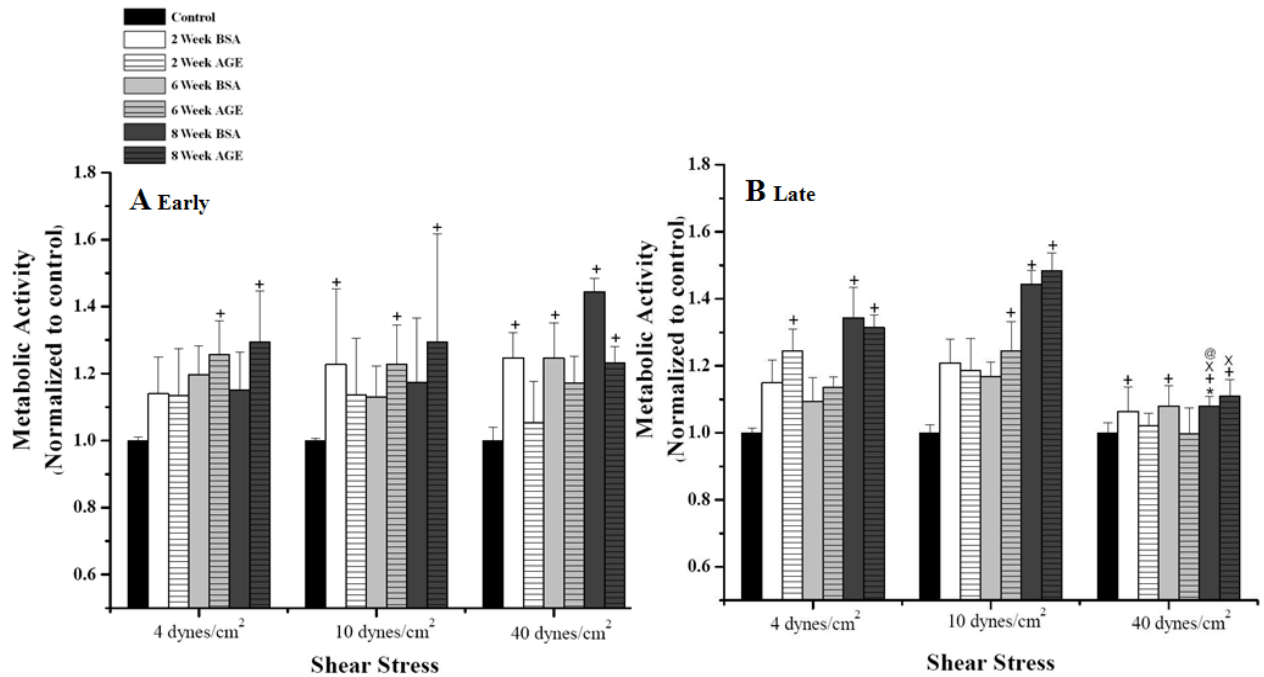


Figure 4.2-Endothelial cell (HUVEC) metabolic activity under dynamic condition early (A) and late culture duration (B), as a function of glycation extent and level of shear stress. Metabolic activity was calculated from 4–5 independent experiments. Each bar represents the mean + standard error of the mean of the pooled data from each experiment. +, significantly different from Control (paired by glycation extent, 3 way ANOVA, $p < .05$); *, significantly different from early culture duration (paired by shear stress level, 3 way ANOVA, $p < .05$); #, significantly different from BSA (paired by glycation duration, 3 way ANOVA, $p < .05$); x, significantly different from 10 dynes/cm² shear stress magnitude (paired by glycation extent, 3 way ANOVA, $p < .05$); @, significantly different from 4 dynes/cm² shear stress magnitude (paired by glycation extent, 3 way ANOVA, $p < .05$).

4.2 Endothelial Cell Viability and Density

To measure the effect of AGEs on the cell viability and density ECs were incubated with 2, 6 and 8 weeks of glycated (AGE) and non-glycated (BSA) albumin for early and late growth durations (Figure 4.3, n=4-5). The overall viability was high for all conditions (~98%). However there was significant decrease in viability of the ECs incubated with 6 and 8 weeks of AGE in the late growth duration compared to the early and paired 6 and 8 weeks BSA samples. The EC density was also compared among the different AGE samples and the results showed an increase in overall cell density over time, with a significant increase in the control, BSA and 2 week AGE sample. However there was significant reduction in the late 6 and 8 week AGE samples compared to their paired non glycated BSA samples. Therefore, the results from Figure 4.3 indicates that longer exposure to 6 and 8 week AGE deteriorates the EC culture conditions.

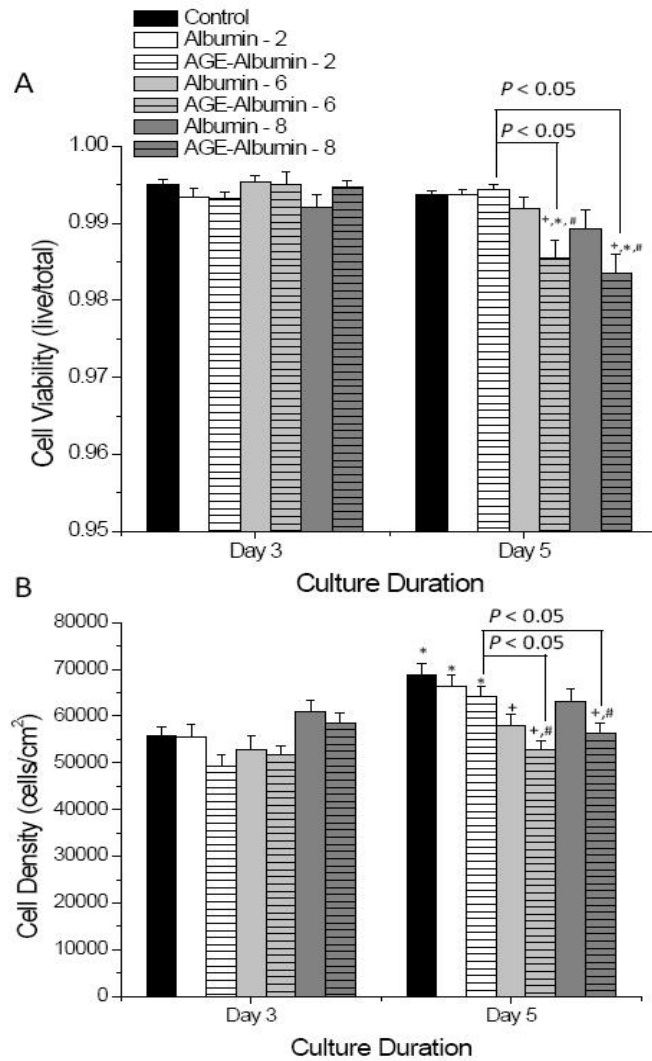


Figure 4.3: Endothelial cell (HUVEC) viability (A) and density (B), as a function of culture duration and glycation extent. Viability and density were calculated from 3–4 images from 4–5 independent experiments. Each bar represents the mean + standard error of the mean of the pooled data from each experiment. +, significantly different from no added albumin (paired by culture duration, two-way ANOVA, $p < .05$); *, significantly different from day 3 (paired by treatment, two-way ANOVA, $p < .05$); #, significantly different from non-glycated albumin (paired by culture duration, two-way ANOVA, $p < .05$). Some data has been collected by the Rubenstein lab. This figure has been taken from (Rubenstein et al. 2011)

4.3 Endothelial Cell Morphology

The effect of AGEs on the EC morphology was determined by measuring the perimeter area for approximately 100 cells per independent culture well, in early and late growth duration (Table 4.1, n=4-5). The results indicated some difference in cell area among the conditions but with no overall trend or significance. However, the percentage of elongated cells in the late growth duration was significantly higher when cells were exposed to 2 and 6 week AGE compared to their paired BSA samples. However, there was no significant improvement in the number of elongated cells for 8 week AGE samples (Table 4.1). Therefore, it can be concluded that, AGEs do not affect the overall cell area, but alters the cells preference to grow with an elongated morphology.

Table 1. Endothelial Cell Area and Morphology				
Condition	Growth duration	Elongated cell area (n)	Circular cell area (n)	Fraction of elongated cells ^a
No added albumin	Day 3	3.61 ± 0.06 ^b (1242)	3.57 ± 0.11 (306)	80.2%
	Day 5	3.61 ± 0.05 (1174)	3.73 ± 0.13 (244)	87.8%
Nonglycated albumin at 2 weeks duration	Day 3	2.99 ± 0.08 (405) ^c	2.69 ± 0.14 (72) ^c	84.9%
	Day 5	3.67 ± 0.12 (328)	3.80 ± 0.54 (13)	96.1% ^{c,d}
Glycated albumin at 2 weeks duration	Day 3	3.28 ± 0.13 (281) ^c	3.03 ± 0.26 (57) ^c	83.1%
	Day 5	3.78 ± 0.10 (324)	3.67 ± 0.24 (42)	88.5% ^{c,d}
Nonglycated albumin at 6 weeks duration	Day 3	3.24 ± 0.09 (349) ^c	2.90 ± 0.17 (63) ^c	84.7%
	Day 5	3.28 ± 0.12 (240) ^c	2.62 ± 0.21 (24) ^{c,e}	91.5% ^{c,d}
Glycated albumin at 6 weeks duration	Day 3	3.31 ± 0.08 (646) ^c	3.35 ± 0.18 (122) ^c	84.1%
	Day 5	3.63 ± 0.11 (274)	3.87 ± 0.35 (31)	91.8% ^c
Nonglycated albumin at 8 weeks duration	Day 3	3.91 ± 0.07 (736) ^c	3.84 ± 0.11 (217) ^c	77.2%
	Day 5	3.84 ± 0.06 (1023) ^c	4.11 ± 0.12 (236) ^c	81.3%
Glycated albumin at 8 weeks duration	Day 3	4.08 ± 0.07 (675) ^c	4.22 ± 0.15 (148) ^c	82.0%
	Day 5	4.34 ± 0.06 (1036) ^c	4.58 ± 0.13 (257) ^c	80.1% ^c

^a These are shown as directly calculated from n; for statistics, the independent experiments were averaged.
^b Data are the mean ± standard error of the mean of the cell area (×1000) μm².
^c Significantly different from no added albumin (paired by culture duration, two-way ANOVA, p < .05).
^d Significantly different from day 3 (paired by treatment, two-way ANOVA, p < .05).
^e Significantly different from elongated (paired by culture duration, two-way ANOVA, p < 0.05).

Table 4.1- Endothelial cell (HUVEC) morphology. The cell area was measured from 2-3 images of 4-5 independent experiments. Some data presented here was collected by the Rubenstein Lab. This table has been taken from (Rubenstein et al. 2011)

4.4 Connexin-43 and Caveolin-1 Expression

4.4.1 Static Condition

The expression of Cx-43 and cav-1 are markers for endothelial gap junction activity and EC angiogenic potential respectively. Here the expression of Cx-43 and cav-1 was measured in two methods; the intensity and relative number of the localized proteins on the EC membrane. The expression of these proteins were compared for the different glycated (AGE) and non-glycated (BSA) conditions, for early and late culture durations (Figure 4.4, n=4-5). In early culture conditions there is no difference in the intensity or relative localization expression among the groups (Figure 4.4(A) and 4.4(B)). However, in the late culture condition, there was an overall increasing trend for both of the expression with the glycation extent and significant increase in Cx-43 intensity was observed in the cells incubated with 8 week AGE, when compared to control and the paired 8 week BSA samples. This result suggests that, presence of AGE could increase Cx-43 expression in EC membrane thereby increasing EC gap junction activity and active network formation potential. The results of the cav-1 expression (Figure 4.4(C) and 4.4(D)) indicate that although there was no significant difference among the different glycated conditions, there was an overall increase in cav-1 intensity and relative localization when the ECs were exposed to different glycation extents of AGE and BSA, compared to control. The cav-1 localization significantly increased when the ECs were incubated with 8 week AGE in late culture duration, compared to control and early cultured samples. The results obtained from Figure 4.4(C) and 4.4(D) indicated that, exposure to higher glycation extent (8 week AGE) for a longer duration could induce new caveolae formation. The results from Figure 4.4 can be further verified from the merged digital images of Cx-43 and cav-1 expression illustrated in figure 4.5.

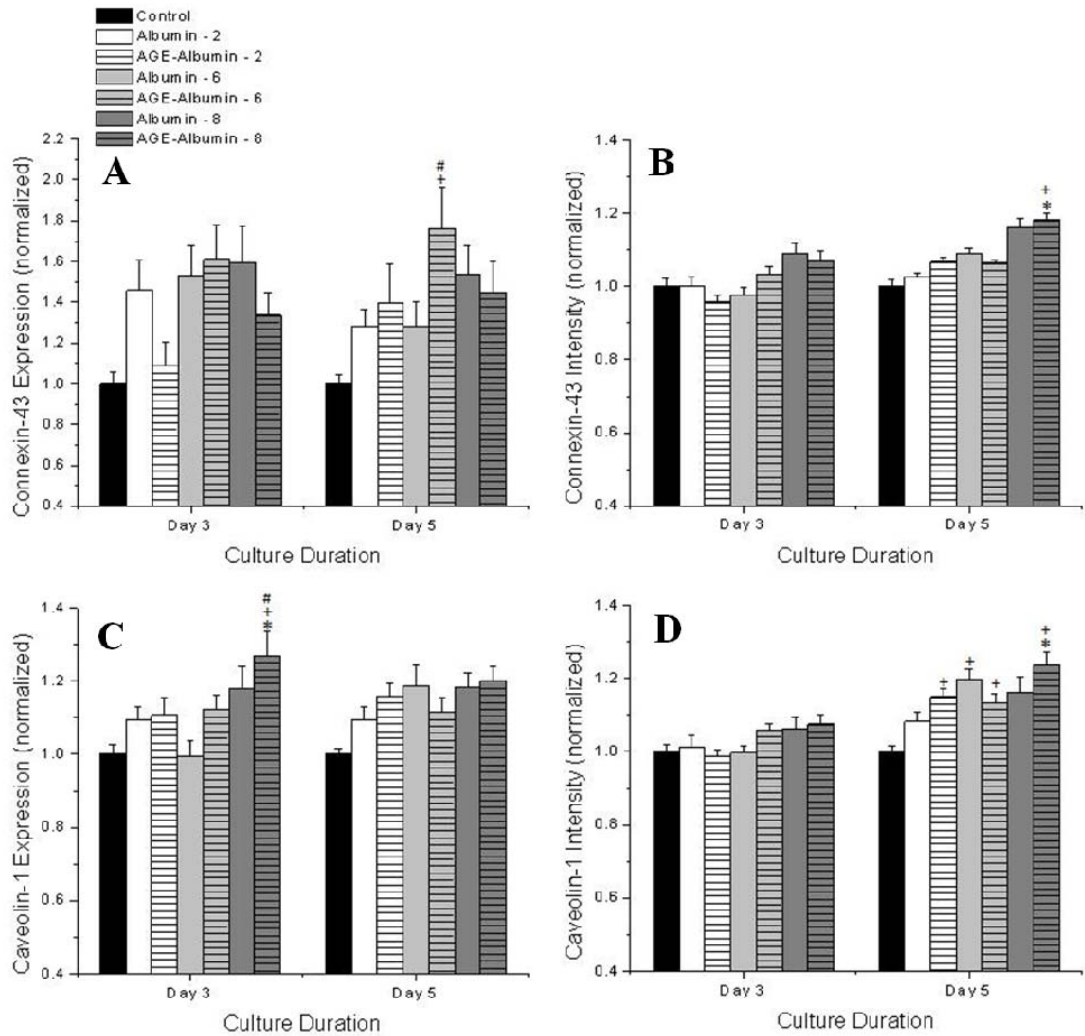


Figure 4.4-Endothelial cell (HUVEC) surface expression of connexin-43 (A, B) or caveolin-1 (C, D) as a function of extent of albumin glycation. The surface expression of these molecules was calculated from 3–4 images for 4–5 independent experiments. Each bar represents the mean + standard error of the mean of the pooled data from each experiment. Intensity is a measure of the expression of these molecules, whereas expression is a measure of the localization of individual molecules to particular regions within the cell. +, significantly different from no added albumin (paired by culture duration, two-way ANOVA, $p < .05$); *, significantly different from day 3 (paired by treatment, two-way ANOVA, $p < .05$); #, significantly different from nonglycated albumin (paired by culture duration, two-way ANOVA, $p < .05$). This figure has been modified from (Rubenstein et al 2011).

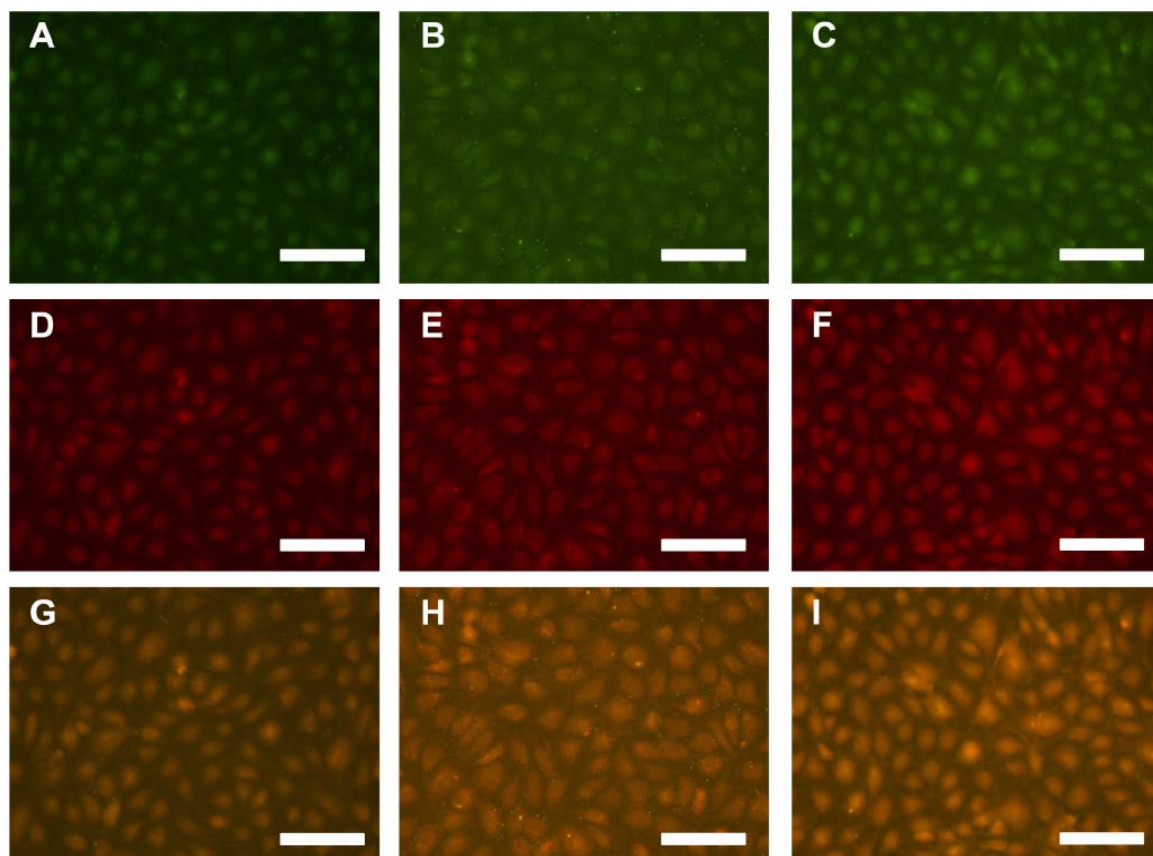


Figure 4.5-Digital images of endothelial cells exposed to no added albumin (A, D, G), albumin glycated for 8 weeks (B, E, H), or non-glycated albumin at 8 weeks for 5 days (C, F, I). The expression of connexin-43 (A, B, C) and caveolin-1 (D, E, F) were quantified as a means to determine changes in angiogenesis potential and gap junction formation (these images generated the data plotted in Figures 4.4A and 4.4C). Merged images (G, H, I) show where these markers were localized under these conditions and suggest that these were nature channels formed (these images were generated the data plotted in Figures 4.4B and 4.4D). All scale bars are 100 μ m.

4.4.2 Dynamic Condition

The objective of this experiment was to determine how the variation in shear stress levels (low, 4 dynes/cm²; medium, 10 dynes/cm²; high, 40 dynes/cm²) would alter the expression of Cx-43 and cav-1 on ECs that have been incubated with different glycated (2, 6 and 8 week AGE) and non-glycated albumin (2, 6 and 8 week BSA) for early and late culture durations. And monitor the combined effect of glycation extent and shear stress level in EC gap junction activity and angiogenic potential.

4.4.2.a Connexin-43 Intensity and Relative Localization

The Cx-43 expression was measured in similar fashion as the static experiments. Both the intensity and the relative localization of Cx-43 protein were measured from the digital images obtained from the immuno-fluorescence microscopy (Figure 4.6, n=4-5). The results from the intensity measurements (Figure 4.6(A) and 4.6(B)) indicated that there were no differences between the early and late culture conditions. When comparing the glycation extents in individual shear groups, the results indicate that when exposed to medium shear stress levels, the Cx-43 intensity was significantly high in ECs that were incubated with 6 and 8 weeks of AGE, compared to the paired 6 and 8 weeks BSA samples and control in early culture conditions. However in late culture condition, although there was no difference between AGEs and the paired BSA samples, the Cx-43 intensity was significantly higher than the control. The combination of high shear stress and 8 week AGE significantly increased the Cx-43 intensity, compared to the paired 8 week BSA and control in both early and late culture durations. Exposure to high shear stress also significantly increased the Cx-43 intensity of ECs incubated with 2, 6 and 8 weeks AGE at late culture duration, when compared with medium shear stress level and control. The Cx-43 relative localization demonstrated similar patterns under the influence of high shear stress (Figure 4.6(C) and 4.6(D)). High shear stress increased relative Cx-43 localization in ECs

incubated with 2 and 6 weeks AGE at late culture duration, when compared to the paired control and medium and low shear stress levels, but with no significant increase for the 8 week AGE samples. The results obtained from Figure 4.6 indicate that shear stress and AGE increase the Cx-43 expression in magnitude dependent manner.

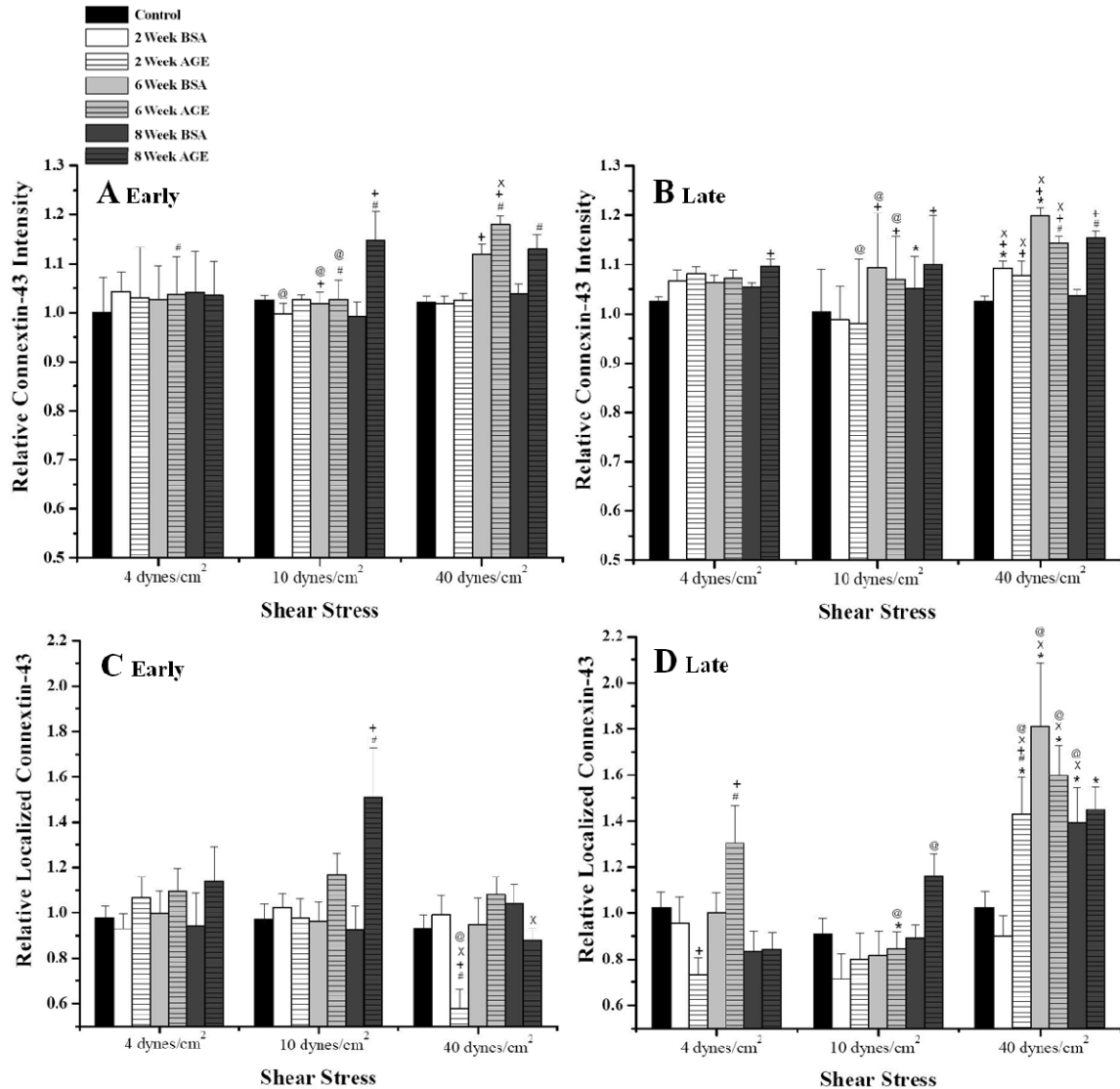


Figure 4.6-Endothelial cell (HUVEC) surface expression for Cx-43 relative localization early (A) late (B); and relative intensity early (C) late(D), as a function of glycation extent and level of shear stress. Cx-43 expression was measured from 4–5 independent experiments. Each bar represents the mean + standard error of the mean of the pooled data from each experiment. +, significantly different from Control (paired by glycation extent, 3 way ANOVA, $p < .05$); *, significantly different from early culture duration (paired by shear stress level, 3 way ANOVA, $p < .05$); #, significantly different from BSA (paired by glycation duration, 3 way ANOVA, $p < .05$); x, significantly different from 10 dynes/cm² shear stress magnitude (paired by glycation extent, 3 way ANOVA, $p < .05$); @, significantly different from 4 dynes/cm² shear stress magnitude (paired by glycation extent, 3 way ANOVA, $p < .05$).

4.4.2.b Caveolin-1 Intensity and Relative Localization

The cav-1 expression was measured in similar fashion as the static experiments. Both the intensity and the relative localization of cav-1 protein were measured from the digital images obtained from the immuno-fluorescence microscopy (Figure 4.7, n=4-5). In the measurement of cav-1 intensity, the results showed no overall differences or trend among the different glycated (AGE) and non-glycated (BSA) samples in early and late culture duration (Figure 4.7(A) and 4.7(B)). Comparing the glycation extents in individual shear stress levels, the results indicate that when exposed to and high shear stress, the cav-1 intensity was significantly higher in ECs that were incubated with 6 and 8 weeks of AGE, compared to control and the paired 6 and 8 weeks BSA samples in early culture conditions. At medium shear stress level there was a significant increase in cav-1 intensity for 6 and 8 week AGE samples compared to control but with no significant difference with the paired BSA samples in late culture conditions (Figure 4.7(B)). When comparing the effect of shear stress on the ECs, it was observed that cav-1 intensity was overall the lowest at medium shear stress level in comparison with low and high shear. There is a significant reduction in cav-1 expression for cells incubated with 2 and 8 weeks of AGE exposed to medium shear stress in comparison with the cells exposed to low and high shear stress at early culture conditions (Figure 4.7(A)). Similarly the intensity of cav-1 is significantly lower for 2 and 6 weeks samples at medium shear in comparison with high shear stress at late culture condition (Figure 4.7(A)). In the measurement of cav-1 localization, no overall trend was observed in early or late culture condition. However, the relative cav-1 localization was significantly of the ECs that were incubated with 8 week AGE and exposed to high shear stress compared to the paired 8 week BSA and control in late culture condition (Figure 4.7(D)). The level of shear stress did not affect the localization of the cav-1 proteins. The results illustrated in Figure 4.7 indicate that, low and high shear stress level plays a role in increasing the overall cav-1 protein expression on the EC cell membrane. The effect of AGE and BSA on the cav-1 expression is in consensus with the static no shear results.

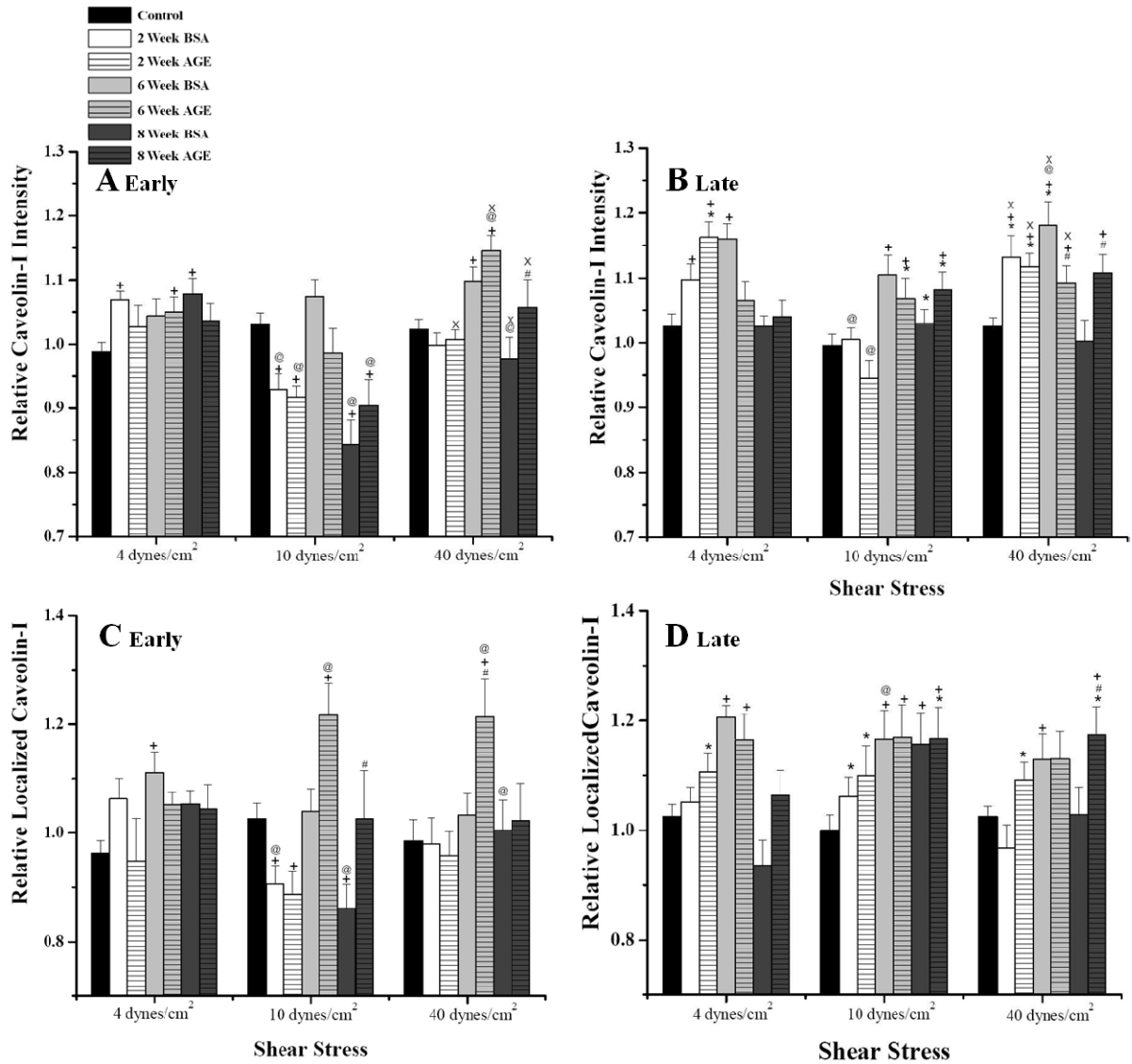


Figure 4.7-Endothelial cell (HUVEC) surface expression for Caveolin-1 relative localization early (A) late (B); and relative intensity early (C) late (D), as a function of glycation extent and level of shear stress. Caveolin-1 expression was measured from 4–5 independent experiments. Each bar represents the mean + standard error of the mean of the pooled data from each experiment. +, significantly different from Control (paired by glycation extent, 3 way ANOVA, $p < .05$); *, significantly different from early culture duration (paired by shear stress level, 3 way ANOVA, $p < .05$); #, significantly different from BSA (paired by glycation duration, 3 way ANOVA, $p < .05$); x, significantly different from 10 dynes/cm² shear stress magnitude (paired by glycation extent, 3 way ANOVA, $p < .05$); @, significantly different from 4 dynes/cm² shear stress magnitude (paired by glycation extent, 3 way ANOVA, $p < .05$).

4.5 Endothelial Cell Cytoskeletal Structure

The objective of this experiment was to determine how the variation in shear stress levels (low, 4 dynes/cm²; medium, 10 dynes/cm²; high, 40 dynes/cm²) would alter the cytoskeleton structure of the ECs that have been incubated with different glycated (2, 6 and 8 week AGE) and non-glycated albumin (2, 6 and 8 week BSA) for early and late culture durations. The effect of shear stress level in the disintegration of fibular actin structure, alignment of actin fibers in the shear direction and cell-to-cell connectivity was observed and documented.

4.5.1 Actin Structure

The actin fibular structure was observed under the varying shear stress levels (Figure 4.8, n=4-5), and the results indicated that, under late culture conditions, the ECs were able to retain significantly high percentage of fibular actin structure at all glycation extents and shear stress levels in comparison with the early culture duration (Figure 4.8(A) and 4.8(B)). When comparing the glycation extents at individual shear stress levels, the results indicated that, ECs incubated with 2, 6 and 8 weeks of AGE and BSA had a significantly lower percentage of fibular actin when exposed to medium shear at early culture conditions (Figure 4.8(A)). However, there were no differences among the AGE and BSA samples that were exposed to low or high shear stress levels. In the comparison among shear stress level, the results indicated that, there was an overall decreasing trend in the percentage of fibular actin structure as the shear stress level increased in both early and late culture duration. A significant reduction in fibrous actin structure was observed with all control, BSA and AGE samples exposed to high shear stress, in comparison with medium and low shear stress in both early and late culture durations. Therefore, Figure 4.8 indicates that, in the combined effect of shear stress level and glycation extent on EC actin structure shear stress had the dominating effect and diminished the fibular actin structure in a

magnitude dependent manner. This is further verified from the digital images obtained from the immuno-fluorescence microscopy illustrated in Figure 4.9.

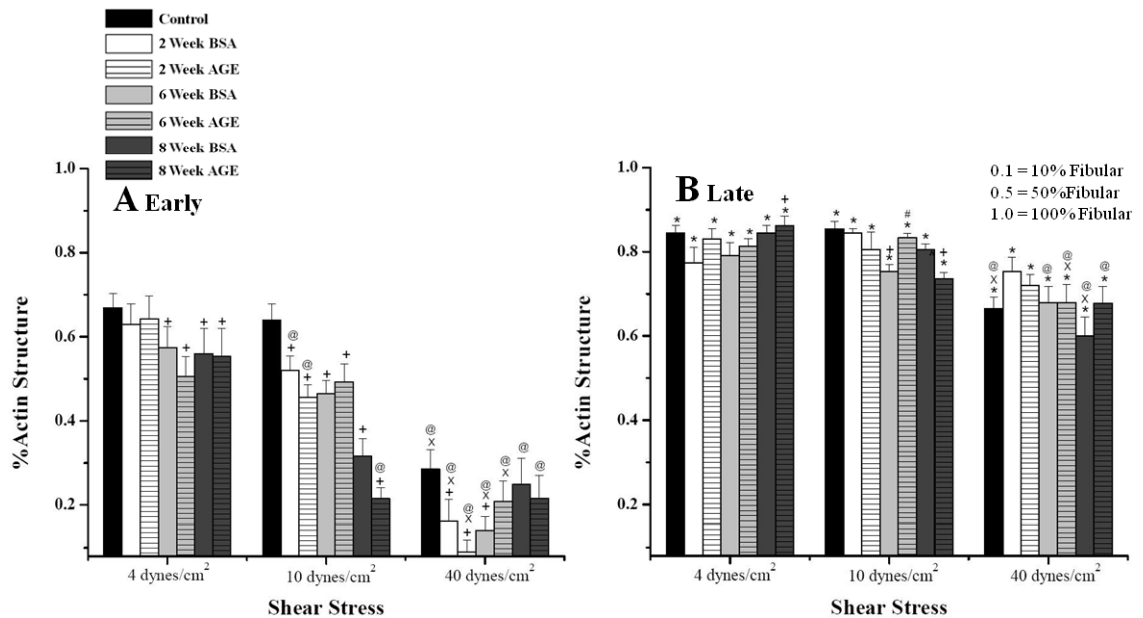


Figure 4.8-Endothelial cell (HUVEC) cytoskeletal actin fiber structure in early (A) and late (B) culture duration, as a function of glycation extent and level of shear stress. The percent actin structure was measured from 4–5 independent experiments. Each bar represents the mean + standard error of the mean of the pooled data from each experiment. +, significantly different from Control (paired by glycation extent, 3 way ANOVA, $p < .05$); *, significantly different from early culture duration (paired by shear stress level, 3 way ANOVA, $p < .05$); #, significantly different from BSA (paired by glycation duration, 3 way ANOVA, $p < .05$); x, significantly different from 10 dynes/cm² shear stress magnitude (paired by glycation extent, 3 way ANOVA, $p < .05$); @, significantly different from 4 dynes/cm² shear stress magnitude (paired by glycation extent, 3 way ANOVA, $p < .05$).

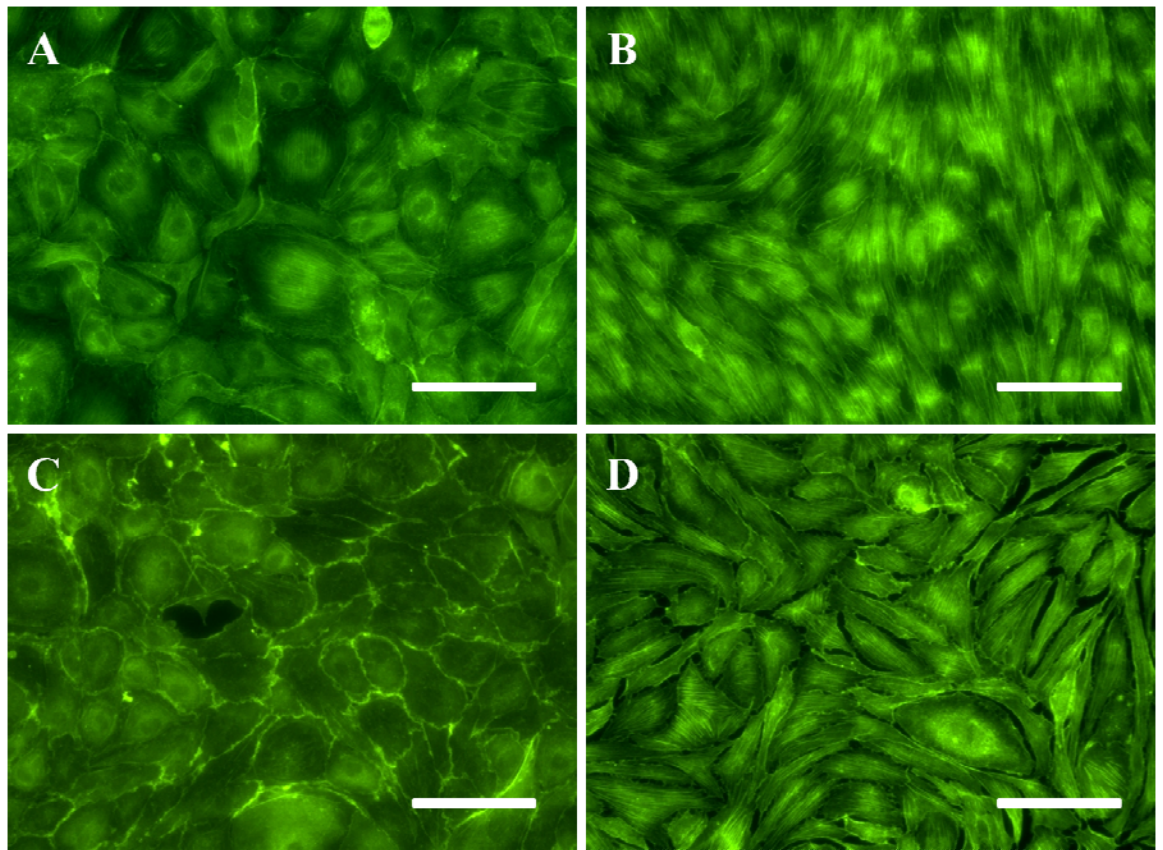


Figure 4.9 – Immunofluorescence microscopy image (20X magnification) of Human umbilical vein endothelial cells (HUVEC) actin fiber structure. A,B – Cells sheared at 4 dynes/cm² of early, late culture durations; C,D – Cells sheared at 40 dynes/cm² of early, late culture durations. The EC sheared at low shear stress levels (image A and B) contain relatively high fibular actin structure, compared to those exposed to high shear (image C and D). The actin structure is more fibular in late culture duration compared to early in both shear stress levels. All scale bars are 100 μ m.

4.5.2 Actin Alignment

The alignment of actin fibers in the shearing direction was observed under the varying shear stress levels (Figure 4.10, n=4-5), and the results indicated that, under late culture conditions, the EC actin fibers were significantly more aligned to the shear direction, in all AGE and BSA samples exposed to medium and high shear stress levels, in comparison with the early culture duration (Figure 4.10(B)). When comparing the glycation extents at individual shear stress levels, the results indicated that, there was no effect of AGE or BSA in actin fiber alignment. In the comparison among shear stress levels, the results indicated that, there was an overall decreasing trend in the percentage of fibular actin alignment as the shear stress level increased in early culture duration. A significant reduction in actin fiber alignment was observed with all control, BSA and AGE samples exposed to high shear stress, in comparison with medium and low shear stress in early culture duration (Figure 4.10(A)). However there were no differences observed in the case of late culture duration. Figure 4.10 indicates that, in the combined effect of shear stress level and glycation extent on EC actin fiber alignment, shear stress had the dominating effect and reduced the actin fiber alignment in a magnitude dependent manner. This is further verified from the digital images obtained from the immuno-fluorescence microscopy and is illustrated in Figure 4.11.

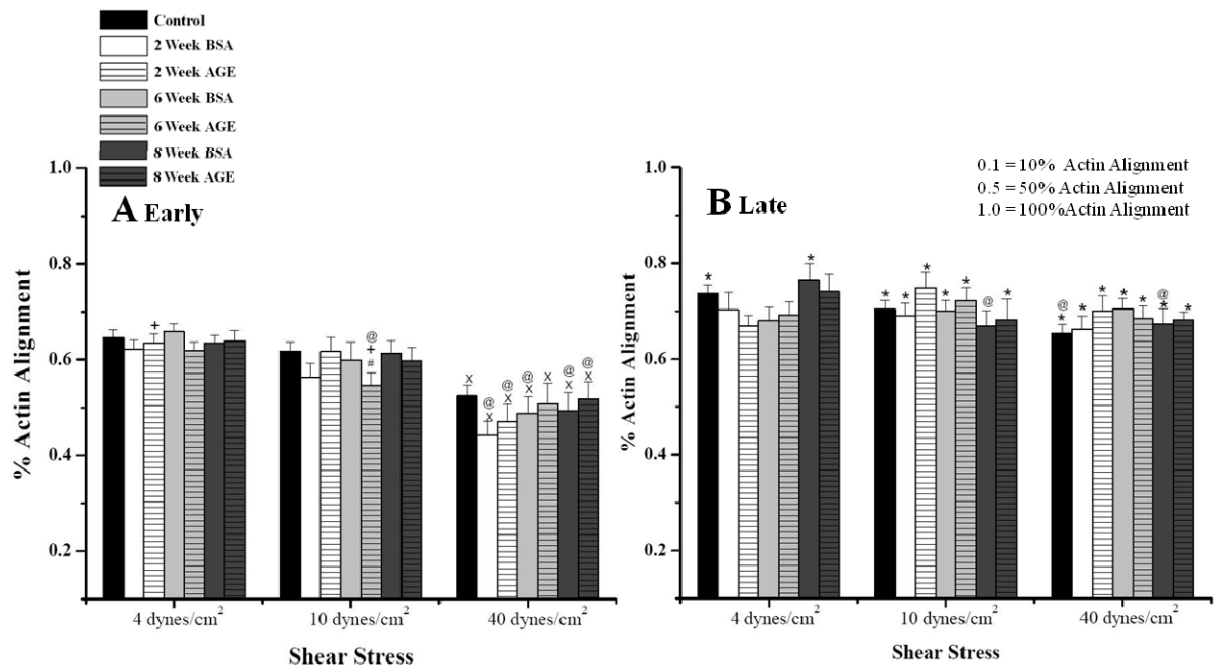


Figure 4.10-Endothelial cell (HUVEC) cytoskeletal actin fiber alignment in early (A) and late (B) culture duration, as a function of glycation extent and level of shear stress. The percent actin fiber alignment with shear direction was measured from 4–5 independent experiments. Each bar represents the mean + standard error of the mean of the pooled data from each experiment. +, significantly different from Control (paired by glycation extent, 3 way ANOVA, $p < .05$); *, significantly different from early culture duration (paired by shear stress level, 3 way ANOVA, $p < .05$); #, significantly different from BSA (paired by glycation duration, 3 way ANOVA, $p < .05$); x, significantly different from 10 dynes/cm² shear stress magnitude (paired by glycation extent, 3 way ANOVA, $p < .05$); @, significantly different from 4 dynes/cm² shear stress magnitude (paired by glycation extent, 3 way ANOVA, $p < .05$).

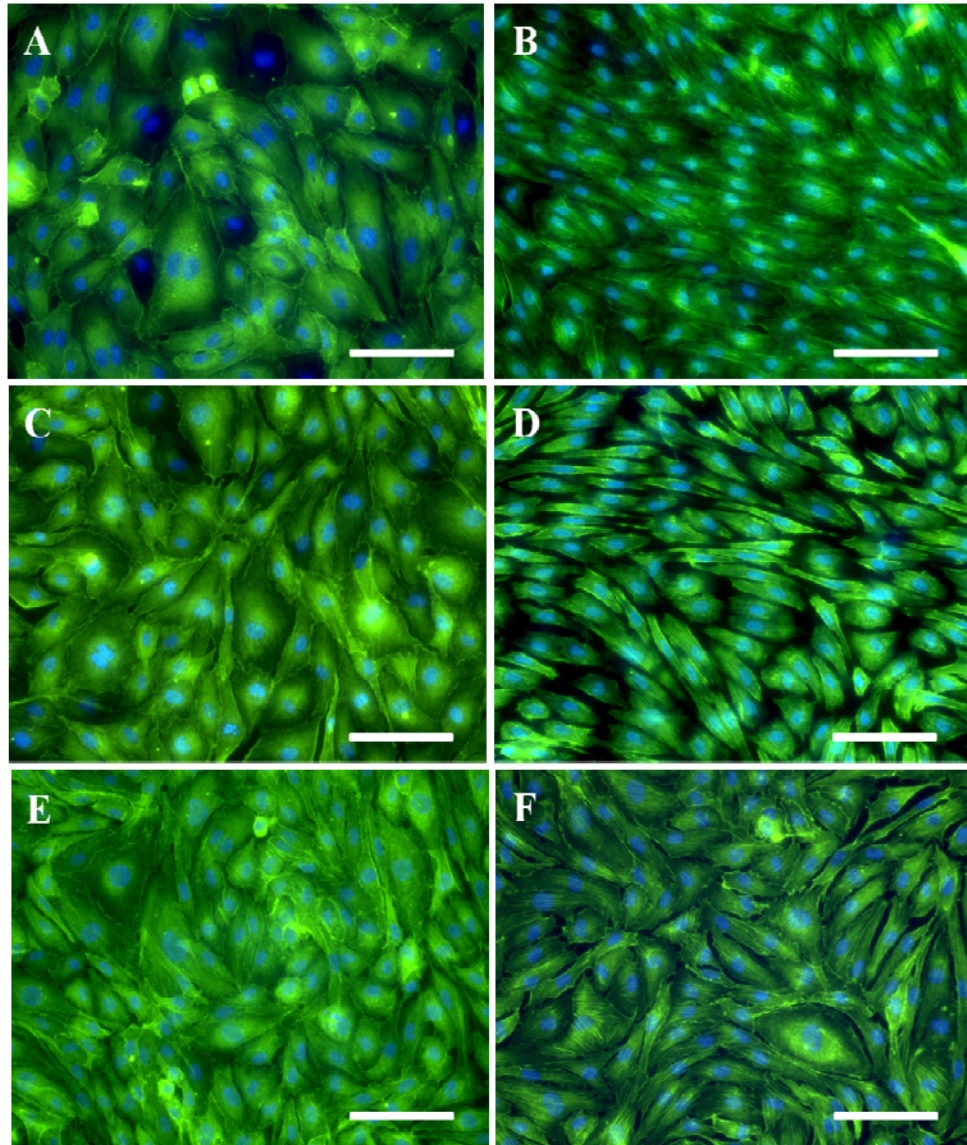


Figure 4.11 – Immuno-fluorescence microscopy image (20X magnification) of Human umbilical vein endothelial cells (HUVEC). A,B – Cells sheared at 4 dynes/cm² of early, late culture durations; C,D – Cells sheared at 10 dynes/cm² of early, late culture durations . E,F – Cells sheared at 40 dynes/cm² of early, late culture duration; D – Cells sheared at 40 dynes/cm² of late culture durations. The actin fibers in low shear stress level (A, B) is relatively more aligned to the shear direction compared to the medium (C, D) and high shear stress (E, F). The actin fibers of ECs in late culture duration (B, D, F) is relatively more aligned compared to early culture duration (A,C,D). All scale bars are 100μm.

4.5.3 Cell Connectivity

The effect of shear stress level in the cell-to-cell connectivity of ECs incubated with the varying glycation extents was monitored for early and late culture durations (Figure 4.12, n=4-5). The results showed no overall difference between the early and late culture duration. This suggested that, the incubation period does not significantly affect the cell-to-cell EC connectivity. Comparing the glycation extent in the individual shear stress levels, it was observed that, ECs exposed to medium shear had a significant reduction in percent connectivity compared to the control in early culture duration (Figure 4.12(A)). However, there was an increase in percent connectivity in the late culture condition compared to the paired early samples (at medium shear stress), but with no significant difference. Under the influence of high shear stress level, there was a significant increase in percent connectivity of ECs incubated with 6 and 8 week AGE compared to the paired 6 and 8 week BSA samples in both early and late culture duration (Figure 4.12(A) and 4.12(B)). This result was verified from the digital images obtained from the immunofluorescence microscopy illustrated in Figure 4.13. The application of high shear stress also induced a significant increase in cell connectivity of ECs exposed to 6 and 8 week AGE samples, when compared to the application of medium shear stress, in early culture condition. The results from Figure 4.12 indicated that, high shear stress level and higher glycation extents (6 and 8 week AGE) could modulate the cell-to-cell connectivity of ECs.

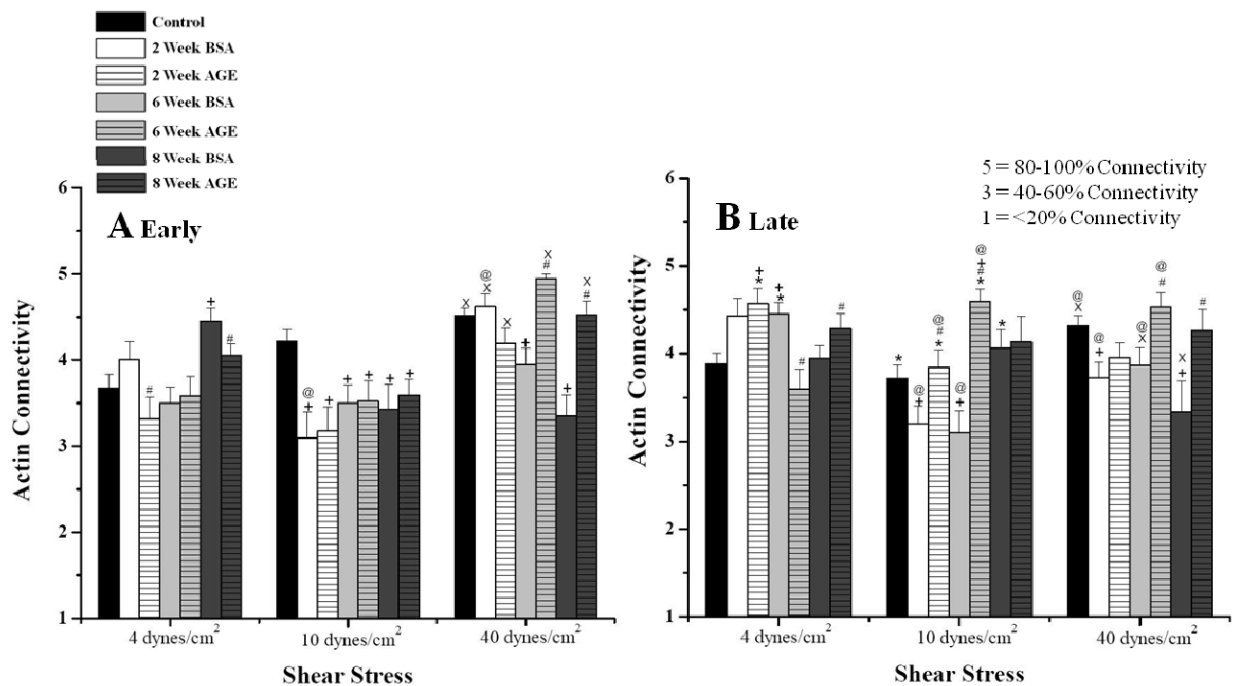


Figure 4.12-Endothelial cell (HUVEC) cytoskeletal actin connectivity at early (A) and late (B) culture duration, as a function of glycation extent and level of shear stress. The percent actin structure was measured from 4–5 independent experiments. Each bar represents the mean + standard error of the mean of the pooled data from each experiment. +, significantly different from Control (paired by glycation extent, 3 way ANOVA, $p < .05$); *, significantly different from early culture duration (paired by shear stress level, 3 way ANOVA, $p < .05$); #, significantly different from BSA (paired by glycation duration, 3 way ANOVA, $p < .05$); x, significantly different from 10 dynes/cm² shear stress magnitude (paired by glycation extent, 3 way ANOVA, $p < .05$); @, significantly different from 4 dynes/cm² shear stress magnitude (paired by glycation extent, 3 way ANOVA, $p < .05$).

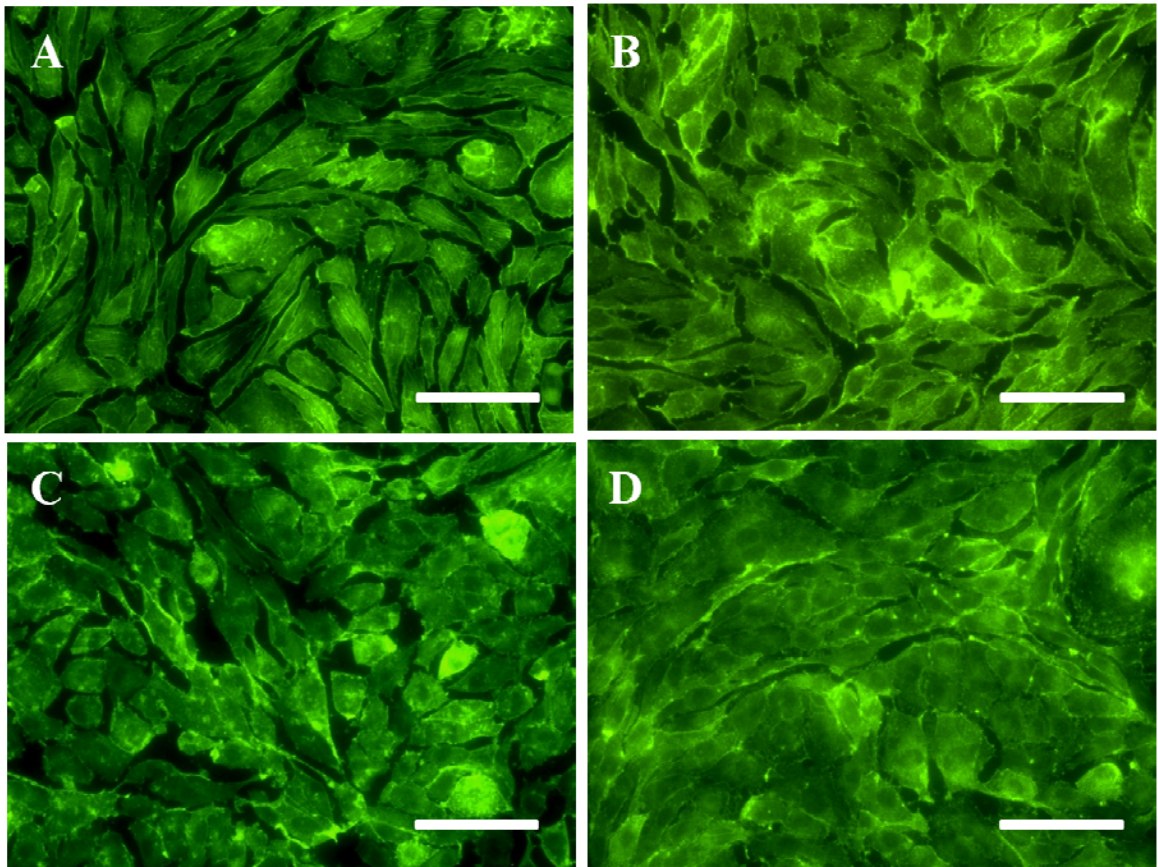


Figure 4.13 – Immuno-fluorescence microscopy image (20X magnification) of Human umbilical vein endothelial cells (HUVEC) actin fiber connectivity. A,B – 6 week BSA, AGE at 40 dynes/cm²; C,D – 8 week BSA, AGE at 40 dynes/cm². Incubation with 6 and 8 week AGE increased the cell to cell connectivity compared to the BSA samples at high shear stress level. All scale bars are 100 μ m.

4.6 Expression of Inflammatory and Thrombotic Mediators

The objective of this experiment was to determine how the variation in shear stress levels (low, 4 dynes/cm²; medium, 10 dynes/cm²; high, 40 dynes/cm²) would alter the inflammatory and thrombotic mediators of ECs that have been incubated with different glycated (2, 6 and 8 week AGE) and non-glycated albumin (2, 6 and 8 week BSA). The effect of shear stress level and the glycation extent on the expression of ICAM-1, thrombomodulin (TM) and tissue factor (TF) on EC membrane was measured and compared (Figure 4.14, n=4-5)

The results for the ICAM-1 expression (Figure 4.14(A)) showed that, comparing glycation extents at individual shear stress level, at low shear stress level, there was a significant increase in the protein expression of ECs incubated with 2, 6 and 8 week AGE compared to the control. At medium and high shear stress level, there was a gradual increase in ICAM-1 expression with the level of glycation, with a significant increase in 8 week AGE samples compared to the paired BSA and control condition. However no overall trend was observed when the shear stress magnitudes were compared. Figure 4.17(A); therefore suggests that, the level of glycation induced higher ICAM-1 expression.

The results for the TM expression (Figure 4.14(B)) showed that, at all levels of shear stress, ECs incubated with AGEs had an overall reduction in TM expression compared to the paired BSA and control samples. The TM expression for the non-glycated BSA samples was equal or higher than the control samples. The reduction in the protein expression was significant for ECs incubated with 8 week AGE at medium and high shear stress. However no overall trend was observed when the shear stress magnitudes were compared. The results for the TF expression (Figure 4.14(C)) indicated that, at shear stress levels, there was an overall increase in the TF expression with the increase of glycation extent (2, 6 and 8 week AGE) compared to the paired non-glycated condition (2, 6 and 8 week BSA). There was a significant increase in TF expression

of ECs incubated with 6 and 8 week AGE at medium and high shear stress when compared to the paired 6 and 8 week BSA and control samples. However no overall trend was observed when the shear stress magnitudes were compared. Therefore comparing Figure 4.14 (B) and 4.14(C), the results indicate that higher levels of glycated albumin (6 and 8 week AGE) significantly impaired the TM expression and enhanced the TF expression on the EC membrane.

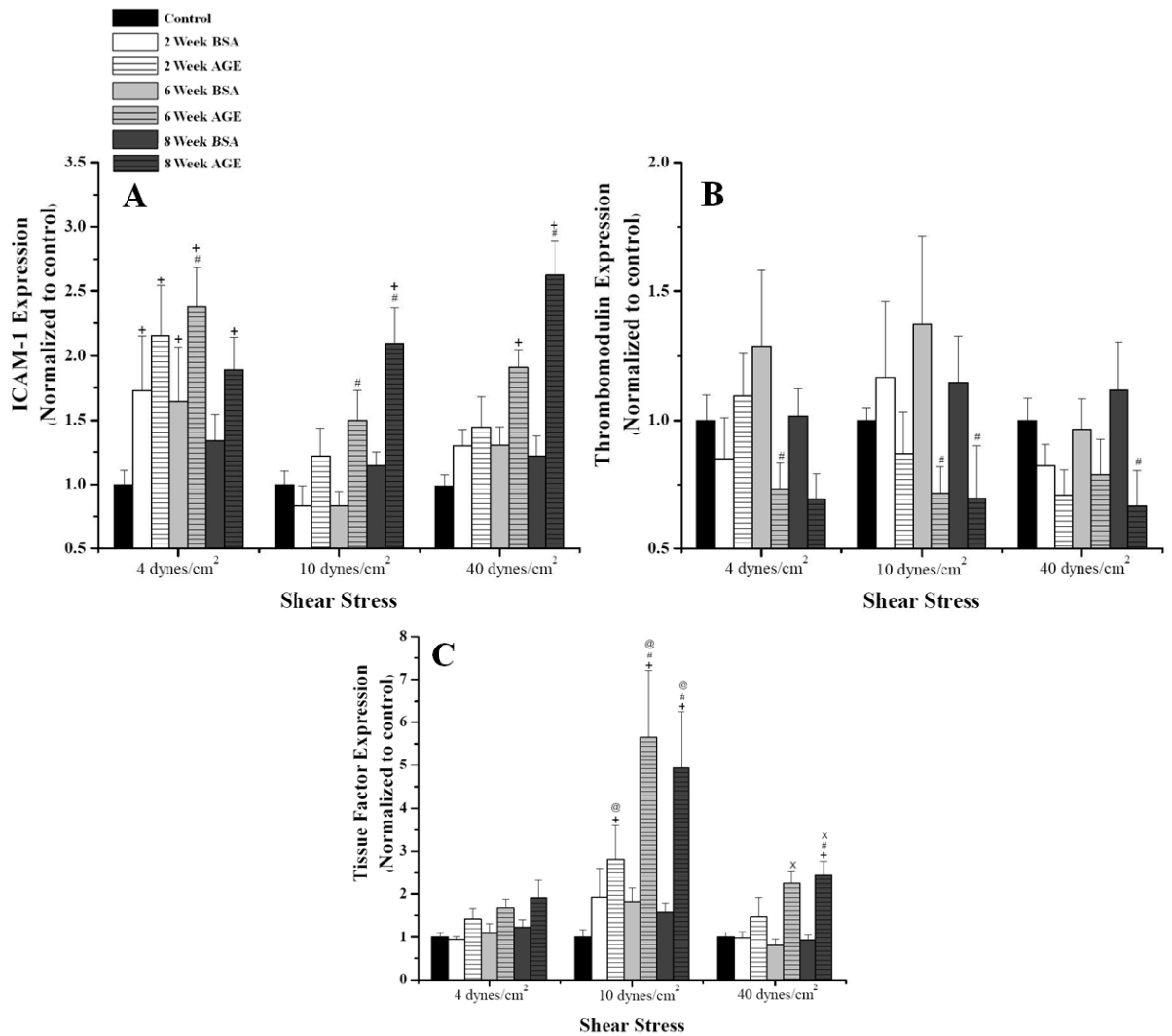


Figure 4.14- Endothelial cell (HUVEC) surface expression of ICAM-1 (A) Thrombomodulin (B) and Tissue Factor (C), as a function of glycation extent and level of shear stress. The percent actin structure was measured from 4–5 independent experiments. Each bar represents the mean + standard error of the mean of the pooled data from each experiment. +, significantly different from Control (paired by glycation extent, 3 way ANOVA, $p < .05$); *, significantly different from early culture duration (paired by shear stress level, 3 way ANOVA, $p < .05$); #, significantly different from BSA (paired by glycation duration, 3 way ANOVA, $p < .05$); x, significantly different from 10 dynes/cm² shear stress magnitude (paired by glycation extent, 3 way ANOVA, $p < .05$); @, significantly different from 4 dynes/cm² shear stress magnitude (paired by glycation extent, 3 way ANOVA, $p < .05$).

4.7 Scanning Electron Microscopy

Scanning electron microscopy (SEM) was used for a qualitative analysis of the EC morphology under the combined effect of different glycation extents (2, 6 and 8 weeks AGE) and shear stress levels (low, 4 dynes/cm²; medium, 10 dynes/cm²; high, 40 dynes/cm²). The images indicated a reduction in cell area as the ECs were incubated with AGE and BSA for a longer period (late culture duration) compared to the control. The obtained images showed that the presence of AGE induced an increase in cell-to-cell network formation in the cultured ECs at all shear stress levels, compared to the control and non-glycated BSA samples (Figure 4.15). The images confirmed that shear stress to some extent modulates the cell alignment and alters the “cobblestone” EC structure to elongated spindle shaped morphology. However the effect of the magnitude of shear stress could not be determined from the images. SEM images for detailed comparison with shear stress level and glycation extent in early and late culture duration are attached in APPENDIX B; this figure is intended for BSA vs. AGE comparisons only.

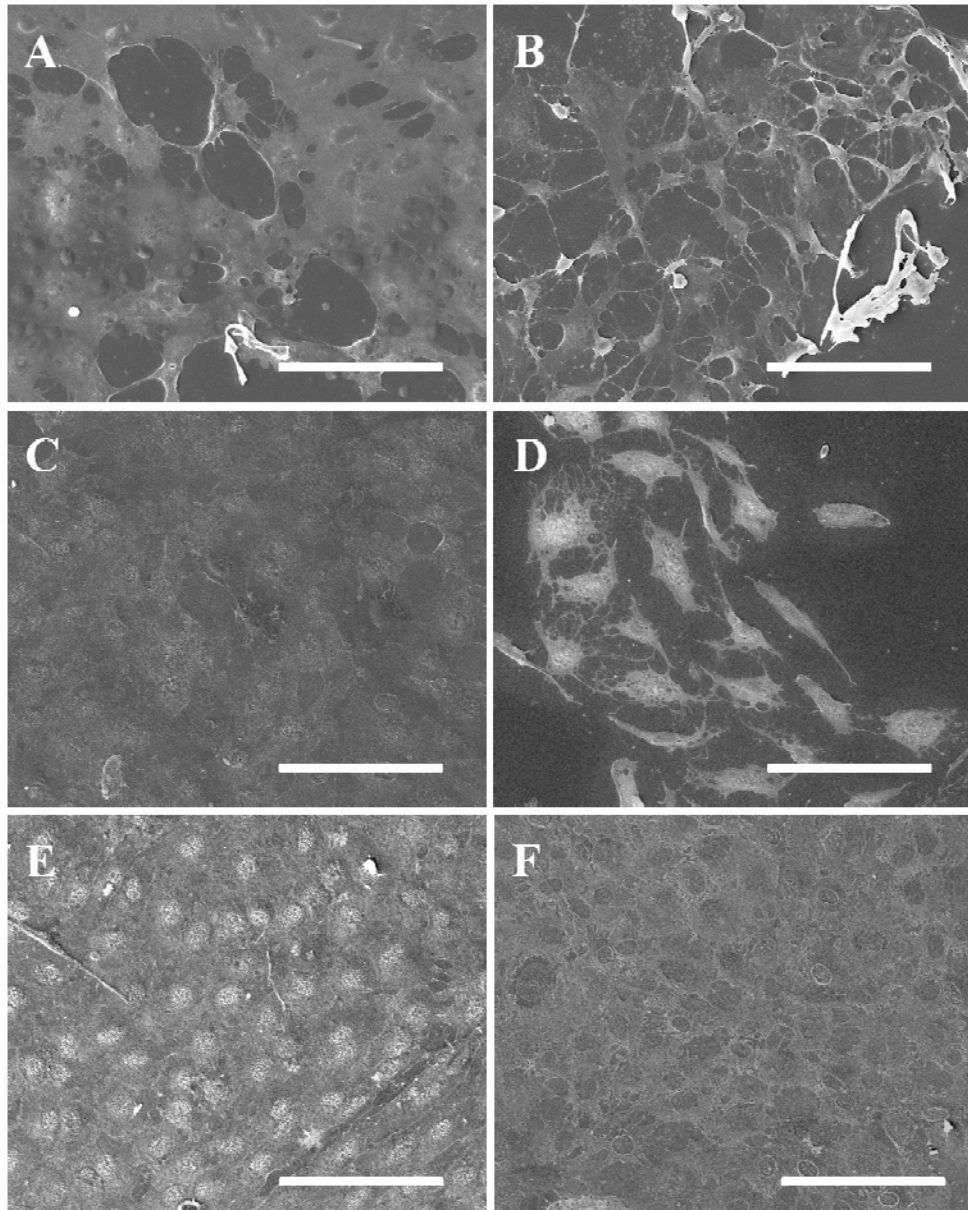


Figure 4.15 – Scanning electron microscopy images of Human umbilical vein endothelial cells (HUVEC). A,B – 2 week BSA, AGE (shear level, 10 dynes/cm² at early culture duration) ; C,D – 6 week BSA, AGE (shear level, 4 dynes/cm² at late culture duration); E,F – 8 week BSA, AGE (shear level, 4 dynes/cm² at Late culture duration). Incubation with 2, 6 and 8 week AGE increased the cell to cell connectivity compared to the paired BSA samples. All scale bars are 100μm.

CHAPTER V

DISCUSSION

5.1 Endothelial Cell Metabolic Activity

5.1.1 Static Condition

The aim of this study was to investigate the effect of different glycation extent (2, 6 and 8 week AGE) and culture duration (early and late) on the metabolic activity of cultured endothelial cells. The results showed an overall increase in metabolic activity of ECs with culture duration, except for cells that were exposed to higher glycation extent (6 and 8 week AGE). There was a significant decrease in metabolic activity when cells were exposed to 6 and 8 week AGE in late culture duration, compared to early, control and paired non-glycated (6 and 8 week BSA) samples. Similar results were reported by Chibber et al. which documented that a higher concentration of AGE had a toxic effect on cultured ECs and reduced EC metabolic activity (Chibber, Molinatti, Rosatto, Lambourne, & Kohner, 1997). In agreement to our results, Nascimento et al. reported that, AGE impaired EC metabolic actions; however this impairment was reversible by the application of pharmacological agents (Nascimento et al., 2006).

5.1.2 Dynamic Condition:

In this study the combined effect of glycation extent (2, 6 and 8 week AGE) in various culture durations (early and late) and exposure to different shear stress levels (low, 4 dynes/cm²; medium, 10 dynes/cm²; high, 40 dynes/cm²) on EC metabolic activity was observed (Figure 4.2). The results showed that, overall ECs showed minimum metabolic activity when exposed to high shear stress (40 dynes/cm²) in late culture duration in all glycated conditions. The metabolic activity of ECs incubated with 8 week AGE and exposed to pathological (40 dynes/cm²) was significantly lower compared to the paired physiological conditions (medium shear stress, 10 dynes/cm²). Previous studies have documented that cultured HUVECs exposed to shear stress at a magnitude of 25 dynes/cm², showed almost 2 folds increase in metabolic activity when compared to 10 dynes/cm² (Frangos, McIntire, & Eskin, 1988; Davies, Mundel, & Barbee, 1995b). In agreement with the previous studies, results from our study suggested that, the overall metabolic activity was high in the case of physiological shear stress (10dynes/cm²). However, the high shear stress magnitude in this study is almost twice the magnitude of the aforementioned studies and therefore could have a different effect on the activity rate due to the pathological level of shear. Therefore, the results obtained from this study suggest that, the combination of pathological shear stress and high glycation extent synergistically decreased overall EC metabolic activity and could lead to possible EC dysfunction.

5.2 Endothelial Cell Viability and Density

In this study the effect of glycation extent (2, 6 and 8 week AGE) for early and late culture duration on EC viability and density was investigated. The results showed, higher glycation extent (6 and 8 week AGE) for a longer culture duration significantly reduced EC viability compared to the control and paired non-glycated (6 and 8 week BSA) conditions (Figure 4.3(A)). The increase in proliferation of cultured ECs with longer culture duration was impaired

by 6 and 8 week AGE as well (Figure 4.3(B)). This result is consistent with previous studies by the Rubenstein lab (Rubenstein, Morton, & Yin, 2010). These results are also in agreement with studies conducted by Xu et al. and Beltramo et al., where the presence of high concentration of glycated albumin for a longer period of time significantly impaired EC viability and viability associated functions (Beltramo et al., 2003; Xu et al., 2003). A reduction of EC viability could induce EC dysfunction and increase the potential for pro-inflammatory and pro-thrombotic responses, which could eventually lead to cardiovascular disease conditions (Baumgartner-Parzer et al., 1995; Du et al., 1998).

5.3 Endothelial Cell Morphology:

The morphological changes of ECs exposed to various glycation extents for early and late culture durations was investigated by measuring the cell perimeter area. And the results showed a heightened preference in elongated morphology as EC were incubated with glycated albumins (2 and 6 week AGE) for longer durations (Table 4.1). In a previous study, Rubenstein et al., associated the change in morphology to EC angiogenic potential (Rubenstein et al., 2007). In a study conducted by Cohen et al., reported that, the change in morphology could be caused by the degradation of the ECM attaching the ECs (Cohen, Hud, Wu, & Ziyadeh, 1995). Therefore, change of the EC morphology could create pathological conditions in the vasculature.

5.4 Connexin-43 and Caveolin-1 Expression

5.4.1 Static Condition

The aim of this study was to observe the effect of different glycation extent (2, 6 and 8 week AGE) and culture duration (early and late) on the EC mature network formation and angiogenesis potential by the measuring the EC surface expression of Cx-43 and cav-1 protein (Figure 4.4). The results showed a significant increase in Cx-43 expression (intensity and localization), when the ECs were incubated with 8 week AGE in the late culture duration, when

compared to control and paired 8 week BSA samples (Figure 4.4(A) and 4.4(B)). So far there has not been a consensus among the previous researches to determine the effect of AGE on Cx-43 expression. However most of these studies have been carried out in varying cell types and culture conditions. In a study conducted by Wang et al. reported a significant down-regulation in Cx-43 expression in a dose dependent manner of AGEs, in cultured human aortic endothelial cells (HAEC) (Wang et al., 2011). Hou et al. reported a significant reduction in Cx-43 expression and gap junction activity in the aortic endothelium of diabetic ApoE mouse (Hou et al., 2008). Previous researches reported that under hyperglycemic conditions Cx-43 expression was reduced in the microvasculature (Sato, Haimovici, Kao, Li, & Roy, 2002). However, in agreement to our results, Abdullah et al. reported that in skin fibroblasts, there was an increase in Cx-43 expression and cell-to-cell communication under diabetic conditions *in vitro* (Abdullah et al., 1999). It was documented by Zhang et al. diabetic conditions enhanced gap junction activity in their particular experimental conditions (Zhang & Hill, 2005). The results from our study suggest that, Cx-43 is highly regulated by the presence of AGEs and is a function of the extent of glycation and exposure duration and alters gap junction activity and the formation of cell-to-cell communicative network.

The results on cav-1 expression showed, that there was an overall increase in cav-1 expression (although not significant) when ECs were exposed to different levels of AGE and BSA when compared to the control. The result showed a significant increase in cav-1 expression when ECs were incubated with 8 week AGE in late culture conditions, in comparison with control and early cultured samples. The results obtained in this study are in agreement with previous studies on cav-1 expression under diabetic conditions. In a study conducted by Bucci et al. reported an increase in cav-1 expression in diabetic mouse in hyperglycemic conditions (Bucci et al., 2004). Similar results were obtained by Komers et al., where AGE induced an increase in cav-1 expression in an *in vivo* study with diabetic mouse (Komers et al., 2006). In another study

Stitt et al. reported an increase in localization of AGE receptors in the caveolae of diabetic endothelium (Stitt et al., 2000). Therefore, it can be concluded that AGEs have an up-regulating effect on cav-1 expression and induce EC angiogenic potential.

5.4.2 Dynamic Condition

The aim of this study was to investigate how the variation in shear stress levels (low, 4 dynes/cm²; medium, 10 dynes/cm²; high, 40 dynes/cm²) would alter the Cx-43 and cav-1 expression of the ECs that have been incubated with different glycated (2, 6 and 8 week AGE) and non-glycated albumin (2, 6 and 8 week BSA) for early and late culture durations. Furthermore we monitored the combined effect of glycation extent and shear stress level in EC gap junction activity and angiogenic potential by observing the surface expression of EC membrane protein Cx-43 and cav-1.

5.4.2.a Connexin-43 Intensity and Relative Localization

The results obtained from this study indicated that, ECs exposed to high pathological shear stress and higher glycation extent (8 week AGE) increased the overall Cx-43 expression (intensity and localization) when compared to control and paired non-glycated BSA samples in late culture duration (Figure 4.6). The Cx-43 expression of EC exposed to high shear stress was also higher compared to the ECs exposed to medium shear stress at late culture duration. In fact, maximum Cx-43 localization was observed in ECs that were exposed to high shear stress at late culture duration in all glycation extents. (Figure 4.6(D)). In agreement to our results, a number of previous studies have reported a shear stress induced up-regulation in Cx-43 expression, localization and junctional activity (DePaola et al., 1999; Kwak et al., 2005). The effect of AGE on Cx-43 expression in dynamic condition (with the application of hemodynamic shear stress) is similar to the results obtained from the static study (without the application of shear stress) (section 5.4.1). In both cases there was significant increase in Cx-43 expression when ECs were

incubated with high levels of glycated albumin. Therefore, our result (Figure 4.6) suggests that, the presence of AGE and high shear stress combined induces higher Cx-43 expression and thereby increases the potential for cell-to-cell network formation, gap junction activity and angiogenesis.

5.4.2.b Caveolin-1 Intensity and Relative Localization

In this study, from the measurement of cav-1 expression (Figure 4.7) the results indicated that, in both early and late culture duration, the overall cav-1 intensity was higher, when cells were exposed to low and high shear stress when compared to the medium shear stress (Figure 4.7(A) and 4.7(B)). At the same time, there was a significant increase in cav-1 expression (intensity and localization) when ECs incubated with higher glycation extents (8 week AGE) were exposed to high shear stress levels in late culture duration compared to control and paired BSA samples (Figure 4.7). The effect of AGE on cav-1 expression in dynamic condition (with the application of hemodynamic shear stress) is similar to the results obtained from the static study (without the application of shear stress) (section 5.4.1). In both cases there was significant increase in cav-1 expression when ECs were incubated with high levels of glycated albumin. At the same time, cav-1 intensity was overall higher, when cells were exposed to high shear stress levels, when compared to the medium shear stress. However, we did not see any overall trends when only the shear stress magnitude is compared. There has not been many studies conducted in the past to observe the effect of shear stress on EC cav-1 expression, however, Rizzo et al. and Sargiacomo et al. reported that, shear stress promotes EC angiogenic potential, which may be related to the shear mediated up-regulation of cav-1 expression (Sargiacomo et al., 1995; Rizzo et al., 1998). Therefore, from the results obtained from this study, it may be concluded that, the combination of high shear stress and high glycation extent play an up-regulating role in cav-1 expression on EC membrane and thereby facilitate EC angiogenesis.

5.5 Endothelial Cell Cytoskeletal Structure

The aim of this study was to investigate the effect of varying shear stress levels (low, 4 dynes/cm²; medium, 10 dynes/cm²; high, 40 dynes/cm²) on the cytoskeleton structure of the ECs that have been incubated with different glycosylated (2, 6 and 8 week AGE) and non-glycosylated albumin (2, 6 and 8 week BSA) for early and late culture durations. The effect of shear stress level in the disintegration of fibular actin structure, alignment of actin fibers in the shear direction and cell-to-cell connectivity was observed and documented (Figure 4.8-4.13).

5.5.1 Actin Structure

The results obtained from this study indicated that, shear stress disintegrated the fibular actin structure in a magnitude dependent manner in both early and late culture conditions for all levels of glycosylated (AGE) and non-glycosylated (BSA) albumin (Figure 4.8(A) and 4.8(B)). The disruption of actin structure was more pronounced in the early culture duration compared to late. However, significant disintegration was observed when ECs were exposed to high pathological shear stress level (40 dynes/cm²) in comparison with medium (10 dynes/cm²) and low (4 dynes/cm²) shear stress levels. It has been observed that in late culture duration ECs were able to retain more of the actin fibular actin structure in comparison with the early culture duration. We hypothesized that, ECs achieved confluency in late culture conditions and therefore, were able to withstand the forces caused by the application of hemodynamic shear stress. It has been documented by previous studies, that shear stress disintegrates the F-actin bundles in the peripheral cortical rim of ECs (Langille et al., 1991; Kim et al., 1989), and is in agreement with the results obtained from this study. However, the previous researches also observed the formation of central stress fibers in ECs at longer durations of shear exposure. ECs are known to be highly adaptive to mechanical forces and they reorganize the cytoskeletal structure to adapt to the environmental changes; however, a certain period of time is required for the adaptation

process to take place. In this study, shear force was applied only for the duration of one hour primarily due to the limitation of the experimental setup. This time period may not have been sufficient for the formation of central stress fibers. The intact EC cytoskeleton is one of the major pathways for mechanochemical signal transduction (Knudsen & Frangos, 1997; Davies et al., 1995b) and is of high importance in the function of a healthy endothelium; therefore the disruption in cytoskeleton structure could lead to the dysfunction of the endothelium and lead to further pathological conditions.

5.5.2 Actin Alignment

The relative alignment of EC actin fibers in the direction of shear was observed for the various shear levels and glycation extent. The results indicated that, in late culture condition, the actin fibers were more aligned in shear direction compared to early culture duration. At the same time an overall reduction of actin fiber alignment was observed with the increase in shear stress magnitude (low, 4 dynes/cm²; medium, 10 dynes/cm²; high, 40 dynes/cm²). A significant reduction in actin fiber alignment was observed with all control, BSA and AGE samples exposed to high shear stress, in comparison with medium and low shear stress in early culture duration (Figure 4.10(A)). However, there was no significant effect of AGE or BSA in the alteration of actin fiber alignment. The higher percentage of actin fiber alignment could be due to higher confluency in longer culture duration. Previous studies on shear mediated actin alignment, have reported, magnitude and exposure dependent alignment of EC actin fibers (Theret et al., 1988; Levesque et al., 1986). However, in this study pathological level of shear stress (High shear stress, 40 dynes/cm²) was applied to ECs cultured in static conditions. We hypothesized that; ECs could not adapt to the sudden application of the high disruptive shear forces and were less aligned, in comparison with those exposed to more physiological shear stress (10 dynes/cm²) levels. Therefore, the results obtained from this study reports, less alignment of actin fibers under pathological shear stress conditions. The alignment of ECs to the flow direction is important to

maintain a healthy vasculature as it reduces the flow resistance (Levesque et al., 1986). However, if the exposure to pathological shear stress inhibits such alignment, the flow resistance might increase in smaller blood vessels and could lead to the activation of ECs and other constituents of the flowing blood resulting in the initiation of disease conditions.

5.5.3 Cell Connectivity

The results obtained from this study demonstrated an increase in cell-to-cell connectivity in the ECs incubated with higher glycation extents (6 and 8 week AGE) and exposed to high level of shear stress compared to the control and non-glycated (6 and 8 week BSA) samples, in both early and late culture durations (Figure 4.12). There have not been many previous studies on the extension of actin fibers among the adjacent ECs in cell culture conditions. However, no significant effect of shear stress on percent connectivity was observed. The results obtained from this study clearly indicated that under the influence of higher glycation extents (6 and 8 week AGE), EC actin fibers undergo an unstable network formation process among adjacent cells and thereby deteriorating the culture conditions. Incubation with AGEs induce ECs to form multiple unstable thin connections between adjacent ECs and the cells do not reach the same level of confluency compared to the cells in control culture conditions (no glycated or non-glycated albumin). Similar results were obtained by the Rubenstein lab (Rubenstein et al. 2011) under static conditions, where ECs were incubated with various levels of glycated albumin without the application of shear stresses. The results obtained from this study is also in agreement with the digital images obtained from the scanning electron microscopy (Figure 4.15), where the small thin branch formation of ECs are more visible under the influence of AGE.

5.6 Expression of Inflammatory and Thrombotic Mediators

In this study the combined effect of shear stress and glycation extent on EC inflammatory and thrombogenic response was investigated. The EC expression for ICAM-1, thrombomodulin (TM) and tissue factor (TF) under different shear stress and glycation levels were measured and compared.

The results for, the inflammatory response marker, ICAM-1 expression (Figure 4.14(A)) clearly indicates that the presence of AGE had an up-regulating effect on ICAM-1 expression at all magnitudes of shear stress. At medium and high shear stress levels, there was a gradual increase on ICAM-1 expression with the level of glycation extent, with a significant increase in 8 week AGE samples compared to control and paired non-glycated BSA samples. Similar up-regulating effect of glycation extent on ICAM-1 expression was observed in previous static studies (without the application of shear) conducted by the Rubenstein lab (Rubenstein et al. 2011). These results are also in agreement with previous researches conducted on the AGE mediated ICAM-1 expression both *in vivo* and *in vitro* (Basta et al., 2002; Mamputu & Renier, 2004). However, the results did not indicate any overall trends when the shear stress magnitudes were compared (Figure 4.14(A)). Although previous researches on the shear stress mediated ICAM-1 expression reported increase in ICAM-1 expression with shear stress (Morigi et al., 1995; Tsuboi et al., 1995), in these studies the ECs were subjected to shear stress levels for a longer duration of time. Our results did not indicate any such conclusions; this could be due the presence of AGEs in culture during the application of shear. The results obtained from this study suggests that, although there was no explicit effect of shear, however the presence of glycated albumin increased ICAM-1 expression on cultured ECs and thereby enhancing inflammation potential which is a hallmark of cardiovascular diseases (Roberts, Won, Pruthi, Lin, & Barnard, 2006).

To observe the effect of AGE and shear stress levels on ECs thrombotic potential, the expression for anti-thrombogenic TM and pro-thrombogenic TF expression was measured and compared (Figure 4.14(B) and 4.14(C)). The results for the TM expression indicated that, there was a decrease in TM expression on ECs in the presence of AGEs in all shear stress levels. ECs incubated with 6 and 8 week AGE had a reduction in TM expression when compared to control and paired non-glycated BSA samples at all shear magnitudes. Similar down regulating effect of glycation extent on TM expression was observed in previous static studies (without the application of shear) conducted by the Rubenstein lab (Rubenstein et al. 2011). These results are also in agreement with previous researches conducted on the AGE mediated TM expression (Wang et al., 2010a). In this study, we did not observe any overall trend in TM expression when the shear stress magnitudes were compared. So far there has been no consensus among previous studies on the effect of shear stress and TM expression; however most of the studies are conducted under varying conditions (level and the time duration of the applied shear stress) and in varying cell types (BAEs, HUVECs and BSMs) (Malek, Jackman, Rosenberg, & Izumo, 1994b; Takada et al., 1994). In this study, the results clearly suggests that, higher levels of glycation extent significantly down regulates anti-thrombotic marker TM. In the study conducted on ECs to measure the TF expression, the results showed a gradual increase in TF expression when cells were incubated with higher levels of glycated albumins at all shear stress levels (Figure 4.14(C)). There was a significant increase of TF expression when ECs were incubated with higher glycation extents (6 and 8 week AGE) and exposed to medium and high shear stress levels when compared to control and paired non-glycated BSA samples. This is in agreement with the previous research conducted by the Rubenstein lab in static culture conditions (Rubenstein et al. 2011). Similar results are also reported in studies conducted Wang et al. and Bierhaus et al., where presence of AGE induced TF factor expression or TF related activity in cultured ECs (Bierhaus et al., 1997; Wang et al., 2010b; Mohamed et al., 1999). However, there was no overall trend observed when comparing the shear stress magnitudes in this study. The

result obtained from Figure 4.14(C) clearly indicates that AGE up regulates pro-thrombotic TF expression and enhances the potential for thrombus formation. At the same with AGE mediated down-regulation of anti-thrombotic TM expression, it could be anticipated that, once initiated, there would be an enhancement in thrombotic potential which is a hallmark of EC dysfunction and cardiovascular disease conditions. Therefore, from the results obtained from this study on EC inflammatory and thrombotic mediators, it can be suggested that, there is a potential risk for cardiovascular disease formation in the diabetic vasculature due to the presence of AGEs.

5.7 Scanning Electron Microscopy

Scanning electron microscopy (SEM) was used for a qualitative analysis of the EC morphology under the combined effect of different glycation extents (2, 6 and 8 weeks AGE) and shear stress levels (low, 4 dynes/cm²; medium, 10 dynes/cm²; high, 40 dynes/cm²). The results demonstrated that, under the influence of shear stress and glycated albumins, the 'cobblestone' structure of ECs were replaced by a spindle like morphology. This is in agreement with the previous researches conducted to observe the shear mediated alteration on EC morphology (Levesque et al., 1986; Langille et al., 1991). However, the SEM images demonstrated, with the alteration of the cobblestone structure, AGE induced thin unstable connections with the neighboring ECs. Therefore results the obtained from this study suggested that the presence of AGE deteriorates EC culture conditions.

CHAPTER VI

CONCLUSION

The major objective of this thesis was to investigate the combined effect of presence of glycosylated albumin, glycation extent and physiological shear stress on endothelial cell function *in vitro*. The obtained results from the static study (without the application of shear stress), indicates that the presence albumin glycosylated to a greater extent for a longer duration of time in cell culture deteriorates EC culture conditions by decreasing cell viability, density, cell metabolic activity and altering the healthy EC morphology (supports Hypothesis 1, Figures 4.1, 4.3 and Table 4.1). The results also show an up-regulation in cellular network formation and angiogenic potential induced by higher levels of glycosylated albumin (Specific Aim 1, Figure 4.4). From these results, it can be concluded that the presence of advanced glycosylated end products in the diabetic vasculature is deleterious to proper EC function and could modulate the cardiovascular pathologies associated with diabetes mellitus. The observations made in this study however are limited by the assumption that the glycosylated albumin formed *in vitro* is similar to what would form under diabetic conditions.

The results from the dynamic experimental conditions (combined effect of shear stress and AGE) showed that a higher magnitude of constant shear stress and higher levels of glycation extent together caused an up-regulation in EC metabolic activity, cellular network formation and angiogenic potential (supports Hypothesis 2, Figures 4.2, 4.6 and 4.7). Observations on EC

cytoskeleton structure and function under varying shear stress levels revealed that, higher shear stress diminished EC actin structure and reduced actin fiber alignment in the shear direction (supports Hypothesis 2, Figures 4.8, 4.9, 4.10 and 4.11). At the same time, presence of glycated albumin induced an unstable morphology of EC cytoskeleton. These results were confirmed by the digital images obtained from scanning electron microscopy (supports Hypothesis 2, Figures 4.12, 4.13, 4.15). Together, it may be concluded that, although EC actin alignment may not be a function of the level of glycated albumin, its presence combined with shear stress significantly deteriorated EC cytoskeleton structure and function.

The results suggest that EC inflammatory and thrombogenic potential under dynamic experimental conditions and in the presence of higher levels of glycated albumin causes significant up-regulation of the inflammatory and thrombogenic mediators (ICAM-1 and TF) (supports Hypothesis 2, Figure 4.15), which could eventually lead to enhanced cardiovascular complications associated with EC activation. However, shear stress did not play a significant role in the modulation these expressions (refutes Hypothesis 2). From these results it may be assumed that higher shear stress in a diabetic vasculature may not be atherogenic. Further experiments are required to verify such assumptions. Combining all shear stress and AGE studies, our data supports that in general, the combination of the presence of AGEs glycated to a greater extent and high magnitude shear stress, deteriorates endothelial cell functions to promote cardiovascular complications during diabetes.

This study was conducted to observe the combined effect of advanced glycation end products and physiological shear stress on EC functionality. The next step would be to incorporate more physiological variables in the experimental and culture conditions. For example, to observe the effect of AGE and shear stress on EC and platelet interactions or under more physiologically relevant shear stress waveforms. Further information and confirmatory results are

required to identify new therapeutic agents for the disease intervention of diabetes mellitus and cardiovascular pathogenesis.

The overall findings of this study have been summarized in the tables 5.1 to 5.3. This is for the purpose of these tables is to give a general view of the overall results to indicate the effect of glycation extent, increasing shear stress (Table 6.1) and the combined effect of shear stress and glycation extent (Table 6.2) on endothelial cell structure and function.

Higher Glycation Extent	Our Findings	Other Studies	
Enhanced	Connexin-43 Expression	Abdullah et al. 1999	Agrees
	Caveolin-1 Expression	Bucci et al. 2004	Agrees
		Komers et al. 2006	
	Actin Connectivity	N/A	
	TF Expression	Wang et al. 2010	Agrees
		Mohamed et al. 1999	
ICAM-1 Expression	Basta et al. 2002	Agrees	
	Mamputu et al. 2004		
Diminished	Metabolic Activity	Chibber et al. 1997	Agrees
		Nascimento et al. 2006	
	EC Culture Conditions	Beltramo et al. 2003	Agrees
		Xu et al. 2003	
TM Expression	Wang et al. 2010	Agrees	
No effect	Actin Alignment	N/A	
	Actin Structure	N/A	
Increasing Shear Stress	Our Findings	Other Studies	
Enhanced	Connexin-43 Expression	Depaola et al. 1999	Agrees
	Caveolin-1 Expression	Sargiacorno et al. 1995	Agrees
		Rizzo et al. 1998	Agrees
Diminished	Metabolic Activity	N/A	
	Actin Alignment	N/A	
	Actin Structure	Langille et al. 1991	Agrees
		Kim et al. 1989	Agrees
No effect	ICAM-1	N/A	
	TF Expression	N/A	
	TM Expression	N/A	
	Actin Connectivity	N/A	
N/A : Either study was not found or was irrelevant			

Table 6.1- The effect of higher glycation extent and increasing shear stress on EC structure and function

Glycation extent And Shear Stress Combined	Our Findings
Enhanced	Connexin-43 Expression
	Caveolin-1 Expression
	Actin Connectivity
Diminished	ICAM-1 Expression
	Metabolic Activity
	EC Culture Conditions
	Actin Alignment
	Actin Structure
No Effect	TM Expression
	TF Expression

Table 6.2- The combined effect of higher glycation extent and increasing shear stress on EC structure and function

REFERENCES

Abdullah, K. M., Luthra, G., Bilski, J. J., Abdullah, S. A., Reynolds, L. P., Redmer, D. A. et al. (1999). Cell-to-cell communication and expression of gap junctional proteins in human diabetic and nondiabetic skin fibroblasts: effects of basic fibroblast growth factor. *Endocrine*, *10*, 35-41.

Aird, W. C. (2007a). Phenotypic heterogeneity of the endothelium: I. Structure, function, and mechanisms. *Circ.Res.*, *100*, 158-173.

Aird, W. C. (2007b). Phenotypic heterogeneity of the endothelium: II. Representative vascular beds. *Circ.Res.*, *100*, 174-190.

Arnout, J., Hoylaerts, M. F., & Lijnen, H. R. (2006). Haemostasis. *Handb.Exp.Pharmacol.*, 1-41.

Basta, G., Lazzerini, G., Massaro, M., Simoncini, T., Tanganelli, P., Fu, C. et al. (2002). Advanced glycation end products activate endothelium through signal-transduction receptor RAGE: a mechanism for amplification of inflammatory responses. *Circulation*, *105*, 816-822.

Baumgartner-Parzer, S. M., Wagner, L., Pettermann, M., Grillari, J., Gessl, A., & Waldhausl, W. (1995). High-glucose--triggered apoptosis in cultured endothelial cells. *Diabetes*, *44*, 1323-1327.

Brandes, R. P., Schmitz-Winnenthal, F. H., Feletou, M., Godecke, A., Huang, P. L., Vanhoutte, P. M. et al. (2000). An endothelium-derived hyperpolarizing factor distinct from NO and prostacyclin is a major endothelium-dependent vasodilator in resistance vessels of wild-type and endothelial NO synthase knockout mice. *Proc.Natl.Acad.Sci.U.S.A*, 97, 9747-9752.

Brouet, A., Dewever, J., Martinive, P., Havaux, X., Bouzin, C., Sonveaux, P. et al. (2005). Antitumor effects of in vivo caveolin gene delivery are associated with the inhibition of the proangiogenic and vasodilatory effects of nitric oxide. *FASEB J.*, 19, 602-604.

Bucci, M., Gratton, J. P., Rudic, R. D., Acevedo, L., Roviezzo, F., Cirino, G. et al. (2000). In vivo delivery of the caveolin-1 scaffolding domain inhibits nitric oxide synthesis and reduces inflammation. *Nat.Med.*, 6, 1362-1367.

Bucci, M., Roviezzo, F., Brancaleone, V., Lin, M. I., Di, L. A., Cicala, C. et al. (2004). Diabetic mouse angiopathy is linked to progressive sympathetic receptor deletion coupled to an enhanced caveolin-1 expression. *Arterioscler.Thromb.Vasc.Biol.*, 24, 721-726.

Busse, R. & Fleming, I. (2006). Vascular endothelium and blood flow. *Handb.Exp.Pharmacol.*, 43-78.

Centers for Disease Control and Prevention. National Diabetes Fact Sheet: national estimates and general information on diabetes and prediabetes in the United States, 2011. Atlanta, GA: U.S. Department of Health and Human Services, Centers for Disease Control and Prevention, 2011.

Chibber, R., Molinatti, P. A., Rosatto, N., Lambourne, B., & Kohner, E. M. (1997). Toxic action of advanced glycation end products on cultured retinal capillary pericytes and endothelial cells: relevance to diabetic retinopathy. *Diabetologia*, 40, 156-164.

Cho, S. J., Roman, G., Yeboah, F., & Konishi, Y. (2007). The road to advanced glycation end products: a mechanistic perspective. *Curr.Med.Chem.*, 14, 1653-1671.

Cines, D. B., Pollak, E. S., Buck, C. A., Loscalzo, J., Zimmerman, G. A., McEver, R. P. et al. (1998). Endothelial cells in physiology and in the pathophysiology of vascular disorders. *Blood*, 91, 3527-3561.

Cohen, M. P., Hud, E., Wu, V. Y., & Ziyadeh, F. N. (1995). Albumin modified by Amadori glucose adducts activates mesangial cell type IV collagen gene transcription. *Mol. Cell Biochem.*, 151, 61-67.

Corada, M., Mariotti, M., Thurston, G., Smith, K., Kunkel, R., Brockhaus, M. et al. (1999). Vascular endothelial-cadherin is an important determinant of microvascular integrity in vivo. *Proc.Natl.Acad.Sci.U.S.A.*, 96, 9815-9820.

Davies, P. F., Mundel, T., & Barbee, K. A. (1995a). A mechanism for heterogeneous endothelial responses to flow in vivo and in vitro. *J.Biomech.*, 28, 1553-1560.

De Matteis, M. A. & Morrow, J. S. (2000). Spectrin tethers and mesh in the biosynthetic pathway. *J.Cell Sci.*, 113 (Pt 13), 2331-2343.

Dejana, E., Corada, M., & Lampugnani, M. G. (1995). Endothelial cell-to-cell junctions. *FASEB J.*, 9, 910-918.

DePaola, N., Davies, P. F., Pritchard, W. F., Jr., Florez, L., Harbeck, N., & Polacek, D. C. (1999). Spatial and temporal regulation of gap junction connexin43 in vascular endothelial cells exposed to controlled disturbed flows in vitro. *Proc.Natl.Acad.Sci.U.S.A.*, 96, 3154-3159.

Dittman, W. A. & Majerus, P. W. (1990). Structure and function of thrombomodulin: a natural anticoagulant. *Blood*, 75, 329-336.

Du, X. L., Sui, G. Z., Stockklauser-Farber, K., Weiss, J., Zink, S., Schwippert, B. et al. (1998). Introduction of apoptosis by high proinsulin and glucose in cultured human umbilical vein endothelial cells is mediated by reactive oxygen species. *Diabetologia*, 41, 249-256.

Dudek, S. M. & Garcia, J. G. (2001). Cytoskeletal regulation of pulmonary vascular permeability. *J.Appl.Physiol.*, 91, 1487-1500.

Endres, M., Laufs, U., Merz, H., & Kaps, M. (1997). Focal expression of intercellular adhesion molecule-1 in the human carotid bifurcation. *Stroke*, 28, 77-82.

Esmon, C. T. (1993). Molecular events that control the protein C anticoagulant pathway. *Thromb.Haemost.*, 70, 29-35.

Esmon, C. T., Esmon, N. L., & Harris, K. W. (1982). Complex formation between thrombin and thrombomodulin inhibits both thrombin-catalyzed fibrin formation and factor V activation. *J.Biol.Chem.*, 257, 7944-7947.

Frangos, J. A., McIntire, L. V., & Eskin, S. G. (1988). Shear stress induced stimulation of mammalian cell metabolism. *Biotechnol.Bioeng.*, 32, 1053-1060.

Frank, P. G., Woodman, S. E., Park, D. S., & Lisanti, M. P. (2003). Caveolin, caveolae, and endothelial cell function. *Arterioscler.Thromb.Vasc.Biol.*, 23, 1161-1168.

Fry, D. L. (1968). Acute vascular endothelial changes associated with increased blood velocity gradients. *Circ.Res.*, 22, 165-197.

Goldin, A., Beckman, J. A., Schmidt, A. M., & Creager, M. A. (2006). Advanced glycation end products: sparking the development of diabetic vascular injury. *Circulation*, 114, 597-605.

Grabowski, E. F., Zuckerman, D. B., & Nemerson, Y. (1993). The functional expression of tissue factor by fibroblasts and endothelial cells under flow conditions. *Blood*, 81, 3265-3270.

Gratton, J. P., Lin, M. I., Yu, J., Weiss, E. D., Jiang, Z. L., Fairchild, T. A. et al. (2003). Selective inhibition of tumor microvascular permeability by cavtratin blocks tumor progression in mice. *Cancer Cell*, 4, 31-39.

Guyton, A.C. and Hall, J.E. (2000). *Textbook of Medical Physiology*. Elsevier Science

Harja, E., Bu, D. X., Hudson, B. I., Chang, J. S., Shen, X., Hallam, K. et al. (2008). Vascular and inflammatory stresses mediate atherosclerosis via RAGE and its ligands in apoE^{-/-} mice. *J.Clin.Invest*, 118, 183-194.

Helmlinger, G., Berk, B. C., & Nerem, R. M. (1995). Calcium responses of endothelial cell monolayers subjected to pulsatile and steady laminar flow differ. *Am.J.Physiol*, 269, C367-C375.

Hori, O., Yan, S. D., Ogawa, S., Kuwabara, K., Matsumoto, M., Stern, D. et al. (1996). The receptor for advanced glycation end-products has a central role in mediating the effects of advanced glycation end-products on the development of vascular disease in diabetes mellitus. *Nephrol.Dial.Transplant.*, 11 Suppl 5, 13-16.

Hotulainen, P. & Lappalainen, P. (2006). Stress fibers are generated by two distinct actin assembly mechanisms in motile cells. *J.Cell Biol.*, 173, 383-394.

Hou, C. J., Tsai, C. H., Su, C. H., Wu, Y. J., Chen, S. J., Chiu, J. J. et al. (2008). Diabetes reduces aortic endothelial gap junctions in ApoE-deficient mice: simvastatin exacerbates the reduction. *J.Histochem.Cytochem.*, 56, 745-752.

Houston, P., Dickson, M. C., Ludbrook, V., White, B., Schwachtgen, J. L., McVey, J. H. et al. (1999). Fluid shear stress induction of the tissue factor promoter in vitro and in vivo is mediated by Egr-1. *Arterioscler.Thromb.Vasc.Biol.*, 19, 281-289.

Hsieh, H. J., Li, N. Q., & Frangos, J. A. (1993). Pulsatile and steady flow induces c-fos expression in human endothelial cells. *J.Cell Physiol*, 154, 143-151.

Jockusch, B. M., Bubeck, P., Giehl, K., Kroemker, M., Moschner, J., Rothkegel, M. et al. (1995). The molecular architecture of focal adhesions. *Annu.Rev.Cell Dev.Biol.*, 11, 379-416.

Kahn, S. E., Hull, R. L., & Utzschneider, K. M. (2006). Mechanisms linking obesity to insulin resistance and type 2 diabetes. *Nature*, 444, 840-846.

Kim, D. W., Langille, B. L., Wong, M. K., & Gotlieb, A. I. (1989). Patterns of endothelial microfilament distribution in the rabbit aorta in situ. *Circ.Res.*, 64, 21-31.

Knudsen, H. L. & Frangos, J. A. (1997). Role of cytoskeleton in shear stress-induced endothelial nitric oxide production. *Am.J.Physiol*, 273, H347-H355.

Komers, R., Schutzer, W. E., Reed, J. F., Lindsley, J. N., Oyama, T. T., Buck, D. C. et al. (2006). Altered endothelial nitric oxide synthase targeting and conformation and caveolin-1 expression in the diabetic kidney. *Diabetes*, 55, 1651-1659.

Kubes, P. & Kanwar, S. (1994). Histamine induces leukocyte rolling in post-capillary venules. A P-selectin-mediated event. *J.Immunol.*, 152, 3570-3577.

Kwak, B. R., Silacci, P., Stergiopoulos, N., Hayoz, D., & Meda, P. (2005). Shear stress and cyclic circumferential stretch, but not pressure, alter connexin43 expression in endothelial cells. *Cell Commun.Adhes.*, 12, 261-270.

Langille, B. L., Graham, J. J., Kim, D., & Gotlieb, A. I. (1991). Dynamics of shear-induced redistribution of F-actin in endothelial cells in vivo. *Arterioscler.Thromb.*, *11*, 1814-1820.

Levesque, M. J., Liepsch, D., Moravec, S., & Nerem, R. M. (1986). Correlation of endothelial cell shape and wall shear stress in a stenosed dog aorta. *Arteriosclerosis*, *6*, 220-229.

Lin, M. C., Almus-Jacobs, F., Chen, H. H., Parry, G. C., Mackman, N., Shyy, J. Y. et al. (1997). Shear stress induction of the tissue factor gene. *J.Clin.Invest*, *99*, 737-744.

Liu, J. & Schnitzer, J. E. (1999). Analysis of lipids in caveolae. *Methods Mol.Biol.*, *116*, 61-72.

Maiti, R. & Agrawal, N. K. (2007). Atherosclerosis in diabetes mellitus: role of inflammation. *Indian J.Med.Sci.*, *61*, 292-306.

Malek, A. M., Alper, S. L., & Izumo, S. (1999). Hemodynamic shear stress and its role in atherosclerosis. *JAMA*, *282*, 2035-2042.

Malek, A. M., Izumo, S., & Alper, S. L. (1999). Modulation by pathophysiological stimuli of the shear stress-induced up-regulation of endothelial nitric oxide synthase expression in endothelial cells. *Neurosurgery*, *45*, 334-344.

Malek, A. M., Jackman, R., Rosenberg, R. D., & Izumo, S. (1994a). Endothelial expression of thrombomodulin is reversibly regulated by fluid shear stress. *Circ.Res.*, *74*, 852-860.

Mamputu, J. C. & Renier, G. (2004). Advanced glycation end-products increase monocyte adhesion to retinal endothelial cells through vascular endothelial growth factor-induced ICAM-1 expression: inhibitory effect of antioxidants. *J.Leukoc.Biol.*, *75*, 1062-1069.

Marchetti, P. (2009) Advanced glycation end products (AGEs) and their receptors (RAGEs) in diabetic vascular disease. *Medicographia*, *100*, 257-264.

Minshall, R. D., Sessa, W. C., Stan, R. V., Anderson, R. G., & Malik, A. B. (2003a). Caveolin regulation of endothelial function. *Am.J.Physiol Lung Cell Mol.Physiol*, *285*, L1179-L1183.

Mohamed, A. K., Bierhaus, A., Schiekofer, S., Tritschler, H., Ziegler, R., & Nawroth, P. (1999). The role of oxidative stress and NF-kappaB activation in late diabetic complications. *Biofactors*, *10*, 157-167.

Moore, K. L., Esmon, C. T., & Esmon, N. L. (1989). Tumor necrosis factor leads to the internalization and degradation of thrombomodulin from the surface of bovine aortic endothelial cells in culture. *Blood*, *73*, 159-165.

Morigi, M., Zoja, C., Figliuzzi, M., Foppolo, M., Micheletti, G., Bontempelli, M. et al. (1995). Fluid shear stress modulates surface expression of adhesion molecules by endothelial cells. *Blood*, *85*, 1696-1703.

Muller, W. A. (2002). Leukocyte-endothelial cell interactions in the inflammatory response. *Lab Invest*, *82*, 521-533.

Muller, Y. A., Ultsch, M. H., Kelley, R. F., & de Vos, A. M. (1994). Structure of the extracellular domain of human tissue factor: location of the factor VIIa binding site. *Biochemistry*, *33*, 10864-10870.

Nagel, T., Resnick, N., Atkinson, W. J., Dewey, C. F., Jr., & Gimbrone, M. A., Jr. (1994). Shear stress selectively upregulates intercellular adhesion molecule-1 expression in cultured human vascular endothelial cells. *J.Clin.Invest*, *94*, 885-891.

Nascimento, N. R., Lessa, L. M., Kerntopf, M. R., Sousa, C. M., Alves, R. S., Queiroz, M. G. et al. (2006). Inositols prevent and reverse endothelial dysfunction in diabetic rat and rabbit vasculature metabolically and by scavenging superoxide. *Proc.Natl.Acad.Sci.U.S.A*, *103*, 218-223.

Palade, G. E. & Bruns, R. R. (1968). Structural modulations of plasmalemmal vesicles. *J.Cell Biol.*, *37*, 633-649.

Patterson, C. E. & Lum, H. (2001). Update on pulmonary edema: the role and regulation of endothelial barrier function. *Endothelium*, *8*, 75-105.

Pober, J. S. & Cotran, R. S. (1990). The role of endothelial cells in inflammation. *Transplantation*, *50*, 537-544.

Pober, J. S., Gimbrone, M. A., Jr., Lapierre, L. A., Mendrick, D. L., Fiers, W., Rothlein, R. et al. (1986). Overlapping patterns of activation of human endothelial cells by interleukin 1, tumor necrosis factor, and immune interferon. *J.Immunol.*, 137, 1893-1896.

Prasain, N. & Stevens, T. (2009). The actin cytoskeleton in endothelial cell phenotypes. *Microvasc.Res.*, 77, 53-63.

Rask-Madsen, C. & King, G. L. (2007). Mechanisms of Disease: endothelial dysfunction in insulin resistance and diabetes. *Nat.Clin.Pract.Endocrinol.Metab*, 3, 46-56.

Rizzo, V., McIntosh, D. P., Oh, P., & Schnitzer, J. E. (1998). In situ flow activates endothelial nitric oxide synthase in luminal caveolae of endothelium with rapid caveolin dissociation and calmodulin association. *J.Biol.Chem.*, 273, 34724-34729.

Roberts, C. K., Won, D., Pruthi, S., Lin, S. S., & Barnard, R. J. (2006). Effect of a diet and exercise intervention on oxidative stress, inflammation and monocyte adhesion in diabetic men. *Diabetes Res.Clin.Pract.*, 73, 249-259.

Rothberg, K. G., Heuser, J. E., Donzell, W. C., Ying, Y. S., Glenney, J. R., & Anderson, R. G. (1992). Caveolin, a protein component of caveolae membrane coats. *Cell*, 68, 673-682.

Rothlein, R., Dustin, M. L., Marlin, S. D., & Springer, T. A. (2011). Pillars Article: A Human Intercellular Adhesion Molecule (ICAM-1) Distinct from LFA-1. *J. Immunol.* 1986. 137: 1270-1274. *J.Immunol.*, 186, 5034-5038.

Rubenstein, D., Han, D., Goldgraben, S., El-Gendi, H., Gouma, P. I., & Frame, M. D. (2007). Bioassay chamber for angiogenesis with perfused explanted arteries and electrospun scaffolding. *Microcirculation.*, 14, 723-737.

Rubenstein, D. A., Morton, B. E., & Yin, W. (2010). The combined effects of sidestream smoke extracts and glycated serum albumin on endothelial cells and platelets. *Cardiovasc.Diabetol.*, 9, 28.

Rubenstein,D.A., Maria,Z. & Yin,Win. (2011). Glycated albumin modulates endothelial cell thrombogenic and inflammatory responses. *Journal of Diabetes Sicin ce and Technology*,5,3.

Ruderman, N. B., Williamson, J. R., & Brownlee, M. (1992). Glucose and diabetic vascular disease. *FASEB J.*, 6, 2905-2914.

Rudic, R. D., Shesely, E. G., Maeda, N., Smithies, O., Segal, S. S., & Sessa, W. C. (1998). Direct evidence for the importance of endothelium-derived nitric oxide in vascular remodeling. *J.Clin.Invest*, *101*, 731-736.

Salameh, A., Zinn, M., & Dhein, S. (1997). High D-glucose induces alterations of endothelial cell structure in a cell-culture model. *J.Cardiovasc.Pharmacol.*, *30*, 182-190.

Sargiacomo, M., Scherer, P. E., Tang, Z., Kubler, E., Song, K. S., Sanders, M. C. et al. (1995). Oligomeric structure of caveolin: implications for caveolae membrane organization. *Proc.Natl.Acad.Sci.U.S.A*, *92*, 9407-9411.

Sato, T., Haimovici, R., Kao, R., Li, A. F., & Roy, S. (2002). Downregulation of connexin 43 expression by high glucose reduces gap junction activity in microvascular endothelial cells. *Diabetes*, *51*, 1565-1571.

Saydah, S. H., Miret, M., Sung, J., Varas, C., Gause, D., & Brancati, F. L. (2001). Postchallenge hyperglycemia and mortality in a national sample of U.S. adults. *Diabetes Care*, *24*, 1397-1402.

Sohl, G. & Willecke, K. (2004). Gap junctions and the connexin protein family. *Cardiovasc.Res.*, *62*, 228-232.

Stitt, A. W., Burke, G. A., Chen, F., McMullen, C. B., & Vlassara, H. (2000). Advanced glycation end-product receptor interactions on microvascular cells occur within caveolin-rich membrane domains. *FASEB J.*, *14*, 2390-2392.

Sumpio, B. E., Riley, J. T., & Dardik, A. (2002). Cells in focus: endothelial cell. *Int.J.Biochem.Cell Biol.*, *34*, 1508-1512.

Takada, Y., Shinkai, F., Kondo, S., Yamamoto, S., Tsuboi, H., Korenaga, R. et al. (1994). Fluid shear stress increases the expression of thrombomodulin by cultured human endothelial cells. *Biochem.Biophys.Res.Commun.*, *205*, 1345-1352.

Theret, D. P., Levesque, M. J., Sato, M., Nerem, R. M., & Wheeler, L. T. (1988). The application of a homogeneous half-space model in the analysis of endothelial cell micropipette measurements. *J.Biomech.Eng*, *110*, 190-199.

Traub, O. & Berk, B. C. (1998). Laminar shear stress: mechanisms by which endothelial cells transduce an atheroprotective force. *Arterioscler.Thromb.Vasc.Biol.*, 18, 677-685.

Tsuboi, H., Ando, J., Korenaga, R., Takada, Y., & Kamiya, A. (1995). Flow stimulates ICAM-1 expression time and shear stress dependently in cultured human endothelial cells. *Biochem.Biophys.Res.Comm.*, 206, 988-996.

van Rijen, H. V., van Kempen, M. J., Postma, S., & Jongsma, H. J. (1998). Tumour necrosis factor alpha alters the expression of connexin43, connexin40, and connexin37 in human umbilical vein endothelial cells. *Cytokine*, 10, 258-264.

Van, R. H., van Kempen, M. J., Analbers, L. J., Rook, M. B., van Ginneken, A. C., Gros, D. et al. (1997a). Gap junctions in human umbilical cord endothelial cells contain multiple connexins. *Am.J.Physiol*, 272, C117-C130.

Vander,A., Luciano,D. & Sherman,J.(2001). Human Physiology: The mechanism of body function, 7th Edition.

Wang, C. Y., Liu, H. J., Chen, H. J., Lin, Y. C., Wang, H. H., Hung, T. C. et al. (2011). AGE-BSA down-regulates endothelial connexin43 gap junctions. *BMC.Cell Biol.*, 12, 19.

Wang, H. J., Huang, H. C., Chuang, Y. C., Liao, P. J., Yang, D. M., Yang, W. K. et al. (2010a). Modulation of tissue factor and thrombomodulin expression in human aortic endothelial cells incubated with high glucose. *Acta Diabetol.*

Wilcox, J. N., Smith, K. M., Schwartz, S. M., & Gordon, D. (1989). Localization of tissue factor in the normal vessel wall and in the atherosclerotic plaque. *Proc.Natl.Acad.Sci.U.S.A*, 86, 2839-2843.

Wolff, S. P., Jiang, Z. Y., & Hunt, J. V. (1991). Protein glycation and oxidative stress in diabetes mellitus and ageing. *Free Radic.Biol.Med.*, 10, 339-352.

Wu, K. K. & Thiagarajan, P. (1996a). Role of endothelium in thrombosis and hemostasis. *Annu.Rev.Med.*, 47, 315-331.

Xu, B., Chibber, R., Ruggiero, D., Kohner, E., Ritter, J., & Ferro, A. (2003). Impairment of vascular endothelial nitric oxide synthase activity by advanced glycation end products. *FASEB J.*, 17, 1289-1291.

Yamagishi, S., Nakamura, K., & Imaizumi, T. (2005). Advanced glycation end products (AGEs) and diabetic vascular complications. *Curr.Diabetes Rev.*, *1*, 93-106.

Yang, G., Lucas, R., Caldwell, R., Yao, L., Romero, M. J., & Caldwell, R. W. (2010). Novel mechanisms of endothelial dysfunction in diabetes. *J.Cardiovasc.Dis.Res.*, *1*, 59-63.

Yang, L., Froio, R. M., Sciuto, T. E., Dvorak, A. M., Alon, R., & Lusinskas, F. W. (2005). ICAM-1 regulates neutrophil adhesion and transcellular migration of TNF-alpha-activated vascular endothelium under flow. *Blood*, *106*, 584-592.

Yeh, H. I., Dupont, E., Coppen, S., Rothery, S., & Severs, N. J. (1997). Gap junction localization and connexin expression in cytochemically identified endothelial cells of arterial tissue. *J.Histochem.Cytochem.*, *45*, 539-550.

Yin, W., Shanmugavelayudam, S. K., & Rubenstein, D. A. (2011). The effect of physiologically relevant dynamic shear stress on platelet and endothelial cell activation. *Thromb.Res.*, *127*, 235-241.

Yin, W. & Rubenstein, D. A. (2009). Dose Effect of Shear Stress on Platelet Complement Activation in a Cone and Plate Shearing Device. *Cellular and Molecular Bioengineering*, *2*, 274-280.

Zhang, J. & Hill, C. E. (2005). Differential connexin expression in preglomerular and postglomerular vasculature: accentuation during diabetes. *Kidney Int.*, *68*, 1171-1185.

APPENDIX A

BASIC PROGRAM USED TO OPERATE CONE AND PLATE SHEARING DEVICE

rem x motor shear stress 4 dynes/cm² and y motor 10 dynes/cm²

joff

sposx 0
sposy 0

accx 0
accy 0

A = 1068
B = 2670

velx A
vely B

jogx
jogy

end

\$

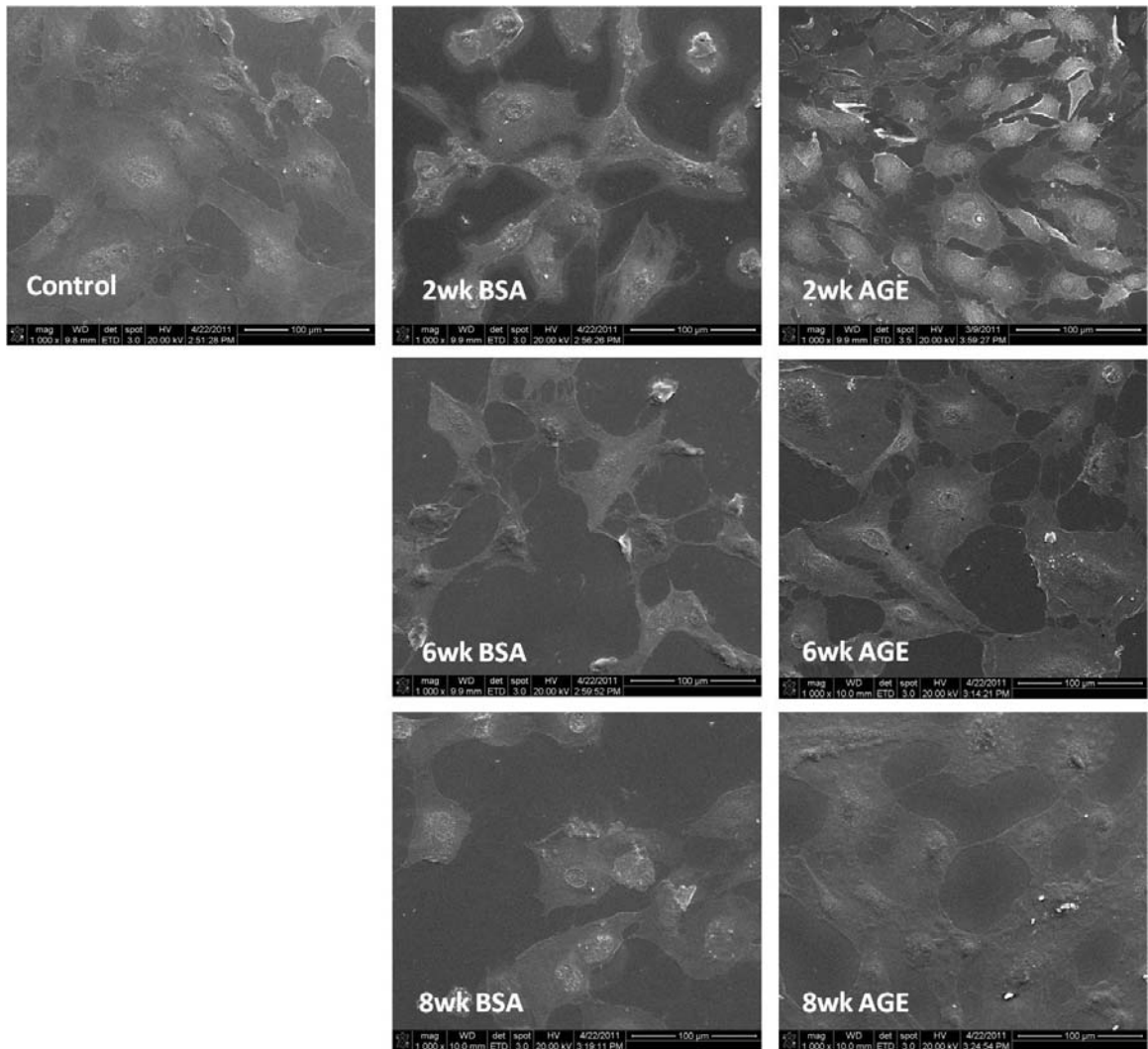
*For 40dynes/cm², the cone speed was set at 10680

APPENDIX B

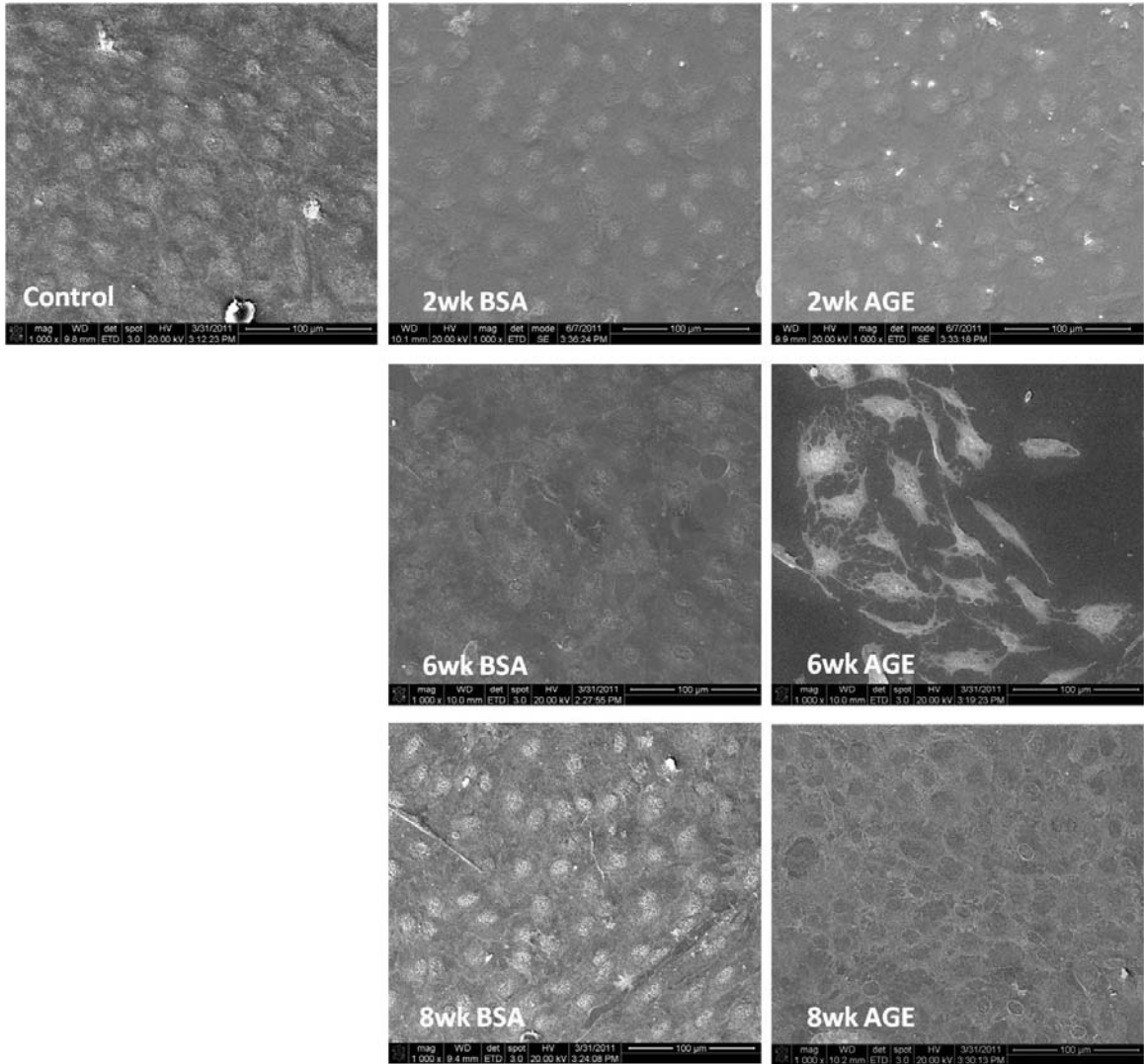
SCANNING ELECTRON MICROSCOPY IMAGE

COMPARISON OF GLYCATION EXTENT FOR INDIVIDUAL SHEAR STRESS AND CULTURE DURATION ON ENDOTHELIAL CELL MORPHOLOGY

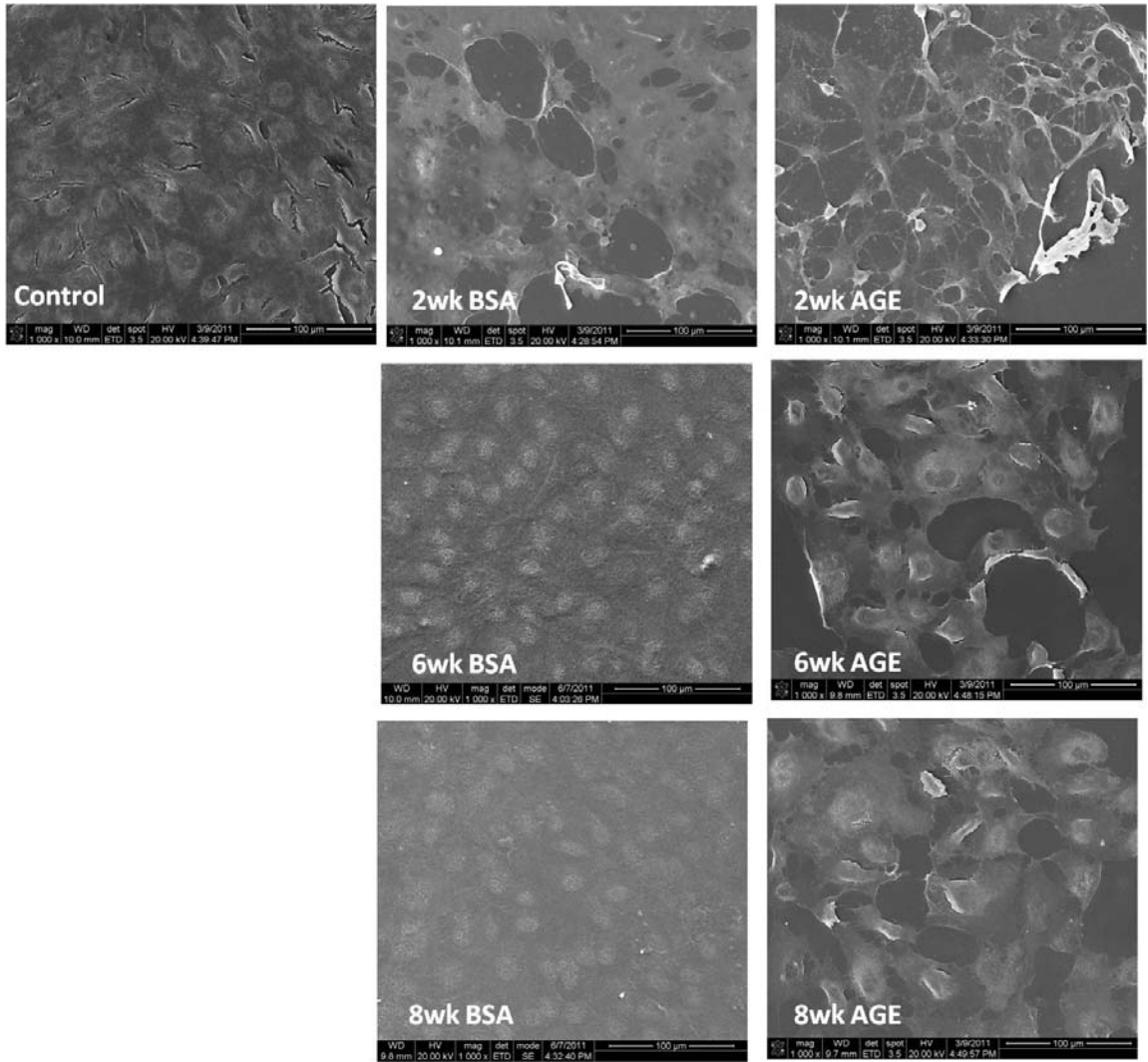
4 dynes/cm² Shear Stress at Early Culture Condition



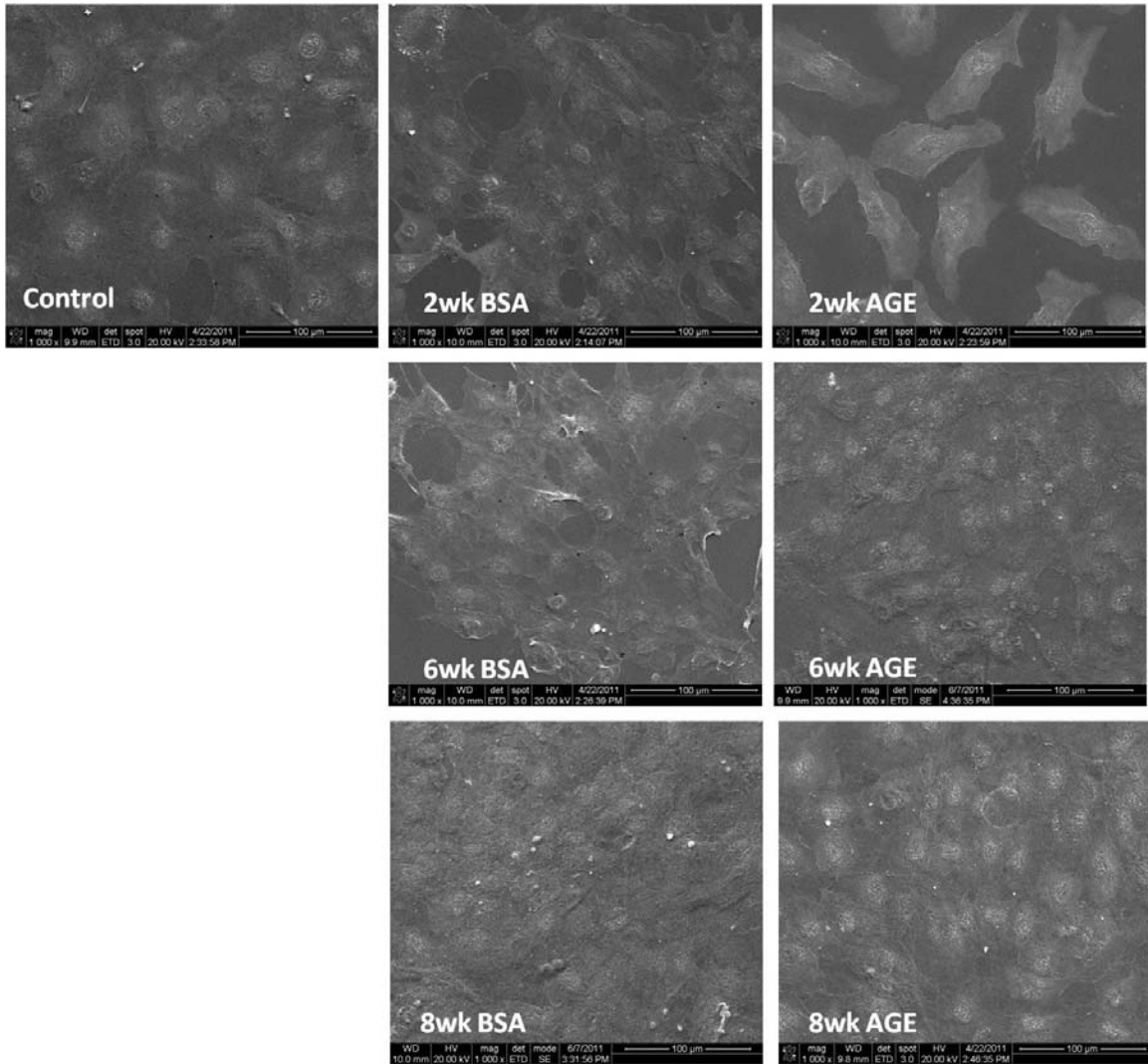
4 dynes/cm² Shear Stress at Early Culture Condition



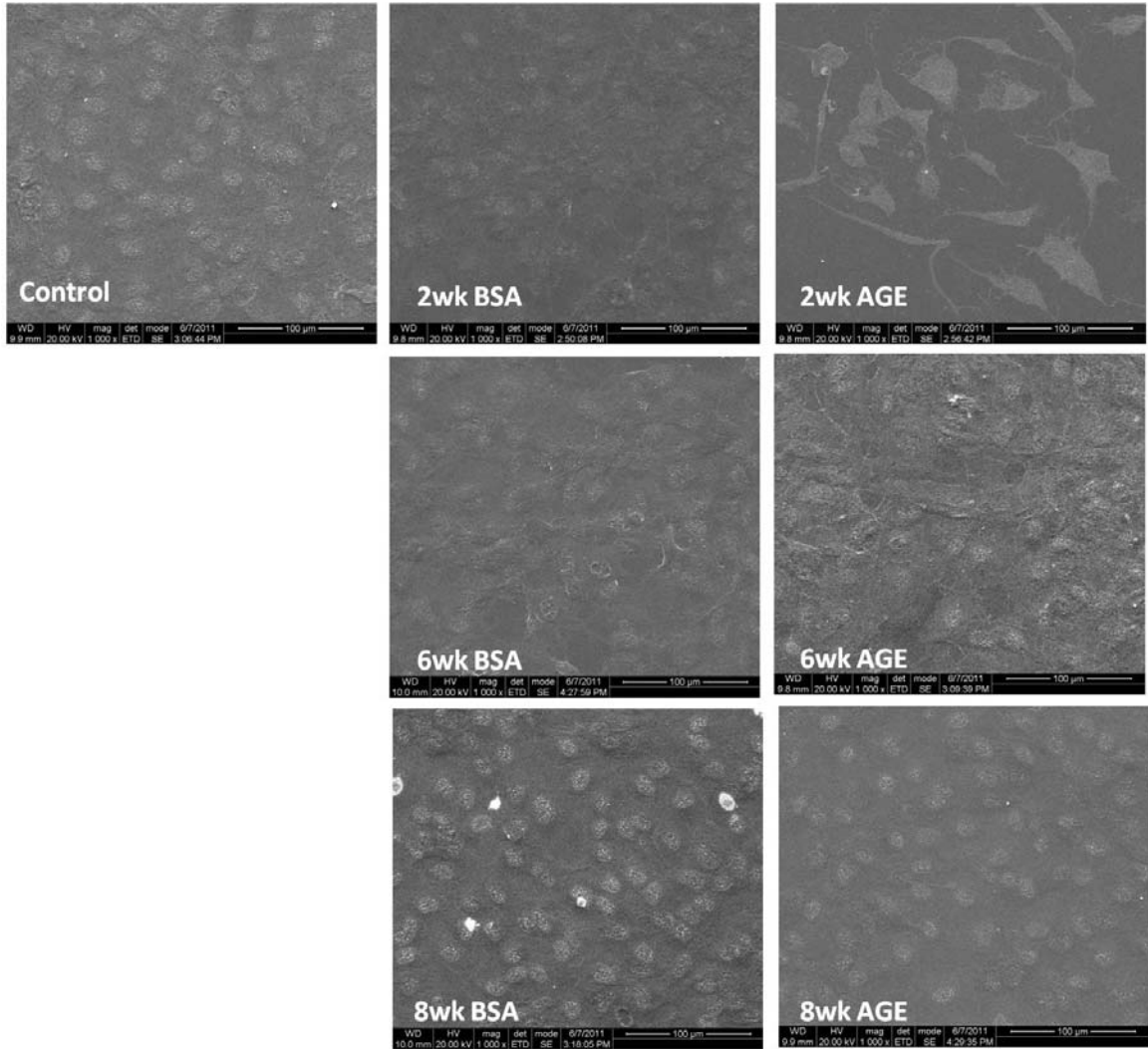
10 dynes/cm² Shear Stress at Early Culture Condition



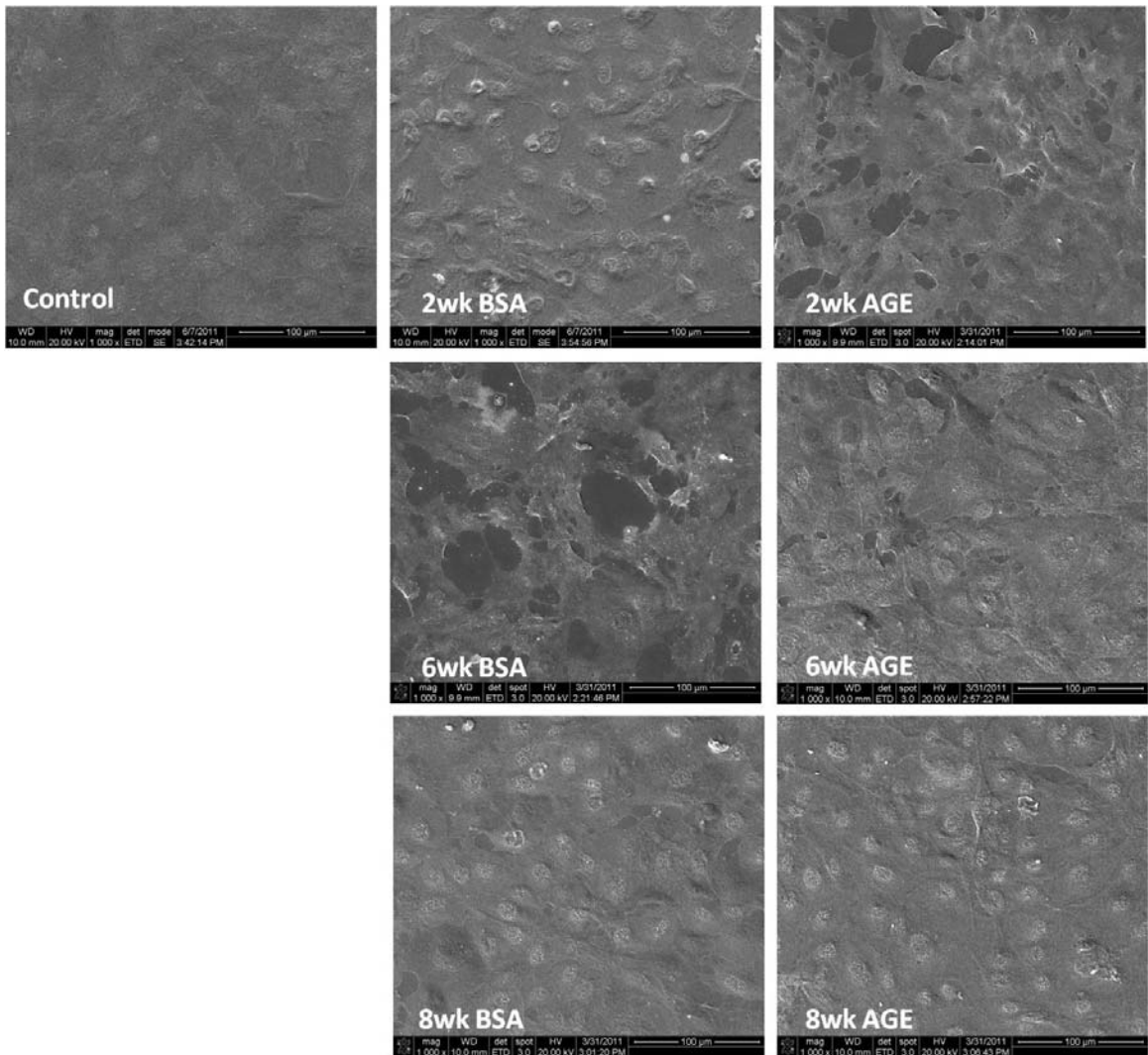
10 dynes/cm² Shear Stress at Late Culture Condition



40 dynes/cm² Shear Stress at Early Culture Condition



40 dynes/cm² Shear Stress at Late Culture Condition



VITA

ZAHRA MARIA

Candidate for the Degree of

Master of Science

Thesis: EFFECT OF GLYCATED ALBUMIN AND SHEAR STRESS ON
ENDOTHELIAL CELL FUNCTIONS

Major Field: Mechanical Engineering

Biographical:

Personal Data: Born in Dhaka, Bangladesh, on October 17th, 1984. Daughter of Azizun Nahar and Kazi Nurul Islam.

Education: Completed the requirements for the Bachelor of Science in Mechanical Engineering at Bangladesh University of Engineering and Technology, 2009

Experience: Graduate Teaching Assistant, from August 2009 to July 2011, Department of Mechanical and Aerospace Engineering, Oklahoma State University. Research Assistant, Biomedical Engineering Lab (BELOS), from August 2009 to July 2011.

Professional Memberships: Student Member, Microcirculatory Society (MCS)

Name: Zahra Maria

Date of Degree: July, 2011

Institution: Oklahoma State University

Location: Stillwater, Oklahoma

Title of Study: EFFECT OF GLYCATED ALBUMIN AND SHEAR STRESS ON
ENDOTHELIAL CELL FUNCTIONS

Pages in Study: 111

Candidate for the Degree of Master of Science

Major Field: Mechanical Engineering

Our goal was to evaluate the combined effect of albumin glycation extent and physiological shear loading on endothelial cell (EC) functions. Cultured ECs were incubated with glycated or non-glycated albumin (2, 6 or 8 weeks of glycation) for up to 5 days. After incubation, ECs were subjected to low, medium or high shear stress (4, 10, 40 dynes/cm²) for 1 hour. EC morphology, shear induced cytoskeletal structure and inflammatory and thrombogenic responses were observed. We hypothesized that the combined effect of high shear stress with glycated albumin would enhance endothelial inflammatory responses to mimic cardiovascular diseases. Results indicated that ECs incubated with advanced (6 and 8 weeks) glycated albumin and exposed to high shear stress had an altered actin alignment and structure. Furthermore, EC metabolic activity in the presence of glycated albumin, decreased with increasing shear stress. Also, ECs treated with glycated albumin induced new communicative network formation. Thus, the results indicate that the presence of advance glycation end products severely affects the function of ECs under various physiological shear stress conditions.

ADVISER'S APPROVAL: Dr. David A. Rubenstein
